November 28, 1984
84042.033

Mrs. Juanita Ellis
President, CASE
1426 S. Polk
Dallas, Texas 75224

Subject: Responses to Cygna Questions from the Independent Assessment Program
         Reviews
         Comanche Peak Steam Electric Station
         Independent Assessment Program - Phase 3
         Texas Utilities Generating Company
         Job No. 84042

Dear Mrs. Ellis:

Enclosed please find copies of responses to questions from the various disciplines associated with Phase 3 of Cygna's Independent Assessment Program.

Feel free to call if you have any questions or wish to discuss the enclosed documents.

Very truly yours,

D. C. Oldag
Administrative Assistant

ajb
Enclosures

cc: Mr. S. Treby (NRC), w/attachments
    Mr. S. Burwell (NRC), w/attachments
    Mr. D. Wade (TUGCO), w/o attachments
    Ms. J. van Amerongen (TUGCO/EBASCO), w/o attachments
    Mr. D. Pigott (Orrick, Herrington & Sutcliffe), w/o attachments

50-445   8412120240 841128
                PDR ADOCK 05000445
                A   PDR

2222
1/1
USe Attorno Dist.
Det 3. Burwell

Attachments

1. L.M. Popplewell (TUGCO) letter to N.H. Williams (Cygna), CPPA-41,195, "Cygna Potential Finding Report (Fisher Valves)," October 2, 1984.

2. L.M. Popplewell (TUGCO) letter to N.H. Williams (Cygna), "Telephone Conversation of October 30, 1984 between L. Weingart, J. Burgess and J. van Amerongen," October 30, 1984.

3. L.M. Popplewell (TUGCO) letter to N.H. Williams (Cygna), "Cygna Review Questions, Reference Cygna telecon dated 10/23/84, Double Trunnion Support MS-1-004-005-C72K," November 1, 1984.

4. J.B. George (TUGCO) letter to N.H. Williams (Cygna), "Cinched U-Bolt Testing & Analysis Program, Additional Information," November 1, 1984.

5. L.M. Popplewell (TUGCO) letter to N.H. Williams (Cygna), "Telephone Conversation of October 30, 1984 between J. Minichiello (Cygna) and J. Finneran (TUGCO)," November 8, 1984.

6. J.B. George (TUGCO) letter to N.H. Williams (Cygna), "Cinched U-Bolt Testing & Analyses Program, Additional Information," November 16, 1984.

TEXAS UTILITIES GENERATING COMPANY

P. O. BOX 1002 · GLEN ROSE, TEXAS 76043

CPPA-41,195

October 2, 1984

CYGNA Energy Services
101 California Street
Suite 1000
San Francisco, California 94111

Attention: Ms. Nancy Williams
Project Manager

COMANCHE PEAK STEAM ELECTRIC STATION
CYGNA POTENTIAL FINDING REPORT
(FISHER VALVES)
REF: CPPA-39,734

CYGNA	
	84042
DATE LOGGED:	10/12/84
LOG NO.:	#89
FILE:	2.1.1 PFC CR
CROSS REF. FILE	2.1 PFC CR log

Gentlemen:

The following is submitted in response to the subject Potential Finding
Report. This report involved several main steam relief valves where the
actual "as-built" loading conditions were not properly qualified or con-
firmed acceptable.

The main steam relief valves (Tag No. PV-2325 through PV-2328) were
subjected to an operability test. They passed the test and no pipe
support rework was required. As previously mentioned in referenced
correspondence, a review of Fisher active and passive valves with similar
support configurations was conducted for potential impact. This review
identified the following valves which also required qualification/acceptance
to the "as-built" loading.

Active:	HV-2185 through HV-2188
	FV-2193 through FV-2196
	HV-2397 through HV-2400
	HV-2401A&B through HV-2404A&B
	HV-4165 through HV-4176
	HV-4178 and HV-4179
	HV-7311 and HV-7312

Passive:	TV-4691 through TV-4694
	HV-5384 and 1-7800
	1-8034 and 1FC-7812
	1-7155 and 1HCV-014

The "as-built" loading/information for these valves was transmitted to
Fisher and have subsequently been qualified. The only physical modifica-
tion required as a result of this qualification was the replacement of
five (5) SMA-1/4 snubbers with SMA-1/2 snubbers. Although the SMA-1/4
snubbers were adequate for the "as-built" loading, Fisher requested that
SMA-1/2's be installed in order to use an existing qualification report
thereby expediting closure of the issue.

CPPA-41,195

CYGNA Energy Services
Page 2.
October 2, 1984

This issue has been addressed in accordance with Deficiency Review Report
(DRR)-054 which identified the concern as a potentially reportable item.
Our subsequent disposition to Significant Deficiency Analysis Report
(SD'R) CP-84-16 indicates no adverse safety conditions would result if
the item r_ined undetected and the issue is not reportable under the
provisions of 10CFR50.55(e).

Please contact this office in the event additional information can be
provided.

Very truly yours,

TEXAS UTILITIES GENERATING COMPANY
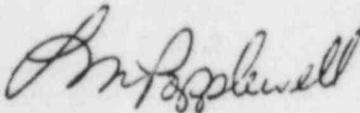
L. M. Popplewell
Project Engineering Manager

LMP/JCF/RPB/cp

cc: ARMS
     D. H. Wade
     J. J. Van Amerongen
     File SDAR-CP-84-16

TEXAS UTILITIES GENERATING COMPANY

P. O. BOX 1002 · GLEN ROSE, TEXAS 76043

October 30, 1984

CYGNA	
JOB NO :	84042
DATE REC'D/LOGGED:	11/2/84
LOG NO.:	#93
FILE:	2.1.1 mc. CR
CROSS REF. FILE	2.1 mc. CR Log

Cygna Energy Services
101 California Street
Suite 1000
San Francisco, California 94111

Attn: Ms. Nancy Williams, Project Manager

REF: Telephone Conversation of October 30, 1984 between
L. Weingart, J. Burgess, and J. Van Amerongen

Dear Ms. Williams:

Attached please find the information requested to close out
the Phase III open issue on the Fisher Main Steam Relief
Valve.

If there are any further questions or comments,
please contact Ms. Jeanne J. Van Amerongen
(Extension 500).

Very truly yours,

L. M. Popplewell
Project Engineering Manager

LMP/JVA/bh

cc: L. Popplewell
D.H. Wade
R.E. Ballard
J. Finneran
J. Burgess
J. Van Amerongen

A DIVISION OF TEXAS UTILITIES ELECTRIC COMPANY

TEXAS UTILITIES GENERATING COMPANY

P. O. BOX 1002 · GLEN ROSE. TEXAS 76043

TSG-6494

September 19, 1984

CCL
P. O. Box 12728
Research Triangle Park, NC 27709

Attention: Mr. Stephen Lehrman

COMANCHE PEAK STEAM ELECTRIC STATION
EQUIPMENT QUALIFICATION DOCUMENTATION
SPECIFICATION 2323-MS-78
P. O. NO. CPF-11167-S, SUPP. 7

Gentlemen:

By copy of this letter, we enclose to the vendor stamped "APPROVED — CHECKED
FOR GENERAL COMPLIANCE WITH PLANS AND SPECIFICATIONS. THIS DOES NOT RELIEVE THE
VENDOR FROM RESPONSIBILITY FOR THE CORRECTNESS OF HIS WORK OR FOR FULFILLING THE
OBLIGATIONS OF HIS CONTRACT WITH TEXAS UTILITIES GENERATING COMPANY", the
following document:

SEISMIC QUALIFICATION REPORT
OF MAIN STEAM RELIEF VALVE
FOR COMANCHE PEAK STEAM ELECTRIC STATION
REPORT NO. A-655-84
Dated September 14, 1984

Please refer to the above "TSG" number in all transmittals resulting from this
letter.

Very truly yours,
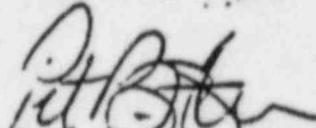
Peter B. Stevens
Supervising Engineer
TUGCO Nuclear Engineering

PBS:CLW:RM:cb

Attachment

cc: ARMS (1L)
    L. Barnes (1L, 1A) PMG-M-997
    E. Q. File (1L, 1A)
    B. F. Jones (1L) PMG
    J. Burgess (1L)
    D. Headrick (1L)

SEISMIC QUALIFICATION REPORT

of

MAIN STEAM RELIEF VALVE

for

COMANCHE PEAK STEAM ELECTRIC STATION
TEXAS UTILITIES GENERATING COMPANY

GIBBS & HILL Specification
Number 2323-MS-78 Rev. 2

Report Date : September 14, 1984
CCL Report Number : A-655-84
CCL Project Number : 84-1813.12
TUGCO P.O. Number:
    CPF-11167-S Supplement 7

By: _Bill R. Black_
    Bill R. Black

Checked By _Stephen A. Lehrman_
    Stephen A. Lehrman, P.E.

Approved By _C. Gary Hughes_
    C. Gary Hughes, P.E.
    CORPORATE CONSULTING AND
    DEVELOPMENT COMPANY, LTD.

Approved By _____
    TEXAS UTILITIES GENERATING
    COMPANY

Prepared By

CORPORATE CONSULTING AND DEVELOPMENT COMPANY, LTD.
P.O. Box 12728
Research Triangle Park, North Carolina, 27709-9998
for

TEXAS UTILITIES GENERATING COMPANY

TABLE OF CONTENTS

4. CONCLUSIONS

The valve has been shown by the testing described in this report to be of sufficient structural integrity to withstand the loads postulated for the valve during the SSE. Neither the valve's pressure retention nor the valve's operability was impaired by the application of static seismic loads. No changes in the performance of the valve were detected during or after the static seismic operability tests.

Fisher Controls International, Inc.
20° th Center Street
Mar alltown, Iowa 50158
Phone 515/754-3011

PMGM- 968

Fisher Controls

FISHER

August 29, 1984

Texas Utilities Generating Company
P. O. Box 1002
Glen Rose, TX 76043

Attention: Manager - TUSI Nuclear Engineering

Subject: Submittal of Fisher Controls Seismic Analysis and
Supplementary Qualification Report

Reference: Comanche Peak Steam Electric Station, Units 1 & 2
Main Steam Relief Valves
TUGCO P.O. No. CP-0078 and CPF-12049-S
Fisher Representative Order No's 1-63500-A,-B and
007D-LF93114
Fisher Project No's NES 170 and LSC 833C910
Fisher Qualification Projects 76NC02 and 84QN89

Gentlemen:

Please find enclosed for your information Fisher Controls Seismic
Analysis and Supplementary Qualification Report FQP-5A-1, Supplement A,
Revision A, dated August 22, 1984, as requested by the referenced purchase
order.

Sincerely,
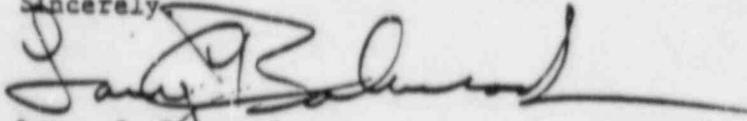
Larry C. Bohnsack
Project Manager
Fisher Controls International, Inc.

LCB:nf

Enclosure - Fisher Controls Seismic Analysis and Supplementary Qual.
Report, FQP-5A-1, Supplement A, Revision A, dated 8/22/84.
(3 copies)

cc: Texas Utilities Generating Company
Attn: Dave Headrick

Vinson Supply Company (Dallas)
Attn: Dick Jacobson

FISHER

cc: Fisher Controls
      Attn: Woody Dickinson
              John Dresser
              1-63500 Base Order (NHS 170)
              7D-LF93114 (8330910)
              Desk

TEXAS UTILITIES GENERATING COMPANY
P. O. BOX 1002 · GLEN ROSE. TEXAS 76043

November 1, 1984

CYGNA	84042 PF
JOB NO :	84042
DATE REC'D/LOGGED:	11/2/84
LOG NO.:	#95
FILE:	2.1.1 Mc. CR
CROSS REF. FILE	2.1 Mc. CRLog

Cygna Energy Services
101 California Street
Suite 1000
San Francisco, California 94111

Attn: Ms. Nancy Williams, Project Manager

COMANCHE PEAK STEAM ELECTRIC STATION
CYGNA REVIEW QUESTIONS

REF: CYGNA Telecon Dated 10/23/84, Double Trunnion
Support Ms-1-004-005-C72K

Dear Ms. Williams:

Attached is TUGCO's response to the above reference Phase
3 follow-up question.

If there are any further questions or comments, please contact
Ms. Jeanne J. Van Amerongen (Extension 500).

Very truly yours,

L. M. Popplewell
Project Engineering Manager

LMP/JVA/bh

cc: L. Popplewell
D.H. Wade
R.E. Ballard
J. Finneran
D. Rencher
J. Van Amerongen

CYGNA QUESTION:

AS part of CYGNA's preparatory review for the Phase 3 double trunnion open issue, CYGNA has found that one support, MS-1-004-005-C72K, may need further review by TUGCO for the weld between the stanchion (item 8) and the pad (item 13). Since this support was modeled in the pipe stress analysis as two supports (i.e., as a moment restraint), there is a theoretical moment carried by this weld. As shown on page 19 of the 8/17/84 calculation, more weld may be required to transmit this moment than presently exists. CYGNA requested TUGCO to clarify.

TUGCO RESPONSE:

The original design of this support relied on the weld between items 8 and 13 to transmit the entire tension or compression load. This weld was designed for a translational force of ±86901 lbs., and no moment.

The revised analysis to include the moment restraining effect of trapeze supports was issued on 5/12/83 (ref. GTN-65560). The problem had previously been qualified without modeling these moment restraining supports in. In both analyses all pipe stress was within allowable limits. However, loads on this support increased due to the restraint of rotation. Calculation by NPSI showed the weld in question was no longer adequate for the increased loads. Hence, two U-bolts were added to accomodate the increased loads.

In the new support configuration, the two cinched U-bolts aid in transferring the moment into a force couple which acts down the axis of each snubber. The weld is not required to transfer 100% of the moment effect. Note that each snubber and the building attachments are designed for the increased loads from the latest analysis. Therefore, the weld between items 8 and 13 is not required to transmit this moment directly, and the connection is adequately designed. Even if the weld and cinched U-bolts were incapable of transferring the moment, the result would be less load on the snubbers and pipe stresses are acceptable either way.

TEXAS UTILITIES GENERAT **COMPANY**

P. O. BOX 1002 · GLEN ROSE, TEXAS 76043

November 1, 1984

Ms. N. H. Williams
Project Manager
CYGNA Energy Services
101 California Street, Suite 1000
San Francisco, California 94111-5894

COMANCHE PEAK STEAM ELECTRIC STATION
Independent Assessment Program Phase 3
Cinched U-Bolt Testing & Analysis Program
Additional Information

REF: (a) N. H. Williams (CYGNA) letter to J. B. George (TUGCO)
"U-Bolt Cinching Testing/Analysis Program-Phase 3
Open Items", 84042.015, dated August 23, 1984

(b) Transcript of "Discussion Between CYGNA Energy Services
and EBASCO Services, Inc.", dated September 13, 1984

(c) R. C. Iotti (EBASCO) letter to N. Williams (CYGNA)
"Additional Information As Follow-up To Meetings of
9/13/84", 3-1-17(6.2) ETCY-1, dated September 18, 1984

(d) N. H. Williams (CYGNA) letter to J. B. George (TUGCO)
"Status of Cinched U-Bolt Testing and Analysis Program",
84042.018 dated October 1, 1984

Dear Ms. Williams:

Reference (a) contained CYGNA's questions on the TUGCO cinched U-bolt testing
and analysis program. All of the questions raised in that reference were
discussed during the meetings of September 13, 1984 (Reference b), and several
of the questions were resolved as a consequence of that meeting and the addi-
tional information provided to CYGNA via Reference (c).

Reference (d) requests additional clarification and/or information on TUGCO's
stated position on those CYGNA comments/questions which have not been fully
resolved.

Accordingly, we are providing in Attachment 1 the information you request as
answers to the questions posed in Reference (d).

A DIVISION OF TEXAS UTILITIES ELECTRIC COMPANY

Ms. N. H. Williams
Page 2
November 1, 1984

We trust this will provide all of the information necessary for you to complete this portion of the Phase 3 Assessment.

Please call if there are any questions.

Very truly yours,

TEXAS UTILITIES GENERATING COMPANY
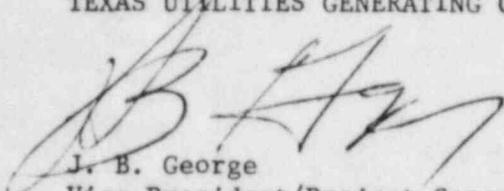
J. B. George
Vice-President/Project General Manager

JBG/LMP/JCF/RCI/gh

cc: D. Wade (TUGCO
     J. Van Amerongen (EBASCO/TUGCO)
     R. Iotti (EBASCO)
     J. Finneran (TUGCO)

TUGCO ANSWERS TO CYGNA'S QUESTIONS
OF OETTER 84042.018, 10/1/84

1. Q. CYGNA Question 2 (transcript page 27)
   Re: Classification of Preload

   TUGCO has classified the pipe stress due to preload as primary in the
   first alternative and increased the allowable primary stress. In the
   second alternative, TUGCO classifies only the membrane portion of the
   preload stress as primary, and then neglects the bending (or membrane)
   portion in the primary plus secondary evaluation. TUGCO's basis for
   this is that the stress is non-cyclic in nature (Robert C. Iotti and
   J. C. Finneran Affidavit Regarding Cinching of U-Bolts, pp. 47 and 67).
   In the first alte itive, CYGNA does not find sufficient justification
   for the use of $3S_m$ for primary stress limits. In the second alterna-
   tive, CYGNA does not find sufficient justification to neglect preload
   as part of the secondary range. In effect, while loads such as dead-
   weight or settlement are non-cyclic in nature, they are compared to
   the appropriate Code allowables. CYGNA believes that the total stress,
   due to all contributions at a point, should be considered in the evalua-
   tion. Therefore, what is the effect of considering preload as a cyclic
   load?

   A. We are surprised that CYGNA still considers the issue of classification
   of preload an open question, since no questions were asked at the con-
   clusion of our stated position in this regard (see transcript page 29).
   To further amplify the explanation provided during the meetings (trans-
   cript at pp 27,28) we are providing below the results of a sample
   fatigue analysis, conducted in accordance with Appendix XIII, Article
   1153, Shakedown Analysis, for the 4-inch Sch 160 pipe.

   The alternating stress, S_{alt}, is given by

   $$S_{alt} = \frac{Ke\ Sn}{2}$$

   where Sn is the peak stress which equals 64.16 KSI when the effect
   of preload is included, and Ke is the simplified elastic/plastic
   damage factor. The latter is given by the equation

   $$Ke = 1 + [(1-n)/n(m-1)] [(Sn/3Sm)-1]$$

   where for the material in question, m=1.7, n=0.3, and 3Sm=50.52/ksi

   $$Ke = 1.9$$

Exhibit 1

EBASCO SERVICES INCORPORATED

BY M. Zupesky DATE 10/22/84

CK'D. BY _____ DATE _____

SHEET ____ OF ____

OFE NO. _____ DEPT. NO. ____

CLIENT TUGC

PROJECT Comanche Peak

SUBJECT Temperature in 10" carbon steel pipe U-BOLT Assembly

pipe at 250°F without insulation contact at the top
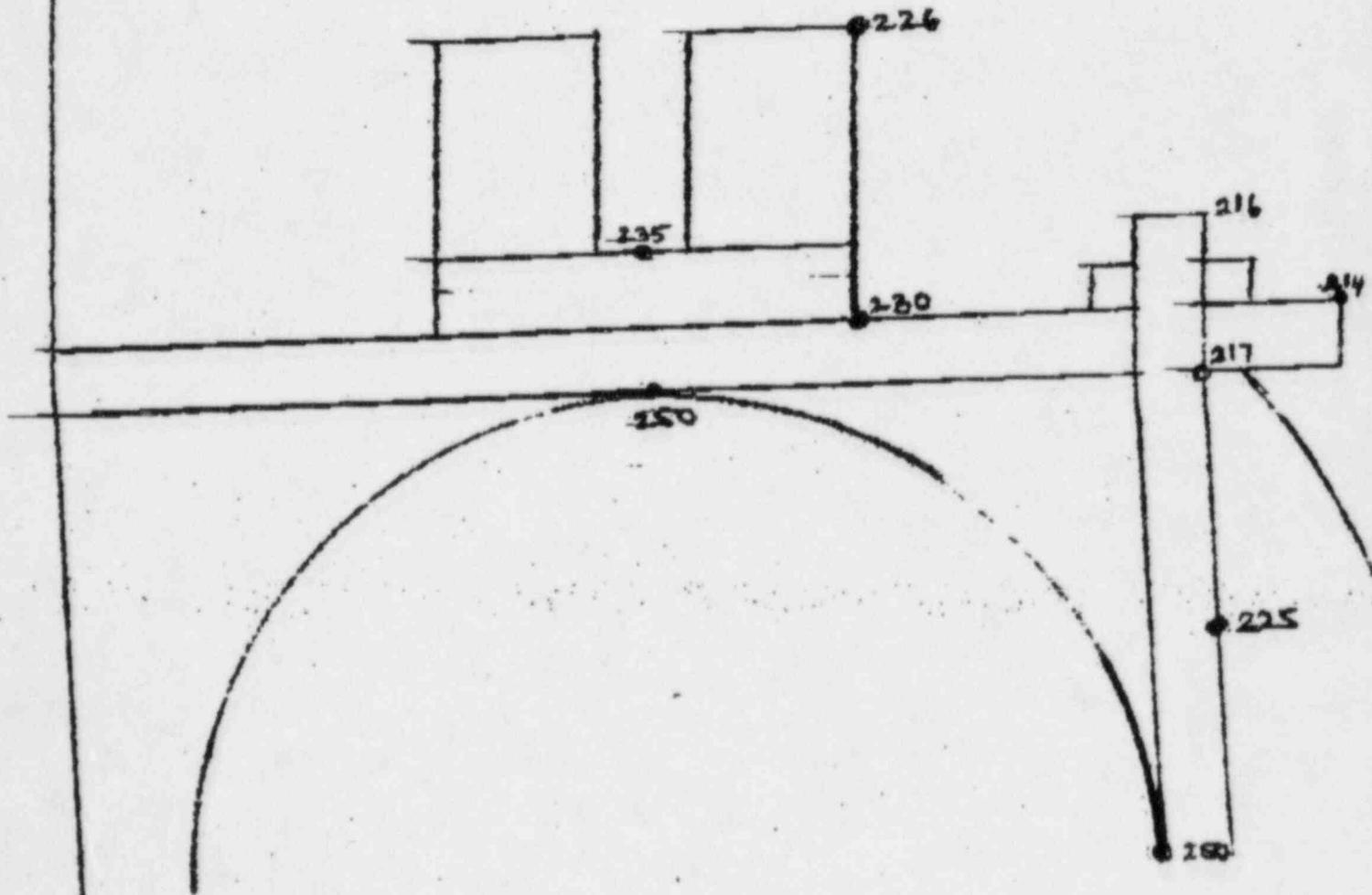
BY M. Zuposky DATE 10/22/84

CHKD. BY ___ DATE ___

SHEET ___ OF ___

OFS NO ___ DEPT. NO ___

CLIENT TUGC

PROJECT Comanche Peak

SUBJECT Temperature in 10" carbon steel pipe V-BOLT Assembly

pipe at 250°F without insulation

no contact at Top

M. Zupersky DATE 10/22/84   SHEET _____ OF _____

CHKD. BY _____ DATE _____   OFS NO _____   DEPT. NO _____

CLIENT ___ TUGC

PROJECT Comanche Peak

SUBJECT Temperature in 10" carbon steel pipe V-BOLT Assembly

pipe at 350°F with 2" insulation
contact at the Top

.EBASCO SERVICES INCORPORATED

Exhibit 4

BY M. Zurosky DATE 10/22/84

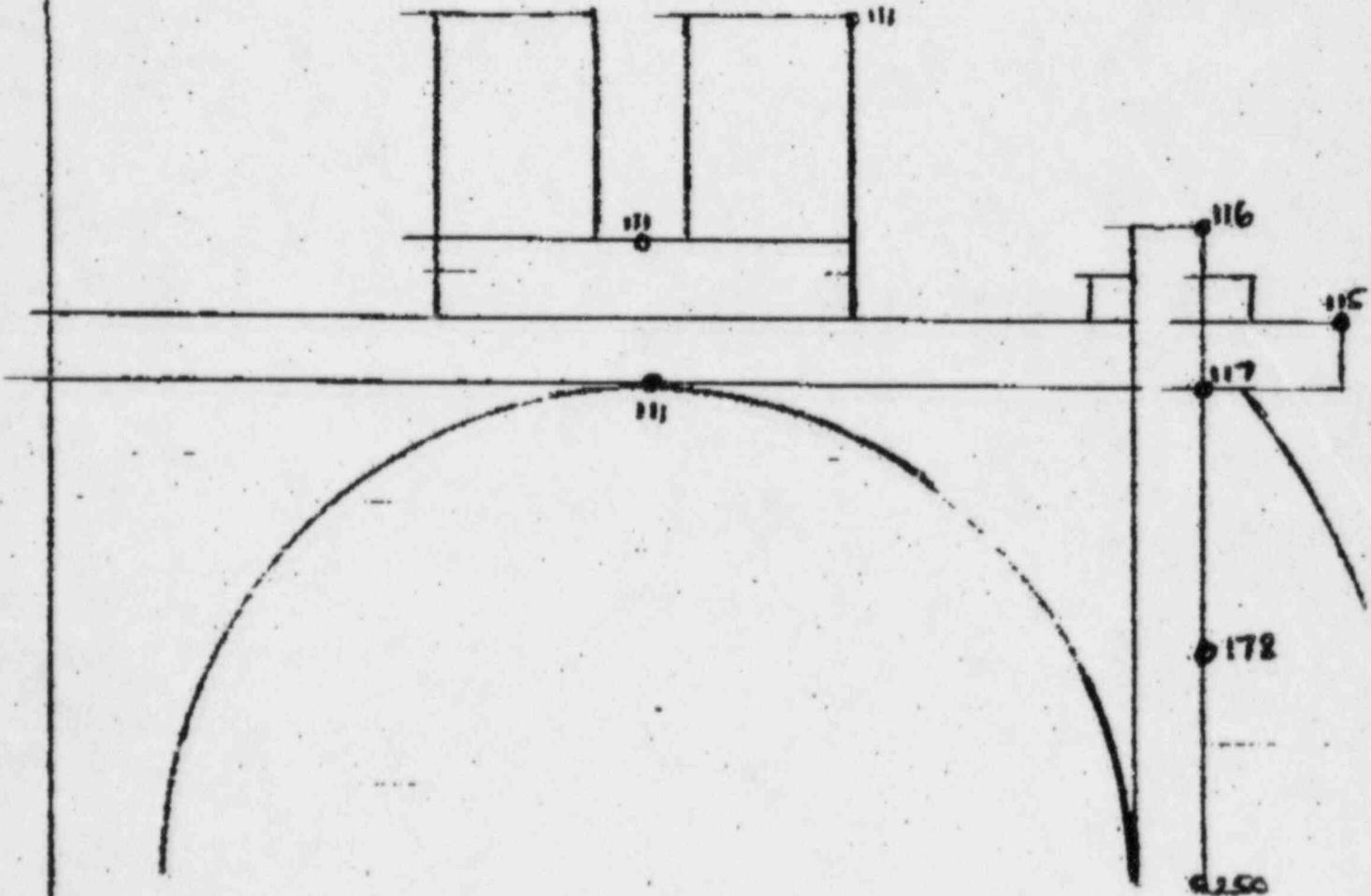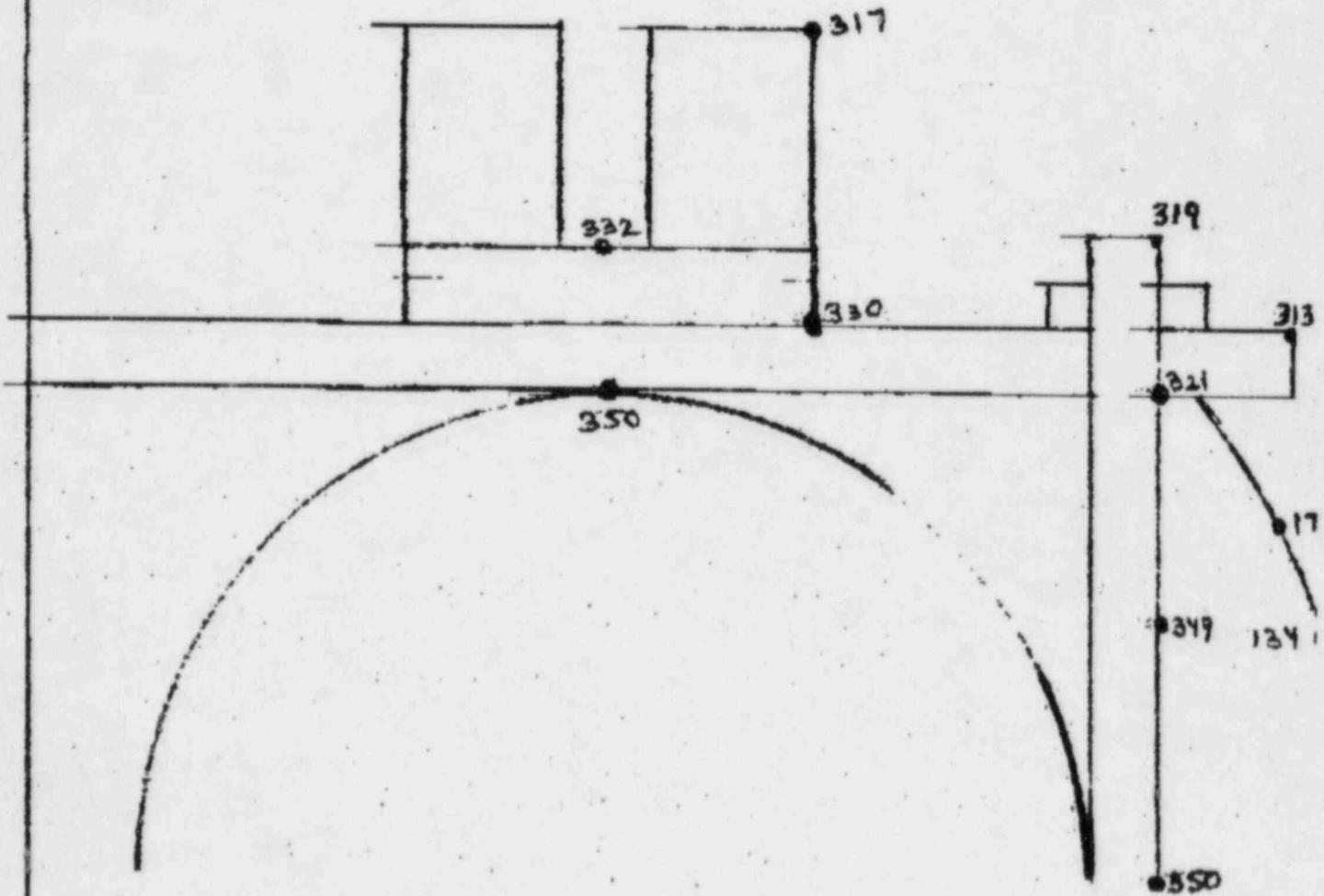CHKD. BY _____ DATE _____

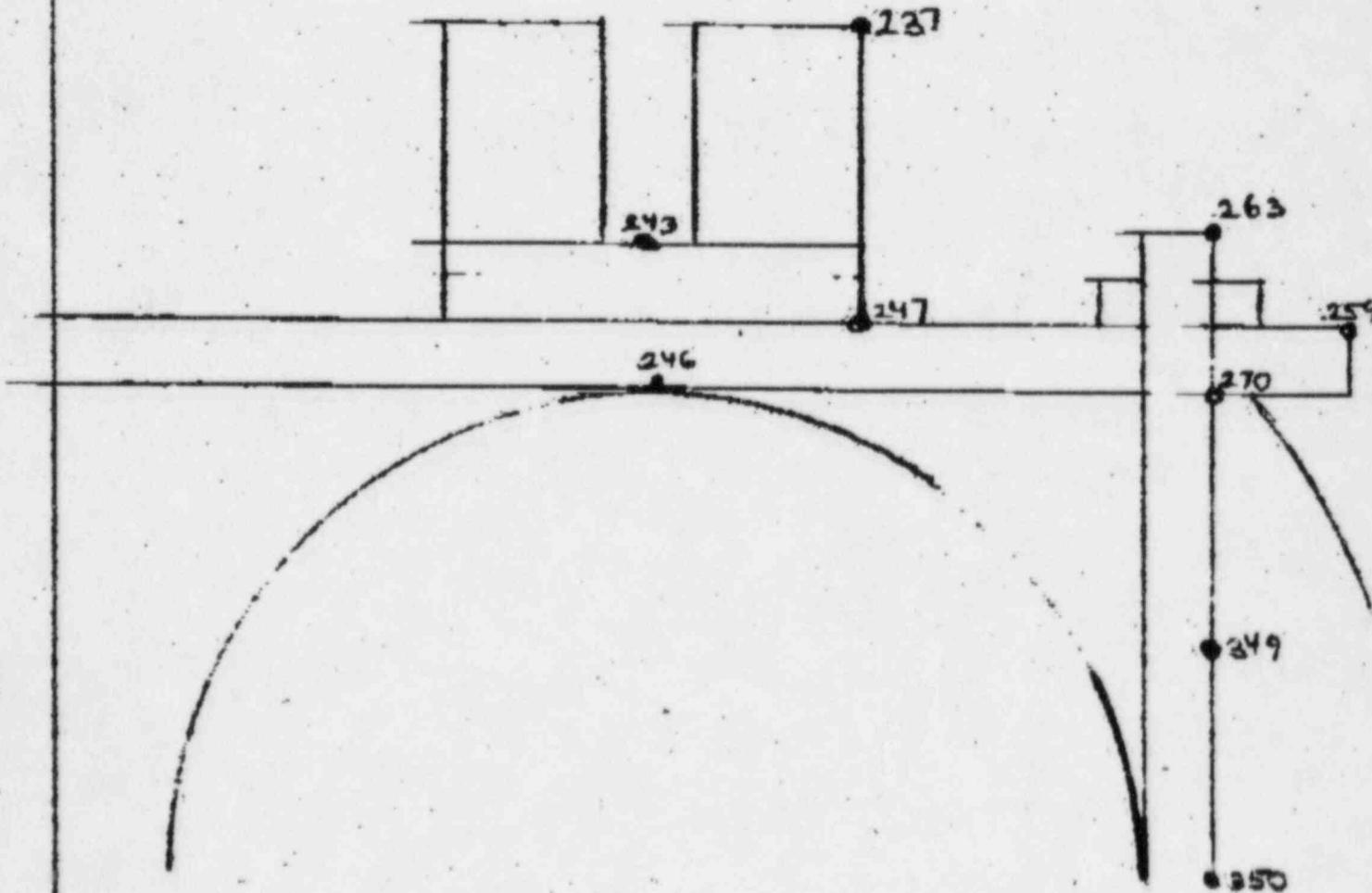OFG NO _____

SHEET ___ OF ___

DEPT. NO ___

CLIENT TUGC

PROJECT Comanche Peak

SUBJECT Temperature in 10" carbon steel pipe U-BOLT Assembly

pipe at 350°F with 3" insulation
no contact at the Top

Exhibits

1-19-84   10" SS Pipe #4 U Bolt / #4 Goosepiece

Thermal Cycling / Thermal Gradient

Ch O Pipe temp.   U Bolt @ 100 ft lbs

Cycle #6

Ch O Pipe temp.	93.7	201.9	250.2	248.9	249.7	250.4	251.2
1 5/8 20327 -1	23032	22930	23050	23027	23025	23028	23025
-4	22743	22292	22290	22267	22266	22263	22265
-8	22538	22567	22568	22550	22550	22550	22555
-11	23261	23276	23266	23242	23240	23248	23240
-12	21949	22000	22000	21980	21979	21976	21973
1/16 #6	79.6	89	106.1	126.2	136.1	140.5	143.7
		836		1551		1690	1591

CYCLE #7

PIPE TEMP.	94.5	201.7	251.7	249.0	249.8	250.8	250.6
20327 -1	23030	23050	23045	23012	23015	23011	23010
-4	22257	22290	22290	22265	22265	22264	22267
-8	22532	22563	22565	22545	22548	22547	23554
-11	23252	23270	23265	23245	23237	23245	23235
-12	21950	21998	22005	21982	21976	21976	21975
	70.5	89.5	99.7	126.8	135.7	140.7	144.3
		1721		1746	30	1:07	3:60

The conditions which permit usage of the procedure above are all satisfied. Namely

(a) The stress range excluding thermal bending stresses is within 3Sm. As previously discussed with CYGNA, this stress range is approximately 35 ksi and hence within 3Sm.

(b) The temperature is well below 800°F.

(c) The material has a ratio of specified minimum yield strength to specified minimum tensile strength of 0.8.

(d) The maximum allowable thermal stress condition of Appendix XIV, Article 1410 is satisfied since in this instance y' = 175 ksi for x = 0.16.

The alternating stress S_{alt} is then equal to 60.95 ksi.

For this alternating stress, the allowable number of cycles is approximately 8000 (see Code Figure 1-9).

CYGNA provides no indication of how many cycles of preload should be considered, and we have already stated our position that preload should not be considered a load that is cyclic in nature. In any case, even if we consider that the 200 cycles, used in our Affidavit at p. 71, are still applicable to the case with preload, the incremental usage factor is

$$U_e = \frac{200}{8000} = 0.025$$

which again indicates that the integrity of the pressure boundary, based on fatigue considerations, would not be significantly affected by the localized U-Bolt effects, regardless of whether the preload is considered as a cyclic or a non-cyclic load.

Finally, we question the choice of words used by CYGNA in regard to the first alternative chosen by Applicants to assess the acceptability of stresses in the pipes.

We do not understand what CYGNA intends when it states that "it doesn't find sufficient justification for the use of 3Sm for primary stress limits." Applicants have clearly stated that this is one of the alternatives used in lieu of direct guidance by the Code and that the use of a 3Sm limit is prompted both from inference from the Code (see footnote 23 of Affidavit at p.54) and the fact that the preload stress has some of the characteristics of a secondary stress, with a preponderant portion of thestress being due to a bending component (Affidavit at 53). We do not understand what additional justification CYGNA would want. Dr. Bjorkman himself has stated that he would consider 3Sm to be the proper allowable for cinching alone and also cinching plus thermal (Tr. at 12996). If CYGNA has justification for not using 3Sm, then CYGNA should state such justification. Otherwise, we are at a loss for replying to a question which we do not understand.

2. Q. CYGNA Question 4 (transcript page 32)
        Re: Use of 250°F for 10" Pipe

        CYGNA has reviewed the thermal operating data for the RHR systems
        and has found that the inlet and outlet to the RHR heat exchanger
        can be at 350°F. This can occur under-normal (inlet) or upset
        (outlet) conditions, both of which must be included in any analysis.

        Please justify that the preload and stress levels due to a 350°F
        insulated pipe are similar to a 250°F uninsulated pipe.

    A. The answer to this question is best provided by first restating
        that the choice of 250°F for the 10-inch pipe temperature is a
        compromise choice which bounds the majority of the systems in the
        plant, and where used with an uninsulated U-bolt configuration is
        also representative of the case where the pipe temperature may be
        350°F but the U-bolt configuration is insulated.

        Second it is important to point out that there is a single cinched-
        up U-bolt which is used on the 10-inch portion of the RHR system.
        This is support RH-1-024-007-S22R which is on line 10-RH-1-24-601-4-2,
        which is connected to the outlet line of the RHR heat exchanger. The
        maximum normal temperature seen by the line is 280°F during initiation
        of RHR operation. Only under upset conditions, when component cooling water
        may be lost, can the maximum temperature of this line reach 350°F.
        There are no cinched-up U-bolts on the inlet side of the RHR heat
        exchanger.

        Third it is germane to point out that the tests conducted on the
        10-inch pipe specimens had a corresponding average temperature of
        the U-bolt equal to approximately 150°F.

        The 150°F is not necessarily the equilibrium temperature of the
        U-bolt, but the temperature reached by the U-bolt during the thermal
        cycle which required approximately 20 minutes to heat the pipe to
        250°F. Finite difference thermal analyses indicate that depending
        on the extent of contact of the pipe with the U-bolt and backing
        plate (there would be contact for a cinched-up U-bolt) the average
        temperature in the straight legs of the U-bolt may range from 175-
        180°F for little or no contact to 225-230°F for well established con-
        tact, when the U-bolt is uninsulated and the pipe wall temperature is
        at 250°F. The U-bolt portion in contact with the pipe would be es-
        sentially at 250°F. For a 350°F pipe with an insulated U-bolt con-
        figuration the corresponding U-bolt average temperatures in the
        straight legs would be about 310°F for the case of poor and good
        contact. The curved portion would be at 350°F in either case. Re-
        sults of the heat transfer analyses are shown as exhibits 1 through 4.

        The effect of the temperature rise on the clamping forces acting on
        the pipe and the U-bolt for the two cases of 250°F pipe, uninsulated
        U-bolt and 350°F pipe, insulated U-bolt, can be estimated by comparing
        the relative growth of the pipe to U-bolt for the two cases, neglecting
        any deformation of the pipe. Since only relative growth is pertinent
        here, the one-directional growth of the U-bolt due to thermal expan-
        sion given as Y_1 where

$$Y_1 = \alpha \Delta TL$$

where L is the projected length of the U-bolt which is given as 2R
and ΔT is the temperature differential between the average U-bolt
temperature and ambient (or a reference temperature), is compared to
the diametral growth of the pipe, Y_2, which is given as

$$Y_2 = \alpha_2 \Delta TD$$

The worst case relative expansion will occur for the stainless steel
pipe and the carbon steel U-bolt. For the 10-inch pipe (10.750D),
coefficients of thermal expansions $\alpha_1 = 6.4 \times 10^{-6}$ in/in/$^{\circ}$F at 180-
230°F or 6.65×10^{-6} at 310-350°F and $\alpha_2 = 9.4 \times 10^{-6}$ at 250°F or
9.53×10^{-6} at 350°F and a reference ambient temperature of 70°F, the
relative expansion for the two cases considered, i.e., 250°F pipe
with bare U-bolt, and 350°F pipe with insulated U-bolt are as follows,
where Case a refers to the instance of good contact between the pipe,
the U-bolt and the backing plate (as would generally be the case for
cinched-up U-bolts) and Case b refers to the instance of poor contact.

1. 250°F   Case a: y = 0.00666 in.   Case b: y = 0.00838 in.

2. 350°F   Case a: y = 0.00920   Case b: y = 0.101 in.

3. 250°F   Test: y = 0.012   Finite El. An.   y = 0.0141*

(* Finite Element Analysis used 210°F)

As seen from the above, theoretical steadystate heat transfer analyses
would predict that the case of 350°F pipe expanding against an insulated
U-bolt could result in a differential pipe expansion which would be ap-
proximately 30-40% larger than could be expected for a 250°F pipe with
uninsulated U-bolt. However, both the tests and the finite element
analyses have been conducted in a manner that would encompass the case
of 350°F, insulated U-bolt. As seen from the third row of relative
expansions, both the test (by having a maximum U-bolt temperature of
150°F) and the finite element analysis, which used a pipe temperature
of 210°F but maintained the U-bolt temperature at 70°F, would yield
relative expansions which are significantly larger.

Another point to be discussed, is that the test has provided informa-
tion on the transient thermal expansion differential between the pipe
and the U-bolt. As seen from a sample of the raw data which is at-
tached as Exhibit 5, the maximum temperature differential between the
pipe and the U-bolt occurred when the U-bolt had reached a represen-
tative temperature of about 100-105° while the pipe had been heated to
250-255°, a difference in temperature of approximately 150°F. This
difference is well simulated in the finite element analysis where a
constant difference in temperature of 140°F. It should also be re-
membered that for these temperature differentials, the amount of
stress caused by the thermal expansion is not very significant.

3. Q.   CYGNA Question 9 (transcript page 130)
        Re: G&H Sample Size for Piping General Stresses

        TUGCO has committed to provide data on the size of the Gibbs & Hill
        sample (transcript page 130).

3. A. The sample size taken by Gibbs & Hill is given in Table 3 of our
        Affidavit. That table includes all of the stress problems reviewed
        by Gibbs & Hill to provide random information to judge the adequacy
        and conservatism of Westinghouse's method of determining maximum
        piping moment stresses in straight sections.

        It must be born in mind that this was the only purpose of the Gibbs
        & Hill review. The purpose was not to determine what the maximum
        straight pipe stress is per pipe size.

4. Q. CYGNA Questions 6, 12, 18, and 19
        Re: CYGNA Question 6

        CYGNA has not received the A-36 steel stress relaxation graph and
        published report on stress relaxation (transcript page 77) nor a
        copy of TU CO's answer to the NRC on this issue (transcript page
        81). This information is necessary to complete our reviews.

    A. The TUGCO's answer to the NRC on this issue has been submitted on
        September 24, 1984 and a copy should have reached CYGNA. In any
        case, we are summarizing below the pertinent portions of the an-
        swer, i.e., that relating to the A-36 stress relaxation.

        There is scant data available on strain relaxation properties of SA-
        36 material. Some relevant data is reported in ASTM DS60 "Compilation
        of Stress-Relaxation Data for Engineering Alloys," for material hav-
        ing the same composition as SA-36 steel (note that this reference
        does not mention the material designation). Unfortunately not much
        data is available directly at the temperatures of interest, i.e., less
        than 500°F although considerable information may be inferred from the
        data at the higher temperatures as will be discussed later. In fact,
        only materials 2 and 25 have data at room temperature. Material 2
        has the proper chemical composition but its physical properties are
        significantly different from those of A-36. Material 25 has physical
        properties similar to A-36 but does not quite meet all

of the chemical specifications. Figure A1 shows the stress strain curve of material 25 at various temperatures within our range of interest, i.e. less than $500^\circ F$. This curve is used to illustrate the meaning of material relaxation (as opposed to overall mechanical relaxation which will be discussed later) for monotonic loading, i.e. noncyclic. For the material to relax, plastic strain is required. Ferritic steels like A-36 exhibit a well defined proportional limit at which plastic strain begins. The yield strengths of these materials are given at the 0.1% or 0.2% elastic strain offset (in general it is the latter, although for material 25 the former is used). In figure A1 the details of the stress strain curve between the proportional limit and the yield point are not shown. From that figure, if the material is strained below the proportional limit no material relaxation will occur. Strains in excess of the proportional limit will result in relaxation, the amount of relaxation being proportional to the amount of plastic strain (or volume of material that has yielded). At room temperature the strain corresponding to the proportional limit is about 0.075 percent. At that level of initial strain, therefore, little or no relaxation should be expected. Figure A4, developed using the information on Material 25 of ASTM DS60, shows that the relaxation is negligible. At $532^\circ F$, the strain corresponding to the proportional limit point is 0.065 percent. Since the material 25 has been strained to .075% relaxation should be expected. Moreover, the heating of the material from room temperature to $532^\circ F$ and the return to

room temperature contributes to relaxation. How this happens is explained by Figure A2, obtained via private communication with M.J. Manjoine, one of the authors of ASTM DS60 and a recognized authority in materials behavior. This figure is an expanded view of a portion of Figure A3, also provided by M.J. Manjoine. Figure A3 deduces the behavior of ferritic steels like A-36 at the lower temperatures from the fact that the behavior exhibited at the higher temperatures (above $700^{\circ}F$) for which the data is available is the same as that exhibited for mild austenitic steels which have data available at all temperatures. The behavior of austenitic steels is shown in figure A7 which is taken directly from reference 4 (see p. 27). As figure A2 shows a material which is strained to or above the proportional limit will lose load at constant strain simply as a result of the lower yield strength at temperature and the higher modulus of elasticity at room temperature than at temperature. Thus, if material 25 had been strained to yield at $532^{\circ}F$, upon its return to room temperature it could exhibit 35 percent of its initial stress. This would occur upon return to room temperature regardless of whether "material" relaxation occurs. If the material is maintained at temperature, loaded for sufficient time, material relaxation would also occur. This can lead to an additional 15-20 percent loss of load. However, for the latter time is needed to redistribute the load. Although we do not know for a fact, it is fairly obvious that the material relaxation characteristics of material 25 at $532^{\circ}F$ must have been determined

at temperature, since as figure A4 indicates, there is some twenty percent relaxation. Similar significant strain relaxation should be expected at all temperatures for initial strains of 0.225 percent, and this is indeed the case.

If the applied load results in a stress below 1/2 of the yield strength at temperature, the corresponding strains would be well below those corresponding to the proportional limits, and thus no relaxation should be expected.

So far only monotonic loads have been discussed. To complete the discussion of material relaxation, it must be pointed out that the stress strain curve for steels are different between the cases of monotonic and cyclic loads. For the monotonic loads discussed so far, the point at which mild ferritic steel materials begins to yield is higher (by approximately 15 percent - private communication with M.J. Manjoine) than the point at which yielding will occur under cyclic loads.

The difference is shown in Figure A5.

It is important that a distinction be made between "cyclic" loads such as are experienced by the U-bolts, whereas the load can be cycled from a low to a high level without stress reversal, and "stress reversal" loads which are cyclic but for which the load causes the stresses to be alternatively tensile and compressive. The relaxation behavior for the two cases can be vastly different. Figure A8 (reference 5) shows that stress strain curve for ferritic steel under reversing constant

amplitude loads (reversing strain). Figure A9 (reference 6)
shows an idealized curve for the kind of mild steel which is
characteristic of both ferritic steels like A-36 and austenitic
steels like A-304. Figure A10 (reference 6) shows the static
(monotonic) stress strain curve and the cyclic (strain reversal)
curve for a material like A-36. The cyclic curve is the envelope
of the stress-strain curves exhibited during the cycling as shown
by the dashed line of figure A9. It is important to compare the
type of relaxation which one can experience under cyclic loadings
with no strain reversal to those which can be experienced for the
latter. To do so we will utilize Figure A11, (provided by M.J.
Manjoine), which combines both types of loadings. In the case of
cyclic loading with no strain reversal, the second cycle will
have a proportional limit PL1 which is about 15 percent lower
than the monotonic proportional limit. However, if the cyclic is
one of relatively large strain reversal (i.e., strains near yield
here defined as .2% offset), then the proportional limit will be
much lower as indicated by point PL2 in the figure.

For strain reversal conditions, according to Mr. Manjoine
there is little difference between the stress strain curve of
ferritic steels like SA-36 and austenitic steels like SA-304.
Thus, the material relaxation properties of SA-36 can be inferred
for cyclic loads from those of SA-304 for which considerably more
data is available.

Figure A6, reproduced from ASTM-DS60 (reference 4) shows the relaxation behavior of SA-304. It can be seen that for cyclic loading with strain reversal there can be always some material relaxation, but that for stresses below $1/2\sigma y$, the amount of relaxation is minor.

Material relaxation, however, is only one of the parameters of interest in the overall relaxation of the U-bolt assembly. Relaxation of the assembly preload can be due to a combination of material relaxation and other mechanical relaxation phenomena that may manifest themselves during the various loading cycles, such as wear, local yielding with load redistribution, etc.

It is difficult to predict the amount of relaxation that might occur as a result of wear or yielding of surface irregularities. It is for that reason that the long term, accelerated vibration test was conducted, i.e., to simulate the number of cycles that the assembly would see during its entire lifetime of operation. It is possible, however, to estimate the amount of mechanical relaxation that takes place due to local yielding, although it is impossible to tell how quickly it will occur since the time required for load redistribution depends on too many factors. Such overall estimates can proceed from a knowledge of the stress state at each location of the assembly, which permits an estimate of the volume of material that might be at yield. This volume of material will relax over time, redistributing load, and giving the appearance that the overall assembly relaxes. It is germane to estimate what amount of

relaxation could occur when the shank of the U-bolt is stressed to a maximum stress of 1/2 yield strength. At such loads there are portions, however small, of the assembly which experience higher stresses and can in fact be at yield. These regions are shown in Figure A12 as points A, B, C, D and E. Points A, B and C yield at the outer fibers when the U-bolt is cinched up and preloaded to relatively low value of loads as a result of straightening the U-bolt legs. Yielding is, however, limited to the outer fibers near and opposite the pipe, and the material which yields occupies negligible volume.

For consistency with future discussion of Westinghouse test data, we will use a yield strength of the material of the U-bolt equal to 36,000 psi, even though actual material yield is about 45,000 psi. Test results obtained by strain gauges have all been referred to the 36,000 nominal yield strength. When the stress in the shank is equal to 1/2 the yield strength in the U-bolt shank area, for instance for the 10-inch assembly (refer to Attachment 1 to the Affidavit) with the 3/4 inch U-bolt, the corresponding load is 7,956 lbs., which gives a threaded area stress in excess of 1/2 of yield, i.e., 23,820 psi. However, as figure A13 indicates, the nut engagement results in stress concentration within the threaded area. Stress concentration can raise the average stress above yield. Since we have two nuts, a similar stress concentration profile will exist in the bolt within the other nut because of the nut engagement to the first one. For the 3/4-inch bolt, the nuts are 5/8 inch thick with six

threads. Approximately half of the bolt volume within both nuts will have stress concentration in excess of 1.5. Thus, a total length of 5/8 inches will have stresses at or close to yield.

The same is true in the other leg of the U-bolt. Thus, about 1.25 inches of material out of a total of 31 inches will experience relaxation of the order 15 percent (relaxation from yield stress - see figure A2) if at room temperature. The remaining threaded area (approximately 5 inches) will experience less relaxation since it is more lightly stressed. The amount of relaxation that it can experience can be estimated using figure 2, suggested by M.J. Manjoine. This additional threaded material would relax approximately 7.5 percent. Thus, one can approximate the overall mechanical relaxation that would occur for loads resulting in stresses in the shank of one-half yield as

$$\frac{5\ (.075) + 1.25\ (.15)}{3.25} = 1.7\%,\ \text{or very low relaxation.}$$

Perhaps more relevant than theoretical calculations to the question of when overall (material and mechanical) relaxation ceases for the U-bolts, is the actual data taken during the various tests conducted by Applicants (see reference 1). One such test is the thermal cycling test.

Results of the thermal cycling test on the 4" Sch 160 stainless steel specimen indicated that the stress in the U-bolt was approximately 31,100 psi (or approximately 86.4% of the assumed yield strength of 36,000 psi and essentially equal to the cyclic yield strength). The total material would thus relax.

After nine cycles the residual stress was measured to be approximately 19,900 psi or 55 percent of the assumed yield strength. (Ambient temperature for pipe and U-bolt was essentially the same before cycling (105°F) and just before the 10th cycle (107.5°F). The U-bolt was heated to an average temperature of about 400°F (see page 16 of Attachment 3 to the Affidavit). From Figure A2 one can deduce that the temperature cycling would result in a relaxation of approximately 36 percent, of which the initial 25 percent would be due to the temperature cycling alone. The result of the thermal cycling test does in fact confirm that the room temperature stress before the thermal cycling, i.e., a nominal 31,100 psi, was reduced to 19,900 or a 36 percent reduction.

Another test which provides insight on the stress relaxation is the creep test which was performed immediately after completion of the thermal cycling test, without retorquing the bolts.

For the 4-inch specimen the microstrain measured in the two U-bolt legs at the ambient temperature before the creep test (77°F) were 856 and 775 microstrain for legs 1 and 2 respectively. (These microstrains correspond to a load of 4,870 and 4,409 lbs.) After the creep test with the ambient temperature being 91.4°F, the strains were measured to be 853 and 773 microstrain, respectively. When one accounts for the fact that at 91.4° there is a preload induced by the difference in thermal expansion between the stainless steel pipe and the carbon

steel U-bolt, and that had the ambient temperature returned to $77^\circ F$ the preload would have been reduced by approximately 45 lbs., the final load at the completion of the creep test would be approximately 4,580 lbs. compared to 4,639 (or 1.2 percent decrease).

Since 4,580 lbs. corresponds to a stress of 23,367 psi (shank area), which is above 1/2 of the assumed yield strength of 36,000, this decrease, if real and not due to instrument uncertainty, would be due to the strain relaxation. The question of whether it may be due to creep is addressed in the answer to the next question.

For the 10" Sch 40 line, where the temperature is low (pipe $250^\circ F$ and U-bolt $150^\circ F$) creep is clearly not a concern. The strains measure prior to the creep test (after the thermal cycling test) were 283 and 280 microstrains respectively in legs 1 and 2 of the U-bolt (at an ambient temperature of $75.8^\circ F$). The initial microstrains correspond to a load of 3,625 and 3,578 lbs. respectively. These loads correspond to a stress equal to 8,200 psi in the shank or 10,800 psi in the thread area of the U-bolt. In either case the stresses are well below the 1/2 yield strength, with the exception of highly local area in the thread within the nut, and hence little, if any, relaxation should be exhibited.

The strains after the creep test were measured to be 281 and 276 microstrains respectively corresponding to an average load of 3,567 lbs.

The drop in load of approximately 39 lbs. is partly due to the lower environment temperatures after the test which was 66.9°F instead of 75.8°F.

The drop in load corresponding to the 9 degrees difference is calculated to be approximately 11 lbs. Thus, relaxation (if any) was less than 0.8 percent.

The seismic test provides further evidence of the relaxation phenomenon. Initial information provided from the test, which is attached as Exhibit A3, indicated a reduction in load from 4,484 lbs. in both U-bolt legs to about 4,291 lbs. and 4,355 lbs. in legs 1 and 2 respectively, when the assembly was vibrated at 9 Hz with a constant amplitude of 7,000 lbs. This relaxation of approximately 12 percent could not be justified on the basis of the applied load which would result, coupled with the initial preload of 4,484 lbs. (50 ft. lb. torque) in maximum load experienced by the U-bolt of approximately 6,100 lbs., and a corresponding stress of 18,200 psi in the threaded area and 13,800 psi in the shank area. This led to questioning the validity of the 7,000 lb. load, and to the realization that the actual applied vibratory load had been higher, and to the results published in the Affidavit, which are included here as Exhibit A4. As seen in the Exhibit, the actual load applied to the U-bolt was in excess of 10,000 lbs during the peak portion of the cycle and initially in excess of 8,600 lbs. during the pull portion of the cycle. On the average the force seen by the U-bolt during the cycling was in excess of 6,600 lbs. (peak load of

more than 8,600 lbs. plus preload of 4,484 lbs.) which would have resulted in a stress in the thread area of about 19,800 lbs. which is 11 percent higher than the nominal 1/2 yield strength, hence justifying the relaxation seen.

Finally, the data obtained during the long term accelerated vibration test merits some attention.

As stated in our Affidavit, the initial preload stress was equal to about 9,020 psi. After the initial reposition of the assembly which occurred approximately 5.15 minutes into the test (see attached raw data - Exhibit A5), and which resulted in an average loss of preload equal to 640 lbs, the preload was seen to decrease slightly, then increase again then decrease with a final preload being about 450 less than the preload existing after the initial adjustment. During the period of time between the 4th sweep (21 minutes) and the 36th sweep (189 minutes) there was essentially no change in the preload. At the latter time is when the sudden cocking mentioned in the Affidavit on p. 30 took place, which resulted in some further preload decrease.

Relaxation of the material discussed within the context of this reply does not change the total strain of the material. (See definition in 2 of Exhibit A2.) The preload at the end of the test is still sufficient to prevent loss of contact between the pipe and backing plate (see figures 17 and 18 of Attachment 1 to the Affidavit with an applied load of 1,500 lbs. and a preload of approximately 3,200 lbs.), thus the motion which resulted in further relaxation is most likely due to accumulated strain over

the more than 10^6 cycles experienced at an applied load of 1,500 lbs. These cycles represent the number that the support may experience during its lifetime, and hence the test results confirm that in spite of some relaxation, adequate preload would be retained throughout life.

Cyclic plastic strain accumulation may occur at these loads, which are abnormally high for the period of time tested. An elasto plastic finite element analyses of a similar U-bolt, backing plate, pipe arrangement, conducted per an 8-inch pipe (same size U-bolt as the 10" pipe, indicates that for sufficiently high preload, the U-bolt can experience some plasticity in the transition region between the straight shank and the curved portion and at the inner surface of the U-bolt apex. This occurs from the bending moment place on the U-bolt from the straightening action of the preload or full external load. This small amount of plasticity occurs even though the average stresses through the U-bolt cross section is low, and in fact, for the particular case examined are only 2,000 psi. Under the large number of cycles seen by the specimen the accumulated plastic strain can result in sufficient permanent deformation to permit relaxation. Also, wear and yielding of surface imperfections can accomplish the same thing.

Figure A1

Figure A2

$$\sigma_R = 0.7 \bar{\sigma_T} + 0.15 \sigma_{yT}$$

for $\bar{\sigma_T} > \frac{\sigma_{yT}}{2}$

$$\sigma_R = \frac{\sigma_{yT}}{2}$$

for $\bar{\sigma_T} < \frac{\sigma_{yT}}{2}$

ESTIMATED for A 36 CARBON STEEL

Figure A3

REF ASTM DS-60

A-36
LOW CARBON STEEL

σ_U (min spec)

STRESS, σ KSI

Expanded in Figure 2

σ_{yT}

σ_R for $\sigma_i = \sigma_{yT}$
$t > 1000 h$

$\sigma_R = f(\sigma_T, T, t)$

$\sigma_R \sim 0.75_T + 0.5 \sigma_{yT}$

INSIGNIFICANT RELAXATION
FOR LOWER STRESSES
(MONOTONIC LOADING)

10 h
100 h
10,000 h

TEMP. (T)

T_R/T_M

SIGNATURE M. MANJOINE   DATE 9-84   CURVE NO. _____
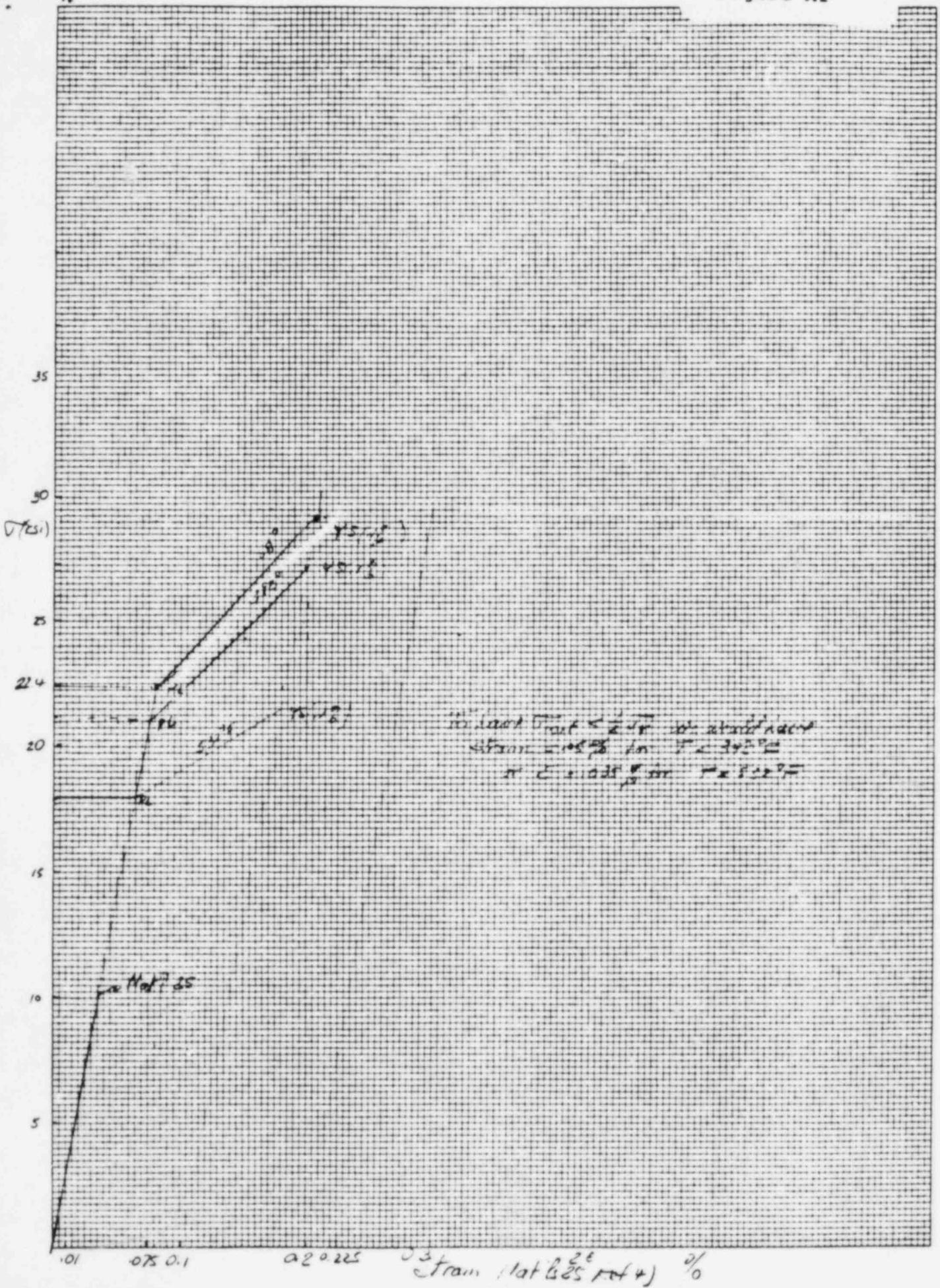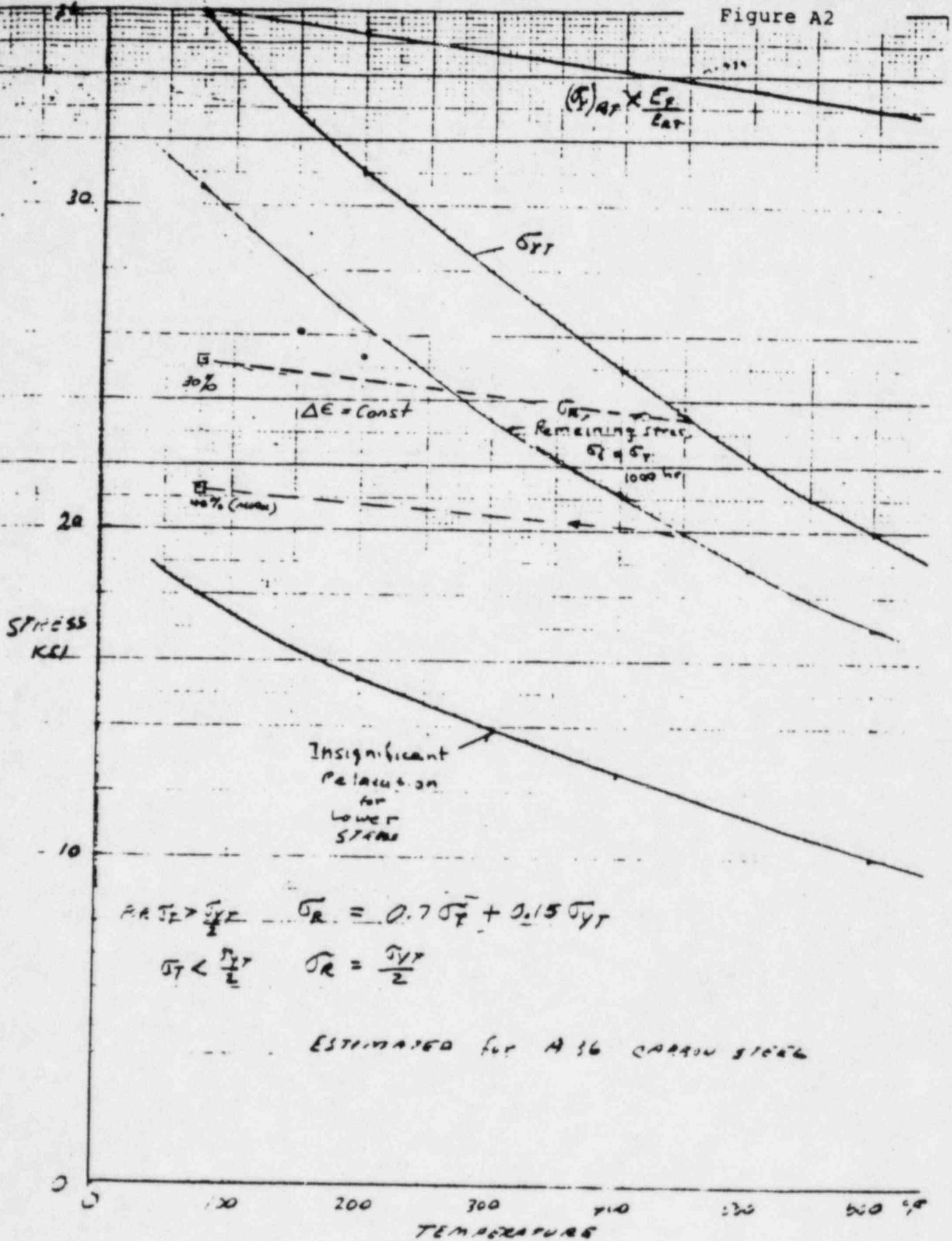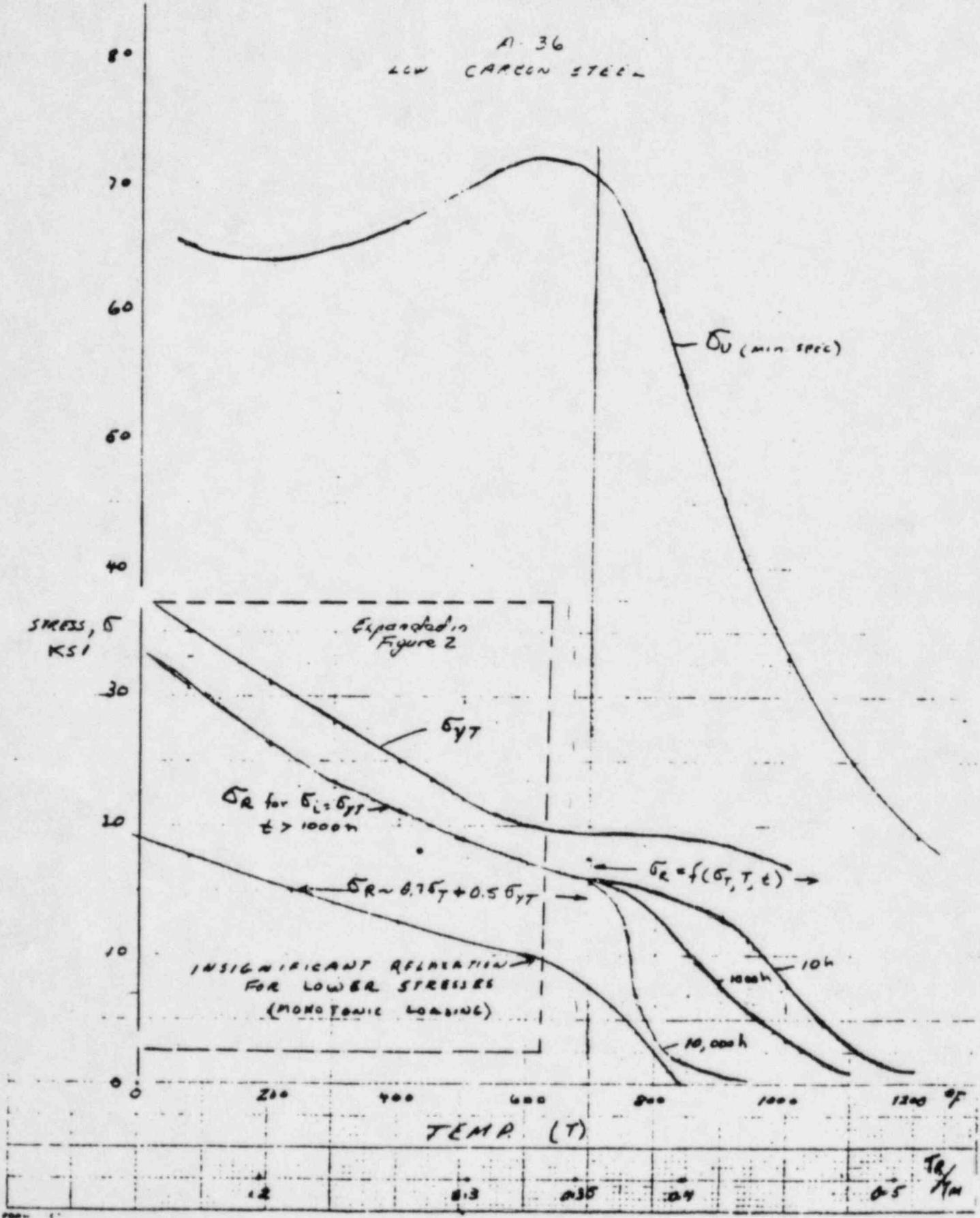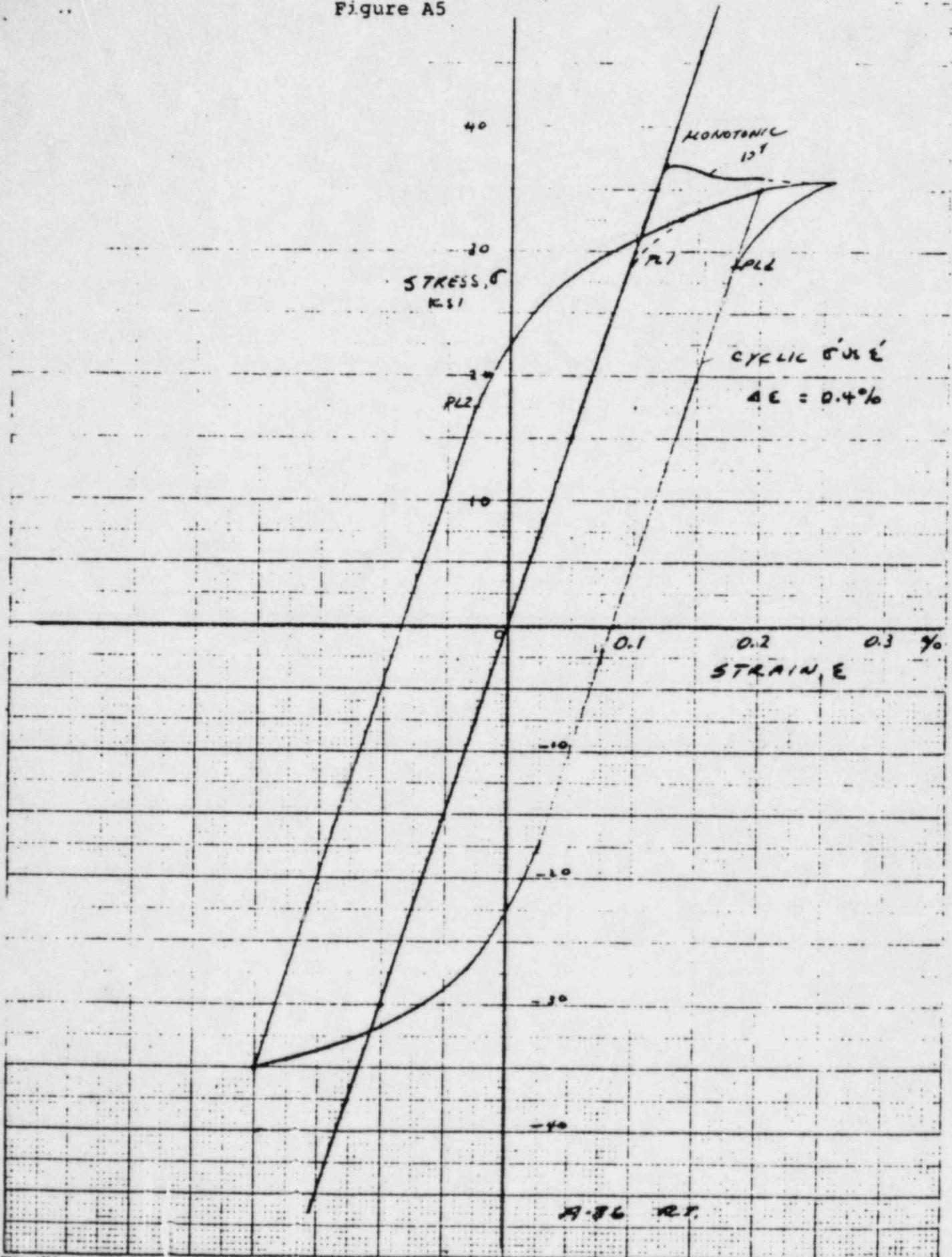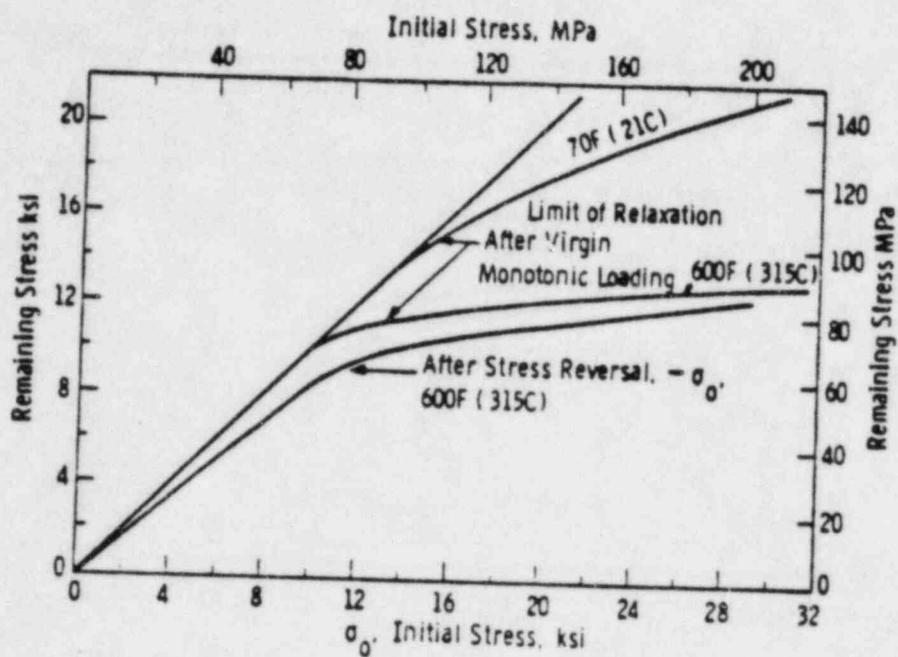
Figure A4

Figure A5

Fig. 2 – Relaxation of solution-annealed type 304 stainless steel
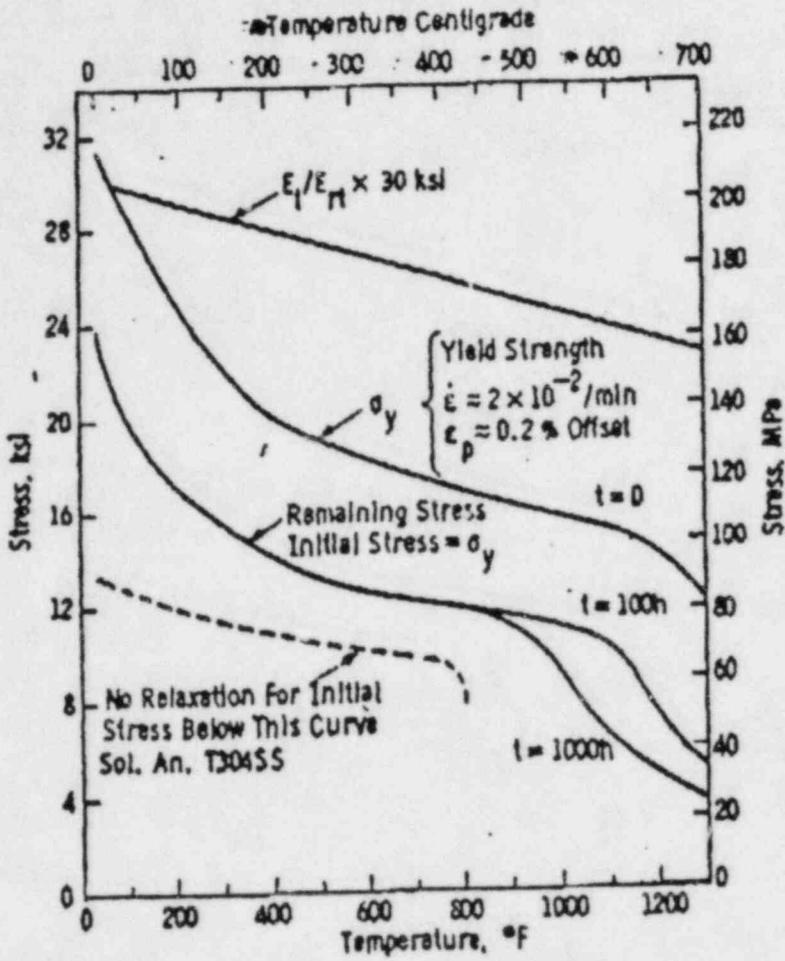
Fig. 4 — Remaining stress for an annealed type 304 stainless steel bar at constant strain as a function of temperature and time.
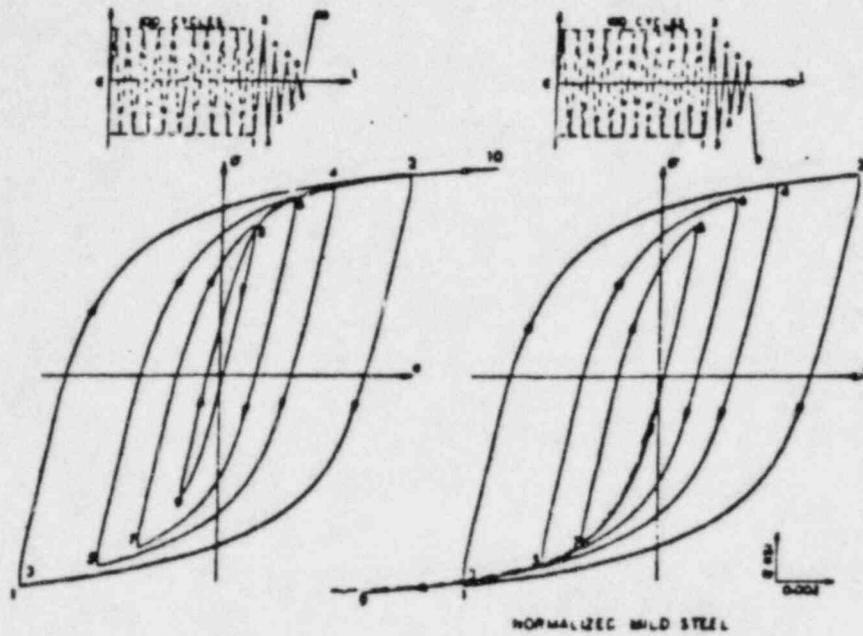
FIG. 7—Hysteresis characteristics of normalized mild steel
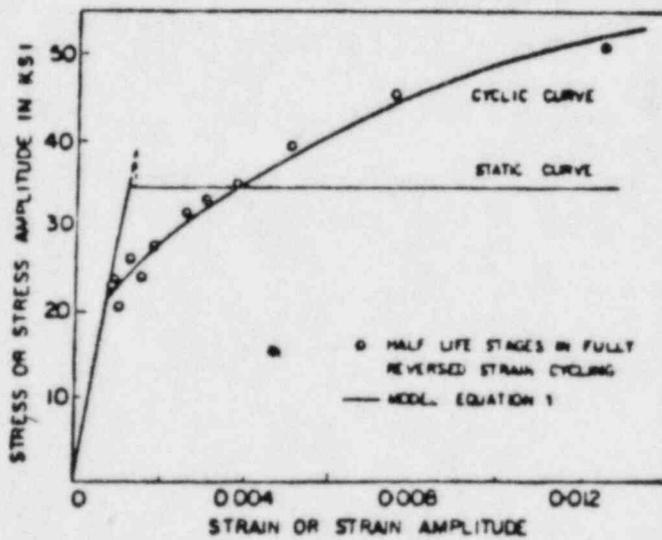
NORMALIZED MILD STEEL

FIG. 9—Static and cyclic stress-strain curves for normalized mild steel
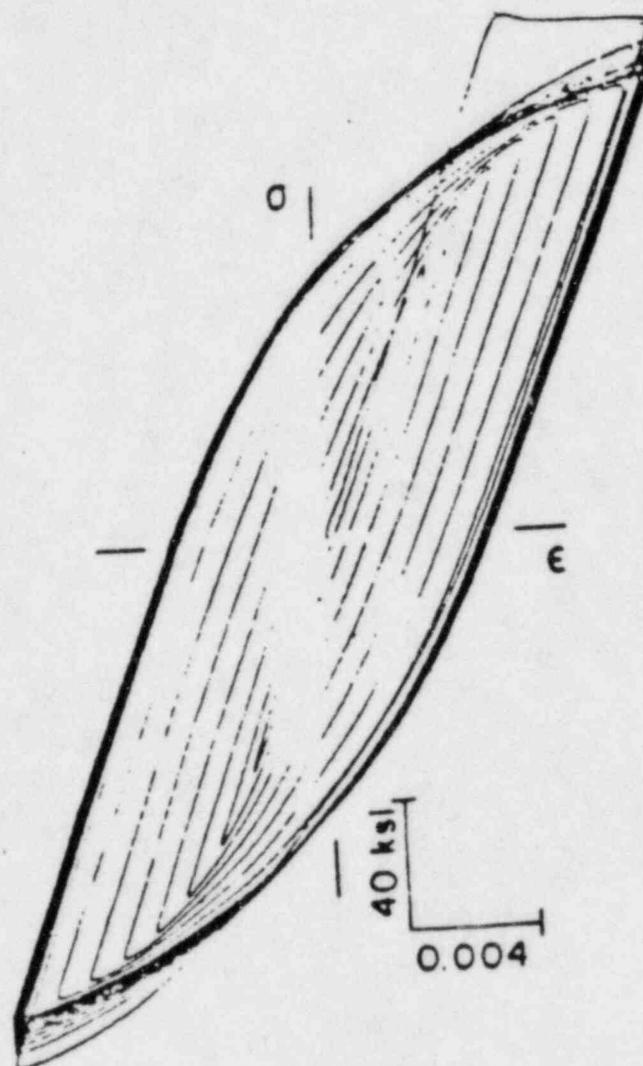
FIG. 4—Stress-strain after recording for initial overstraining

	σ_y	σ_{cy}	σ_u
A(108)	83	35	60
B(4130)	113	82	130
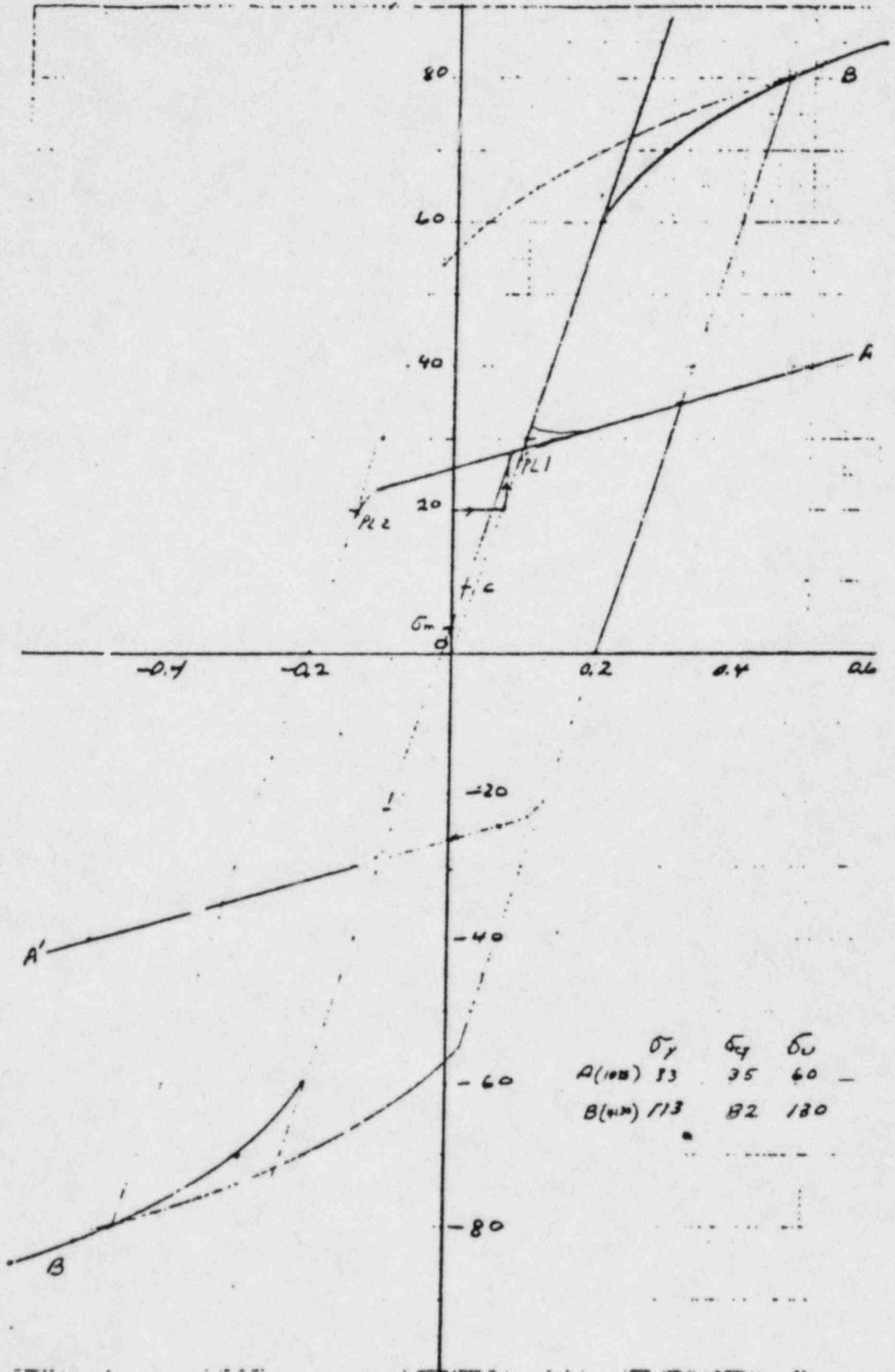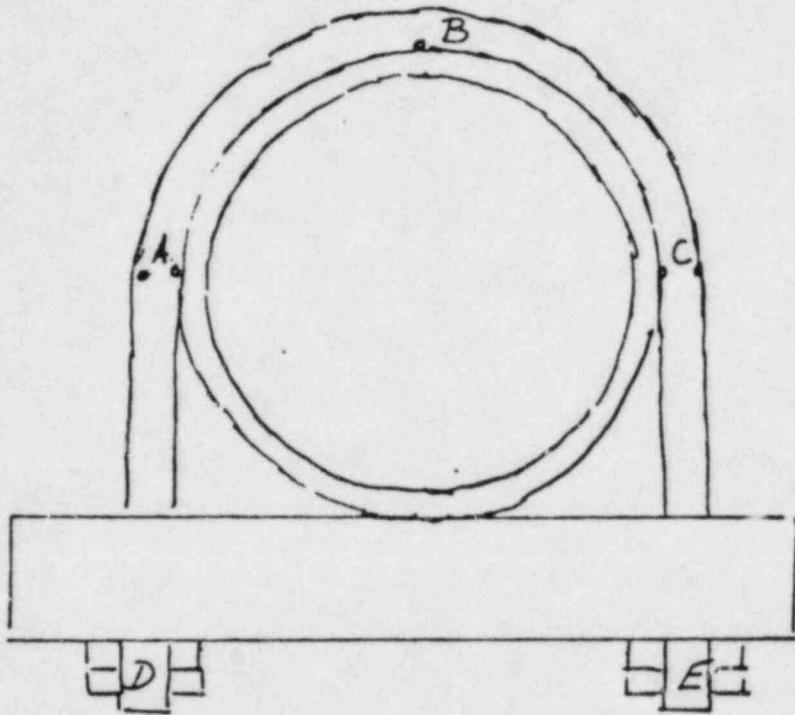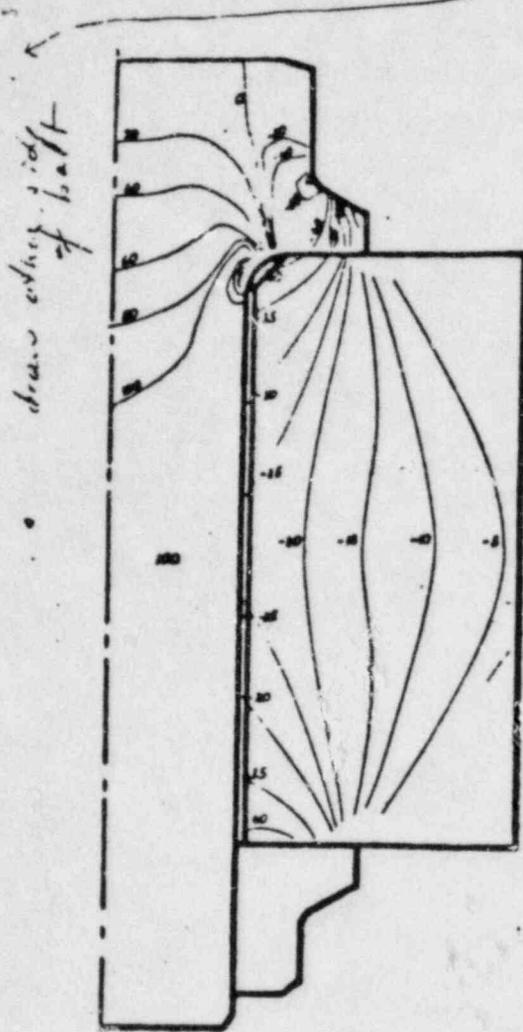
Fig Lines of equal axial stresses in a bolted joint obtained by the axisymmetric finite element method are shown for a 9/16 - 18 bolt preloaded to 100 KSI. Positive numbers are tensile stresses in KSI; negative numbers are compressive stresses in KSI.
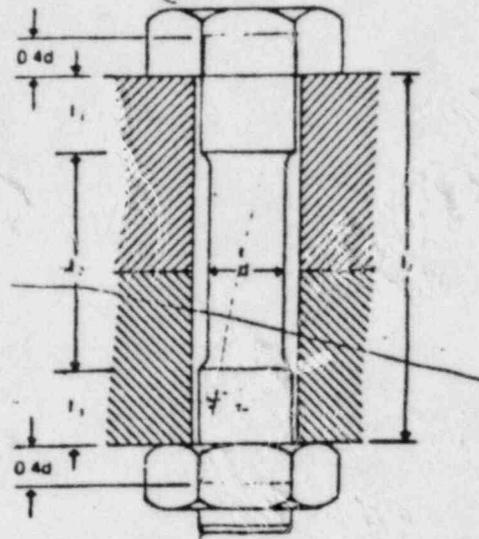
Fig Analysis of bolt lengths contributing to the bolt spring rate.

$$\frac{1}{K_B} = \frac{1}{K_1} + \frac{1}{K_2} + \cdots + \frac{1}{K_n}$$

DESIGNING AGAINST FATIGUE
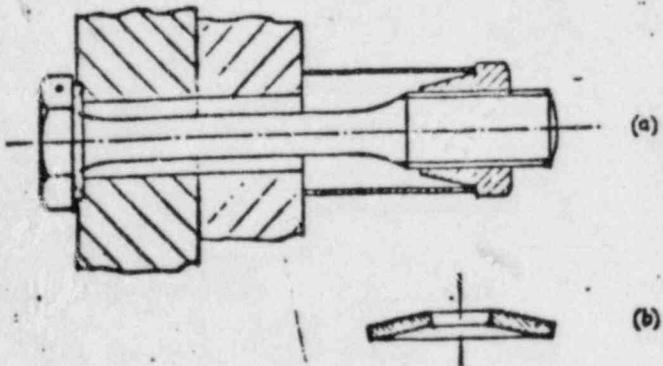
FIG. (a) A low-stiffness bolt assembly; (b) Belleville spring washer

(a)

(b)

TOP OF NUT

CONVENTIONAL NUT

BOTTOM OF NUT

Stress Concentration Factor

STRESS AT THREAD ROOTS DUE TO NUT ENGAGEMENT

(Private Communication from M J Manjoine)

2

5. Q. Re: CYGNA Questions 12 and 19

Please provide U-bolt torque values that will be used in the field for all pipe sizes and the corresponding lower bound preload level expected as discussed on transcript pages 123 and 94, respectively. Also, please provide preload versus torque data scatter and lower bound curves to be used (transcript page 100).

A. The U-bolt torque values that will be used in the field has not been established yet for all pipe sizes and will be made available as soon as the information is finalized. However, the methodology that is employed in arriving at such values is provided herein, and is applied as an example to the values reported in our affidavit, so that CYGNA will be able to understand how all values are derived. The important thing to recognize is that we will determine the minimum preload level to be applied to the various pipe sizes and schedules. The torque to be applied is then derived from knowledge of the "mini-mum" preload necessary and the test data of preload versus torque.

The data scatter obtained from all the tests where preload versus torque was measured is given in Exhibits 5.1 through 5.4 for the four specimens tested. Also shown in those exhibits are dashed lines which have been used to derive the linear relationship between pre-load and torque for each pipe size. It is to be noted that the cor-relations derived for each pipe size tested represent the condition whereby the lowest preload is achieved for the highest applied torque in the range of interest for each pipe size. The correlation is the usual
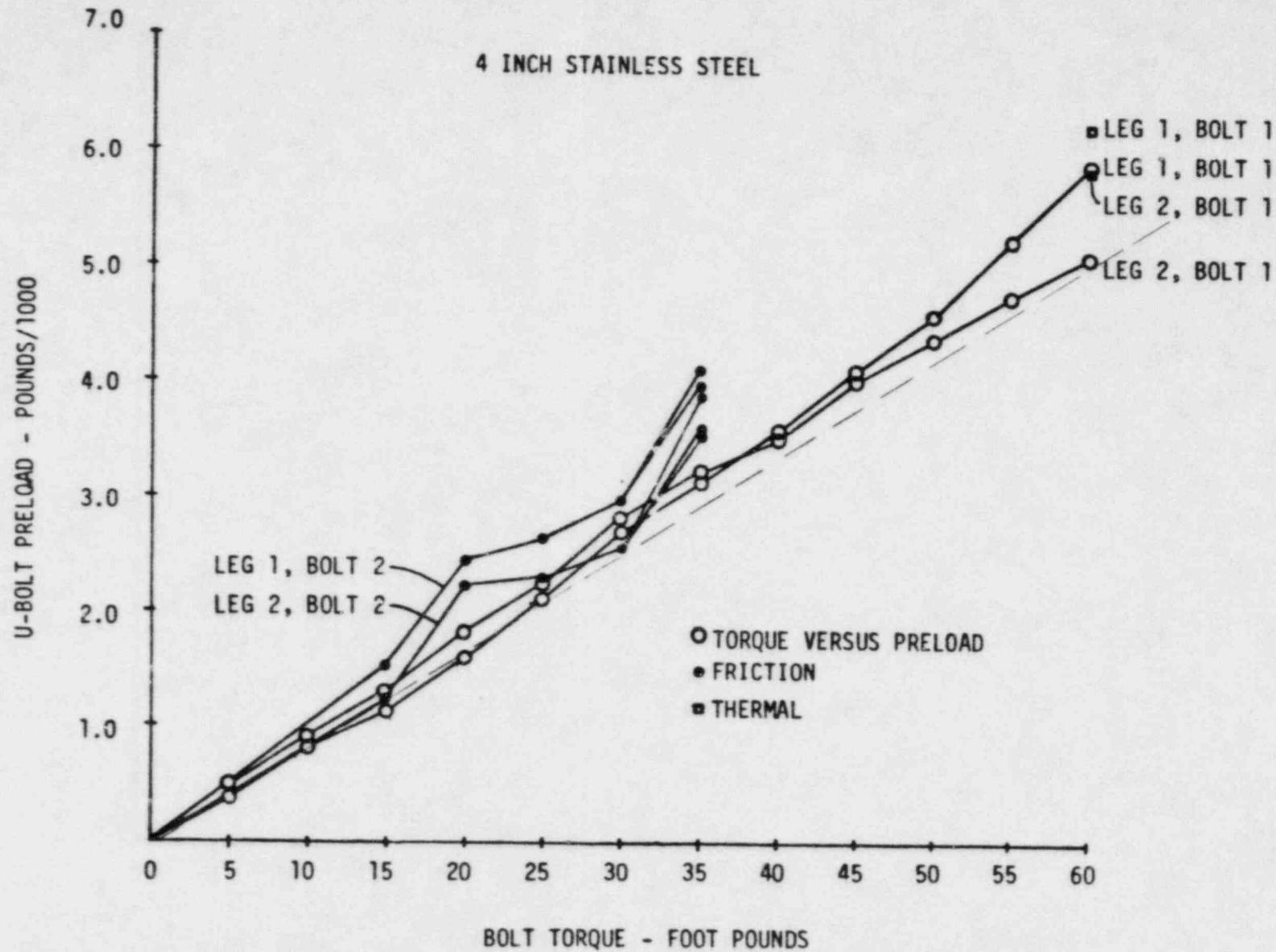
$$\tau = KTD$$

where τ is the torque in ft.-lb., T is the preload in lbs., D is the U-bolt diameter and K is a coefficient derived from test. For the four specimens tested, the coefficients, K, that would result in the lowest preload for a given torque are as follows
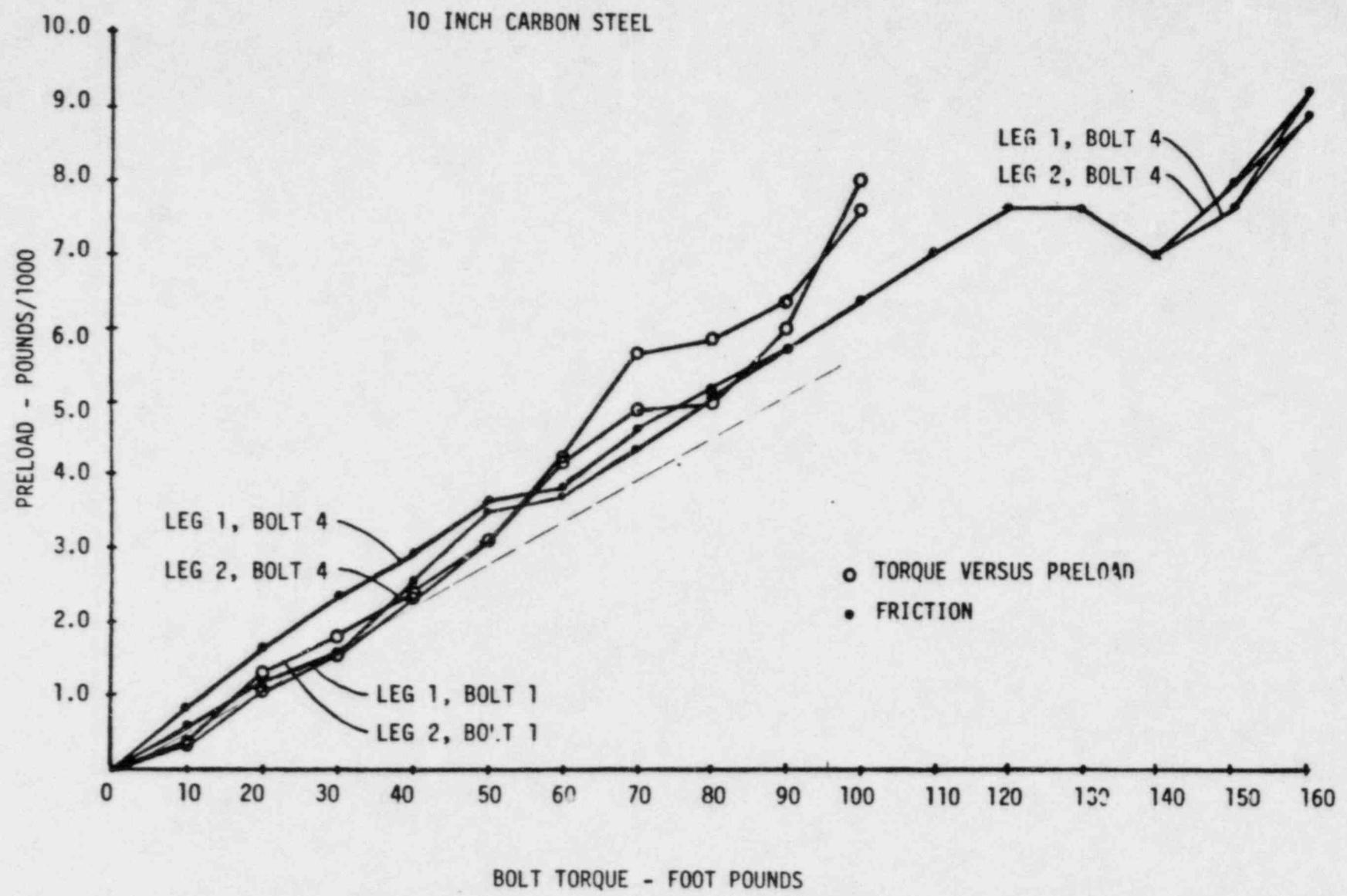
SPECIMEN	K
4" Sch 160	0.288
10" Sch 40	0.353
10" Sch 80	0.276
32" MS	0.403

Obviously average coefficient would be less and would vary between 0.25 and 0.35 as stated in our affidavit. To ensure that the minimum required preload is achieved in the field, the highest value of the coefficient is used regardless of pipe size, i.e., K=0.040.

To arrive at the torque value, the following examples derived for the 4" Sch 160 and 10" Sch 40 pipes will serve as illustration. From the answer to the next question, the minimum value of preload necessary to maintain "stability" for the 4" Sch 160 assembly is 0.37 kips. With an average value of K (used in finite element analyses of the Affidavit) the torque value corresponding to this preload would be 5 ft.-lbs. With the maximum K value the torque is 6.16 ft.-lbs. Considering that the specimen is subject to thermal cycling and possible relaxation, a 40%

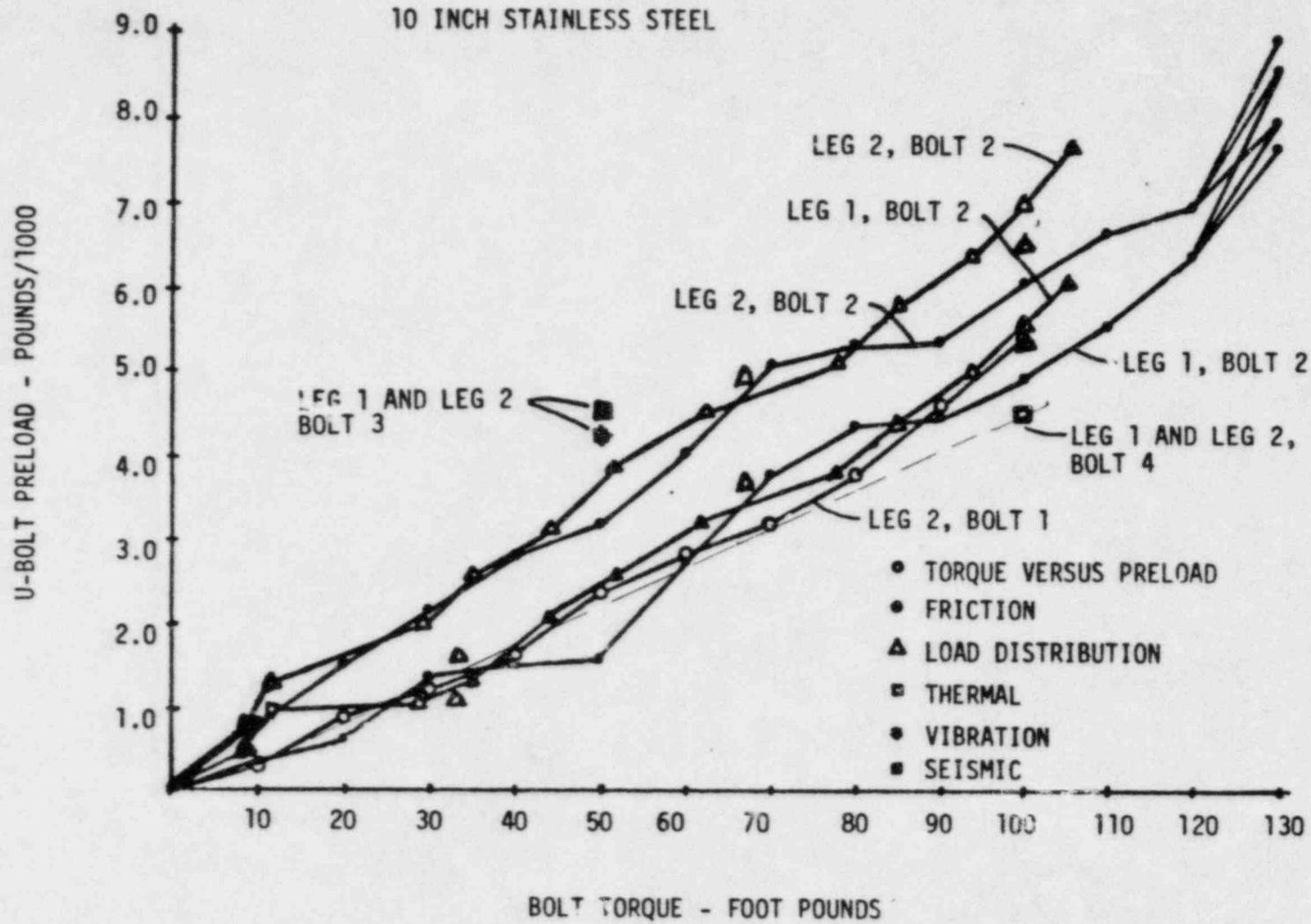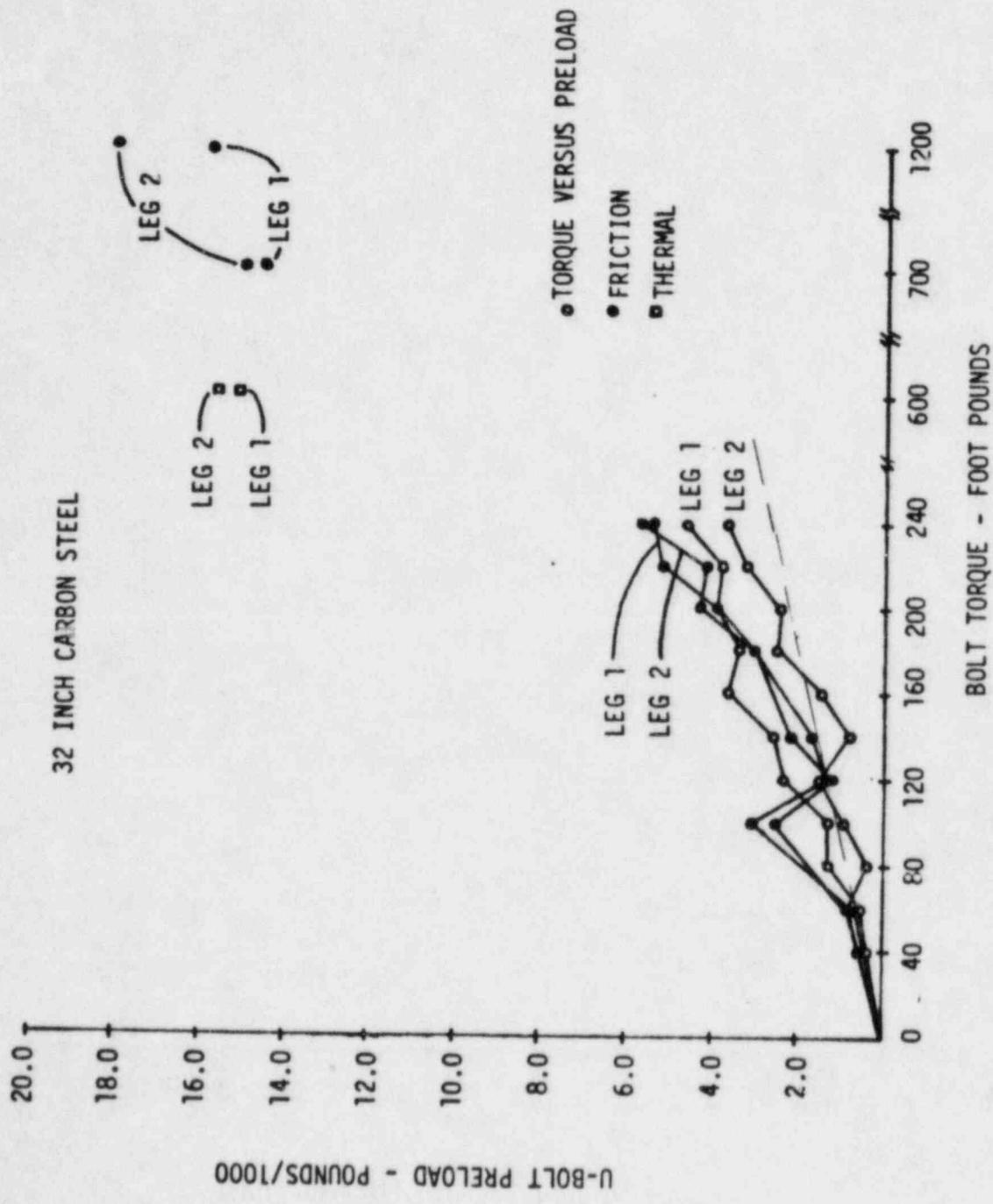4 INCH STAINLESS STEEL

LEG 1, BOLT 1
LEG 1, BOLT 1
LEG 2, BOLT 1
LEG 2, BOLT 1

LEG 1, BOLT 2
LEG 2, BOLT 2

○ TORQUE VERSUS PRELOAD
● FRICTION
▫ THERMAL

U-BOLT PRELOAD - POUNDS/1000

BOLT TORQUE - FOOT POUNDS

10 INCH CARBON STEEL

Exhibit 5.2

Exhibit 5.3

10 INCH STAINLESS STEEL

LEG 2, BOLT 2

LEG 1, BOLT 2

LEG 2, BOLT 2

LEG 1, BOLT 2

LEG 1 AND LEG 2, BOLT 3

LEG 1 AND LEG 2, BOLT 4

LEG 2, BOLT 1

U-BOLT PRELOAD - POUNDS/1000

BOLT TORQUE - FOOT POUNDS

● TORQUE VERSUS PRELOAD
● FRICTION
△ LOAD DISTRIBUTION
▣ THERMAL
● VIBRATION
■ SEISMIC

32 INCH CARBON STEEL

TORQUE VERSUS PRELOAD
FRICTION
THERMAL

BOLT TORQUE - FOOT POUNDS

U-BOLT PRELOAD - POUNDS/1000

Exhibit 54

7

margin is added to account for it, leading to a torque of about 9 ft.-lb. required for stability.

The total load experienced by the U-bolt with a torque level of 9 ft.-lb., coupled with a peak thermal expansion and peak pressure expansion load is approximately 4000 lbs. (see Table II-1 of Attachment 3 of Affidavit). For this load the stress in the U-bolt threaded area would be 28,200 psi, which is approximately 78% of the minimum yield strength at room temperature. With thermal cycling at this level of stress, a stress relaxation of between 30 and 40 percent may be possible (see figure A2 of preceding Question 4).

In the affidavit a value of 25 ft.-lb. was chosen as a compromise between the 9 ft.-lb. and 35 ft.-lb. which tests showed resulted in good contouring of the U-bolt around the pipe (see Affidavit at 74).

For the 10" Sch 40 pipe, as another example, the minimum required preload is computed to be 1.4 kips, which leads to a torque of 35 ft.-lb.

Little or no relaxation would be expected in such specimen for such relatively low torque. Nevertheless, if one were to consider a 30% relaxation, then the minimum applied torque would be less than 50 ft.-lb. Note that a preload of 50 ft.-lb. (equal to a tension of 2000 lbs.), plus thermal and pressure expansion loads equal to 1600 lbs., and an external 10,000 pull load, the total tension with U-bolt would be 5800 lbs., which produce a stress of 17350 psi, which is less than ½ of yield. Thus no significant relaxation should be expected.

6. Q. Re: CYGNA Question 18

What is the minimum level of preload required to maintain stability for the anticipated worst loading condition for stability (i.e., preload plus push at 5°)? This question does not appear to have been answered by the finite element analysis (transcript page 122). Specifically, the first objective on page 1 of the finite element analysis has not been safisfactorily addressed. The fact that "adequate frictional forces exist" requires a judgment based upon what are known to be the necessary frictional forces for stability under the anticipated worst loading condition for stability. Since the necessary frictional forces for stability under this loading condition have not been determined, it is not possible to know if an adequate margin exists between the minimum expected preload in the field nad the preload level necessary to maintain stability.

Without knowing the minimum preload required to maintain stability with a push load at 5°, a judgment as to what constitutes adequate preload cannot be made. Maintaining a tensile load in the U-bolt legs does not guarantee stability.

A. To respond to the question:

> "What is the minimum level of preload required to maintain stability for the anticipated worst loading condition for stability (i.e., preload plus push at 5°)?"

requires a two-part answer. The first, related to the finite element

analysis performed, and the second, pertaining to piping systems that
have lower normal operating temperatures and pressures than evaluated
in the finite studies.

Part one, the finite element analyses adequately addresses the first
objective of the U-bolt testing and analytical program. This objective
being to determine if;

> "adequate frictional forces exist at the pipe/pipe
> support interface to balance a moment created when
> the U-bolt legs are not parallel to the strut so
> that the U-bolt strut assembly support is stable."

The analysis program addressed the stability of four specific U-bolt
pipe support systems assuming that the SSE seismic push force occurs
at the system normal operating temperature and pressure conditions.
Stable solutions are summarized in the finite element analysis report
for minimum and maximum preload torque values. The minimum preload
torque values given are not the actual lower-bound minimum values
for stability but the lowest preload evaluated in the analytical
study. The actual lower-bound minimum torque value required for
stability could be much smaller.

The second part, to assure stability for a push force, it is necessary
to maintain a difference in U-bolt leg forces, this difference pro-
duces a couple which balances the induced moment due to the 5 degree
push force. This difference in U-bolt leg forces will result from a
small amount of cross piece "rolling" on the pipe. If the U-bolt were
a cable, no shear or moment capacity, the U-bolt leg tensile forces
would have to be large enough to create fricitional forces between the
pipe and U-bolt to maintain moment equilibrium. Since the U-bolt
has shear and moment capabilities, the U-bolt leg tensions can be
less than required for a cable.

The effect of reducing the pipe system temperature and pressure is to
reduce the total preload. The reduced preload will result in lower
frictional force resistance capacity. Although the finite element
analysis did not explicitly determine the absolute minimum U-bolt
leg tension required for stability, they do show that the minimum
U-bolt leg tension for the stability approaches zero. It is necessary
that the U-bolt leg forces be tensile (greater than or equal to zero)
to ensure that the U-bolt legs will be active and resist the applied
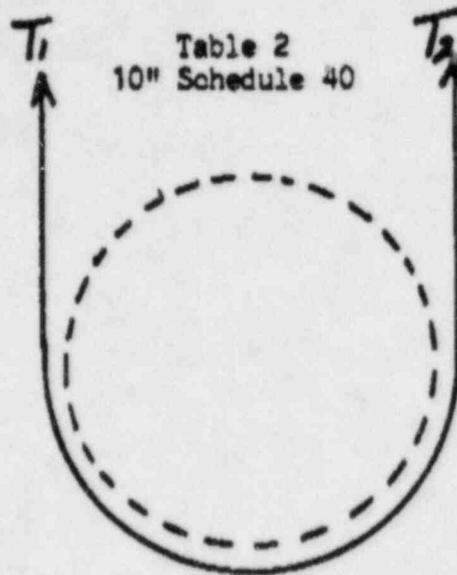seismic strut loads.

With one exception, the finite element analysis results are used to
project minimum preload tension and torque values that ensure stability
for the PRELOAD + PUSH (@5°). The exception is the 10" Sch 40 SS speci-
mens for which test data is directly available on preload reduction as
function of externally applied push load (see figure 18 of Attachment 1
to the Affidavit). The projected values are given in Tables 1 to 4. As
seen from these tables, the recommended torque values given in the tes-
timony are equal to or higher than these minimum perload values except
for the 32 inch U-bolt. Very large U-bolt leg tensions result from
temperature and pressure in the 32 inch pipe/U-bolt system. Since the
temperature and pressure preload effects are not present in the 32 inch
pipe/U-bolt assembly, an additional preload torque is required for this
pipe/U-bolt assembly. Therefore, for the 31 inch pipe, and similar
pipe/U-bolt assemblies, care must be taken before assigning a torque

Table 1
4" Schedule 160
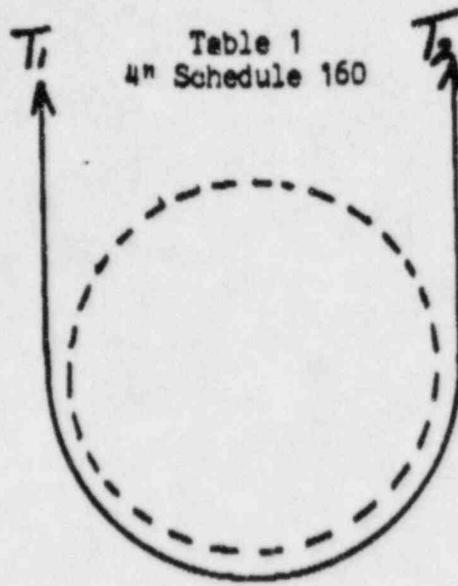
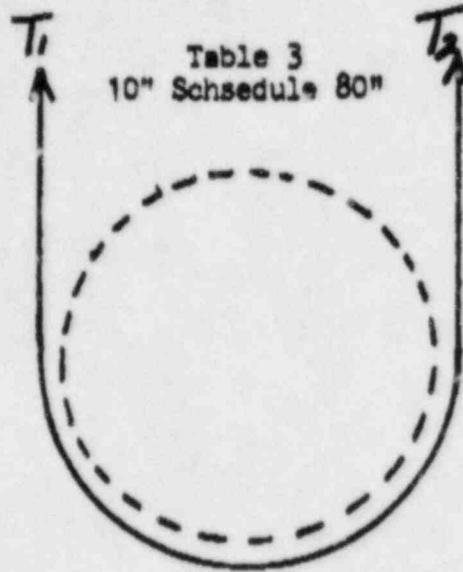|	Tension T_1 (kips)[1]	Tension T_2 (kips)[2]
1. Leg force needed to provide resistance couple	0.0	.12
2. Amount of unloading due to push	.37	.25
3. Total preload necessary (Sum 1+2)	.37	.37

$$\text{Minimum Preload Moment} = \frac{.37}{5.41} \times 60 \text{ FT-LB} = 5 \text{ FT-LB}$$

Note: This table is based on results given in Table II-1 of Attachment 3 to "Applicants' Summary Disposition of CASE's Allegations Regarding Cinching Down of U-Bolts"
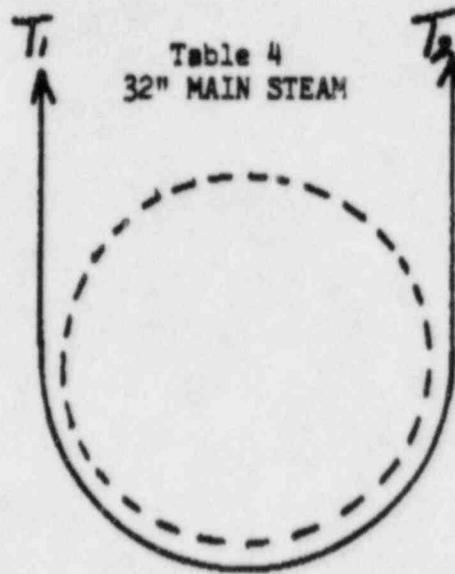
Table 2
10" Schedule 40

	Tension T_1 (kips)[1]	Tension T_2 (kips)[2]
1. Leg force needed to provide resistance couple	0.0	.35
2. Amount of unloading due to push	2.79	1.05
3. Total preload necessary (Sum 1+2)	2.79	1.44

Minimum Preload Moment = (0.4)(0.75) 1400/12 = 35 ft.lbs.*

Note: This table is based on results given in Figure 18 of Attachment 1 to "Applicants' Summary Disposition of CASE's Allegations Regarding Cinching Down of U-Bolts"

It is important to note that this particular torque had been applied to the 10" Sch 40 SS assembly subjected to a 2½ minute accelerated vibration test with a sinusoidal force input of 1000 lb. peak to peak, and the assembly was noted to experience no motion (see Affidavit at 29). The assembly had rotated and walked where the torque was only 20 ft.-lb. Hence, there is confirmation of the stability of the assembly at the 35 ft.-lb. torque. For this test neither pressure nor temperature were present in the assembly.

Table 3
10" Schsedule 80"

	Tension T_1 (kips)[1]	Tension T_2 (kips)[2]
1. Leg force needed to provide resistance couple	0.0	.43
2. Amount of unloading due to push	1.51	1.51
3. Total preload necessary (Sum 1+2)	1.51	1.51

$$\text{Minimum Preload Moment} = \frac{1.51}{7.51} \times 100 \text{ FT-LB} = 20 \text{ FT-LB}$$

Note: This table is based on results given in Table II-3 of Attachment 3 to "Applicants' Summary Disposition of CASE's Allegations Regarding Cinching Down of U-Bolts"

Table 4
32" MAIN STEAM

	Tension T_1 (kips)	Tension T_2 (kips)
1. Leg force needed to provide resistance couple	0.0	8.1
2. Amount of unloading due to push	29.0	20.9
3. Total preload necessary (Sum 1+2)	29.0	29.0

$$\text{Minimum Preload Moment} = \frac{29.0}{6.04} \times 380 \text{ FT-LB} = 1825 \text{ FT-LB}$$

Note: This table is based on results given in Table II-4 of Attachment 3 to "Applicants' Summary Disposition of CASE's Allegations Regarding Cinching Down of U-Bolts"

value, to examine the normal operating temperature and pressure conditions of the pipe and their effects on preload.

A further note needs to be added to the minimum preload required for the main steam line (32" MS). We do not consider it appropriate to determine the minimum required preload for this line in the absence of pressure and temperature. This would only occur when the line is not functioning.

Under such condition, the line fulfills no safety function related to maintaining the plant in a cold shutdown condition. Further analyses conducted on the portion of the main steam line which has the cinched-up U-bolts, in the absence of these supports, indicate that no adverse consequences would result. For this reason Applicants have elected to retain 240 ft.-lb. torque as the minimum required for stability.

7. Q. Re: CYGNA Questions 6, 12 and 18

   Given that lower bound values of preload versus torque are to be provided in the field, how will these lower bound values be reduced to account for observed reductions in preload which occurred during the testing program (thermal cycling, vibration testing, etc.)? Also, what values of "necessary preload for stability" will these reduced values be compared to determine the margin against instability?

   A. The manner in which the lower bound value of preload are "augmented" to account for relaxation phenomena that may occur, so that a correspondingly higher torque would be used in the field has been described in our prior answer.

TEXAS UTILITIES GENERATING COMPANY
P. O. BOX 1002 · GLEN ROSE. TEXAS 76043

November 8, 1984

Cygna Energy Services
101 California Street
Suite 1000
San Francisco, CA 94111

Attn: Ms. Nancy Williams, Project Manager

Ref: Telephone Conversation of Octoner 30, 1984 between
J. Minichiello (CYGNA) and J. Finneran (TUGCO)

Dear Ms. Williams:

Attached, please find the TUGCO clarification to the calculations for
MS-1-002-005-5RR.

If there are any further questions or comments, please contact Ms. Jeanne
J. Van Amerongen.

Very truly yours,

L.M. Popplewell
Project Engineering Manager

LMP/JVA/ljh

cc: D.H. Wade
    R.E. Ballard
    J. Finneran

A DIVISION OF TEXAS UTILITIES ELECTRIC COMPANY

CYGNA QUESTION

Cygna has reviewed TUGCO's calculations for MS-1-002-005-S72R (done in response to the 10/4/84 telecon between Cygna and TUGCO). Cygna has found the calculations correct. Cygna requested TUGCO to provide documentation showing the AWS calculation is an appropriate method for evaluating this type of local stress.

TUGCO'S Response

We have attached a copy of the paper "Basics for Tubular Joint Design" by P.W. Marshall and A.A. Toprac. Their paper presents the background data for the local failure design criteria in AWS. Although that criteria is expressed in terms of punching shear, it also includes considerations of flange width to thickness ratio, branch member to main member ratio, and axial and bending stresses in the main member. Thus, as the paper makes clear, it is really a total joint design approach, not just punching shear. CYGNA should note on the third page of the paper that the authors state that for a γ less than 7, the joint may be said to have a 100% punching shear efficiency. On page 5 of the paper, γ for tube steel is defined as b/t where b = half the width of the tube steel shape minus the thickness t. For MS-1-002-005-S72R, γ equals $(4 - .5)/(.5 + .72) = 2.8$.

Basis for Tubular Joint Design

Design criteria of the codes that govern construction of offshore drilling platforms are analyzed and evaluated

BY P. W. MARSHALL AND A. A. TOPRAC

Introduction

Recently published codes (Refs. 1,2) include criteria for the design and construction of welded connections for circular tubes, which have been in use for a number of years in offshore drilling platforms. The purpose of this paper is to document the background data underlying these criteria, in terms of static and fatigue strength.
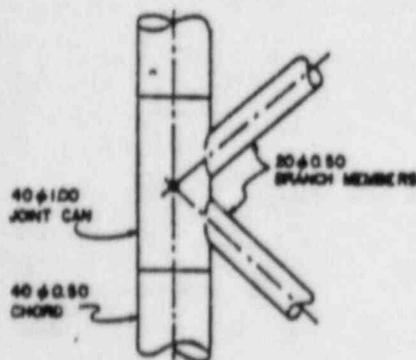
Fig. 1 — Simple joint

P. W. MARSHALL is Staff Civil Engineer, Offshore Construction, Shell Oil Company, New Orleans, La. A. A. TOPRAC is Professor of Civil Engineering, The University of Texas at Austin.

Paper is based on a survey sponsored by the WRC Subcommittee on Welded Tubular Structures.

Static Strength

Simple and Punching Shear Joints

Currently the most popular style of welded connection for intersecting circular tubes as used in fixed offshore structures is the "simple" joint illustrated in Fig. 1. The tubular members are simply welded together, and all load is transferred from one branch to the other via the chord, without any help from stiffening rings or gusset plates. To prevent excessively high localized stresses in the chord, a short length of heavier section (joint can) is often used in the connection area. In such cases, the problem of 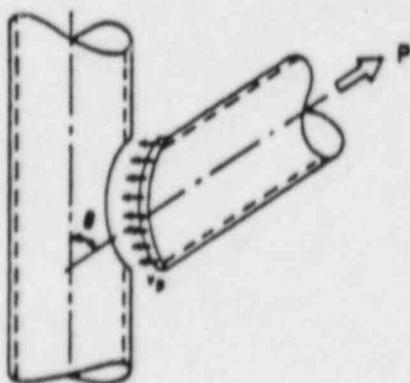joint design reduces to that of sizing the joint can, particularly where complete joint penetration groove welds (as defined for tubular structures (Ref. 2) are used at the ends of the branch members.

Although the complete stress picture is much more complex, the concept of punching shear, Fig. 2, has been quite useful in correlating test data and formulating design criteria. The average (or nominal) punching shear stress, v_p, acting on the potential failure surface is calculated as:

$$v_p = \tau \left(\frac{f_a \sin\theta}{k_a} + \frac{f_b}{k_b} \right) \qquad (1)$$

Fig. 2 — Punching shear

Fig. 3 — Intersection line effects

LINE LOAD Q K/in — LINE LOAD Q Q — CLOSED RING — UNIT WIDTH STRIP BEAM

KELLOGG

TEST DATA FOR TUBULAR JOINTS

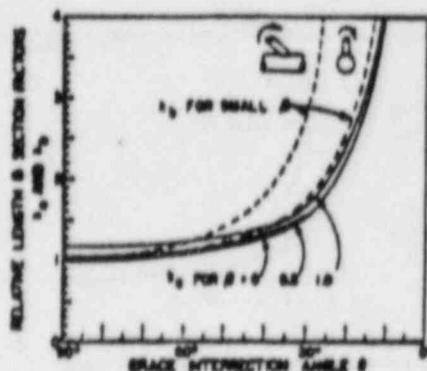$$\text{AT YIELD} \quad v_P = \frac{Q}{t} \cdot f(\beta)\, \frac{F_Y}{0.5\,\gamma}$$
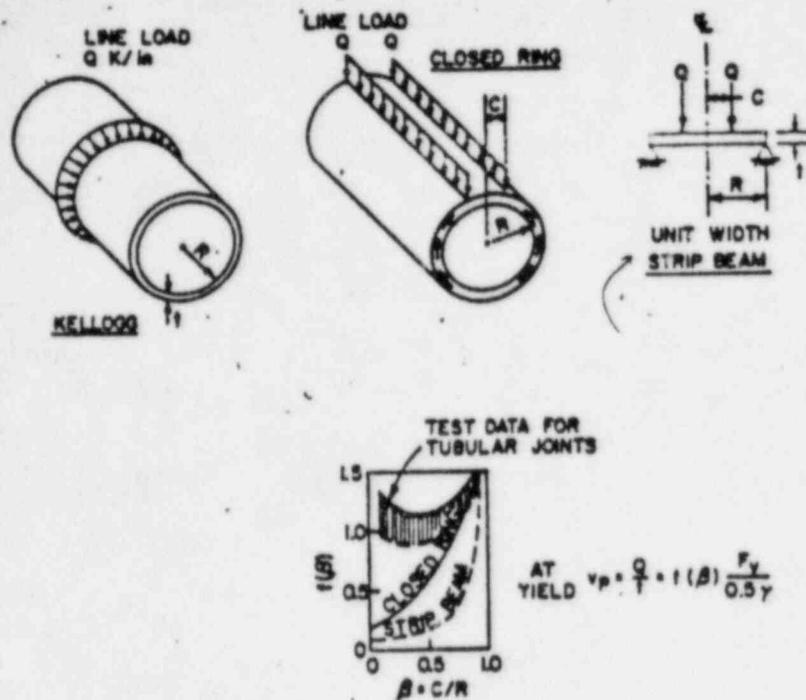
$\beta = C/R$

Fig. 4 — Simplified punching shear criteria

Table 1 — Closed Ring and Kellogg Solutions for Punching Shear and Line Load Capacities

Case	Closed ring	Kellogg
Punching shear capacity	$v_P = \dfrac{F_Y}{0.5\,\gamma} \times f(\beta)$	$v_P = \dfrac{F_Y}{2.34 \times \gamma^{0.5}}$
Total joint capacity proportional to	$t^2 \times \text{length} \times f(\beta)$	$t^{1.5} \times \text{perimeter}$

where $\gamma = t_b/t$ = ratio of branch thickness to chord thickness,

θ = angle between member axes (see Fig. 2),

f_a and f_b = nominal axial and bending stresses in branch, respectively.

It is to be noted that only the component of the branch member load which is perpendicular to the main member (chord) wall is considered because this component is responsible for most of the localized stresses. The terms K_a and k_b relate to the length and section modulus, respectively, of the tube-to-tube intersection, which is kind of a saddle-shaped oval (Ref. 3). Specifically the terms represent the ratio of the true perimeter (or section modulus) to that of the circular brace; they are plotted in Fig. 3, as a function of θ (defined above) and β, where

$\beta = \dfrac{R_b}{R}$ = brace to chord diameter (or radius) ratio

To specify design allowable values for the punching shear stress theoretical and experimental considerations are discussed below.

Theoretical Approach. Solutions for elastic stresses in cylindrical shells subjected to localized line loads are available for the very simple load cases shown in Fig. 4. The closed ring solution and Kellogg formula (Ref. 4) indicate punching shear and line load capacities as shown in Table 1. Note that punching shear capacity is defined in relation to the very important nondimensional parameter γ where

$\gamma = R/t$ = chord thinness ratio, radius/thickness

This is analogous to the span to depth ratio of a strip beam, for which similar relationships may be derived (see Fig. 4).

These two relatively crude physical models might be expected to bracket the behavior of simple tubular joints, since the branch member loads the chord along a combination of longitudinal and circumferential lines. Unfortunately they yield divergent results and tend to indicate disturbingly high stresses in practical design situations. However, they both do reflect the strong dependence of total joint capacity on chord thickness and branch member perimeter. The addi-

tional effect of diameter ratio, $f(\beta)$, as indicated by Roark, was considered paradoxical in that test data with tubular connections did not show the same monotonic increase in joint efficiency as depicted in Fig. 4. In fact, T-joint tests cited by Toprac (Ref. 4) showed joint efficiency (in terms of the ratio of hot spot stress to punching shear) passing through a minimum in the midrange of diameter ratios.

A sophisticated analytical solution (Ref. 5) yields the more realistic picture presented in Fig. 5. These results are consistent with those obtained experimentally and with finite element analyses (Ref. 6), insofar as stress levels in the chord and load transfer across the weld (Q) are concerned. For this joint, the stress concentration factor is 7.3, and the calculated average punching shear stress, v_p, at which first yield at the hot spot occurs ($F_Y = 36$ ksi) is only 2.5 ksi. Comparable punching shears for Roark and Kellogg would be 2.2 ksi and 3.4 ksi, respectively.

Figure 6 summarizes the results of a parameter study made with computer programs based on Ref. 5. The punching shear stress, v_p, at which yield stress is predicted for axially loaded T-connections, is presented as a function of chord thinness ratio, γ, and brace/chord diameter ratio, β. As was previously noted experimentally, joint efficiency (in terms of punching shear at yield) passes through a minimum for a diameter ratio in the range of 0.4 to 0.7. Throughout this range, punching shear efficiency is more or less independent of diameter ratio, but varies inversely with the 0.7 power of chord thinness ratio γ.

Correspondingly, the overall capacity of the connection would be proportional to the product of brace perimeter (or intersection length) and $t^{1.7}$, where t is chord thickness — a result which is surprisingly consistent with the oversimplified approaches considered earlier.

However, the use of first yield as a failure criterion shows that elastic theories seriously underpredict the available static strength of practical tubular connections. For example, a mild steel scale model of the connection in Fig. 5 actually carried the load shown (appropriately scaled down). Naturally, a hot spot stress of 160 ksi for mild steel is unrealistic and the material is beyond yield, and subjected to strains in excess of 5300 μ in./in. Under these circumstances, it appears that theoretical elastic analyses will be of limited use in formulating practical design criteria for static or quasi-static loading conditions.

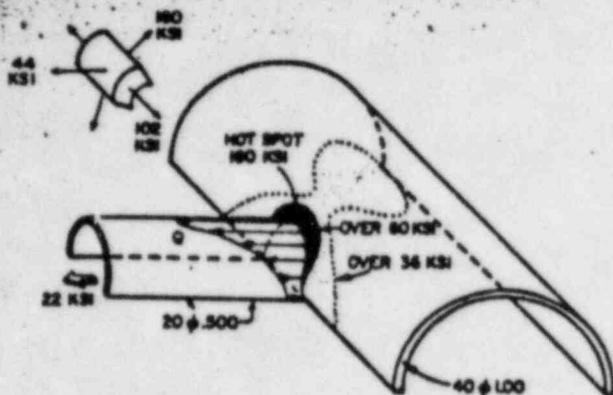*Empirical Approach.* Tubular joints have a tremendous reserve capacity beyond the point of first yield (Ref. 7),

Fig. 5 — Theoretical elastic stresses — axially loaded T-joint

PUNCHING SHEAR
AT FIRST YIELD
$v_p/F_y = f(\gamma, \beta)$

AXIALLY LOADED
TEE JOINT $\tau = 1.0$

Fig. 6 — Parameter study

as illustrated in Fig. 7. If a section through the chord at its intersection with the brace is considered for small loads in the elastic range, the distribution of circumferential stresses on the outside surface are shown as Stage 1 in the figure. Beyond yield, the connection deforms (Stage 2) while the applied load continues to increase. Finally, at loads 2.5 to 8 times that at first yield, the joint fails — by pullout failure as shown for tension loads or by localized collapse of the chord for compression loads (Stage 3).

The average punching shear stress at failure*, v_p, has been plotted in Fig. 8 relative to specified minimum yield strength, F_y, and as a function of chord thinness ratio, γ; 38 static tests which failed in the punching shear mode are represented, along with two specimens which failed after only a few cycles of fatigue loading. The solid circles represent K-joints; the rest are T and cross joints. Data are from Toprac (Refs. 4, 7) and other sources (Refs. 8, 9).

For relatively stocky chord members — thickness greater than 7% of diameter or γ less than 7 — the joints may be said to have a 100% punching shear efficiency, in the sense that the shear strength of the material is fully mobilized on the potential failure surface. This criterion is met by ASTM A-53 standard weight pipe under 2 in.

diam, by extra strong pipe under 5 in. diam, and by double extra strong pipe through 12 in. diam.

Larger and/or thinner chords should be treated on the basis of a reduced punching shear capacity as given by the curve in Fig. 8 and

$$\text{Ultimate } v_p = \frac{F_y}{0.5 \times \gamma^{0.7}} \quad (2)^{**}$$

$$\text{Allowable } v_p = \frac{F_y}{0.9 \times \gamma^{0.7}} \quad (2a)$$

Here, the design allowable punching shear stress incorporates a safety factor of 1.8 with respect to the empirical curve for ultimate punching shear. Its intended range of application is for the mid-range of diameter ratios for which v_p is more or less independent of β.

Since the proposed empirical design curve makes use of the post-yield reserve strength of simple tubular connections, it will be instructive to review the sources of this extra capacity. These are:

1. The difference between elastic and plastic bending strength (localized) of the cylindrical shell, a factor of 1.5.

2. Restraint to plastic flow caused by triaxial stresses at the hot spot, a factor of 1.6 for the situation of Fig. 5.

3. Strain hardening — for the mild steels represented in the test data, the ultimate tensile strength (which is at least locally utilized when a joint fails by separation of the material) is greater than the specified minimum yield strength, F_y, (which is used for the empirical correlation and design formula) by factors from 1.6 to 2.4. Correspondingly, it is suggested that F_y used in calculating the allowable v_p should not exceed two-thirds (2/3) the tensile strength.

4. Further increases in capacity result from the redistribution of load, which occurs as the connection yields and approaches its limit load. If the cylindrical shell is visualized as a network of rings and stringers, the sequence of events may occur as illustrated in Fig. 9.

Plastic behavior, triaxial stresses, strain hardening, load redistribution and large deformation behavior place extraordinary demands on the ductility of the chord material. Some localized yielding will occur at design load levels. These considerations should be kept in mind when selecting steels for tubular structures (Ref. 8).

Further Refinements

By and large, design codes represent a consensus of engineering practices in a particular field. There was a general feeling that, while the data of Fig. 8 (as replotted in terms of β in Fig. 10) did not justify taking diameter ratio β into account, experience indicated a beneficial effect as the diameter ratio approaches unity, as indicated by the heavy dashed line in Fig. 10.

Square Tubes. Considerable insight into the effect of β on the ultimate

---

* Failure was defined as first crack for tension loads. This would functionally impair the joint for subsequent fatigue service.

** The ultimate strength criteria developed by Reber (Ref. 9) reduces to:

$$\text{Ultimate } v_p = f(\beta) \frac{F_y}{0.55 \times \gamma^{0.4}}$$

All simple T, Y and K connections are tested on a common basis. Although K connections have lower elastic stresses than the corresponding T and Y connections, they also have less reserve strength, so that the ultimate capacities come out similar. The chief difference between Reber's results and equation (2) is in the degree of conservatism with respect to the scatter band shown by the test results. Reber provides a good average fit whereas the curve for equation (2) falls on the safe side of most of the data. Reber's $f(\beta)$ shows relatively little influence of diameter ratio; i.e., $f(\beta) = \beta^{0.1}$
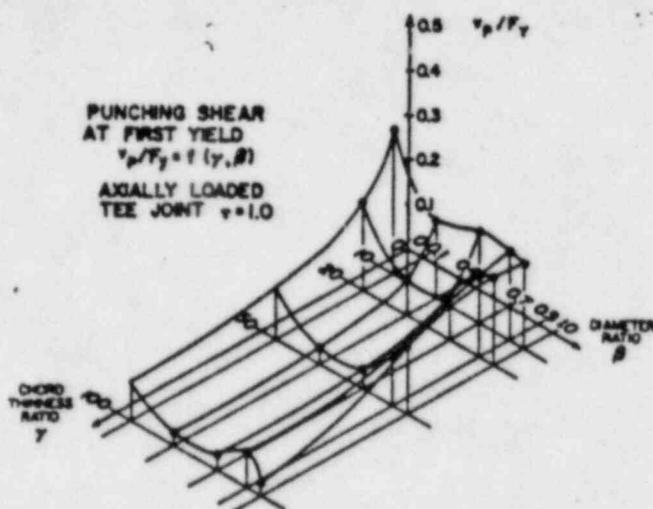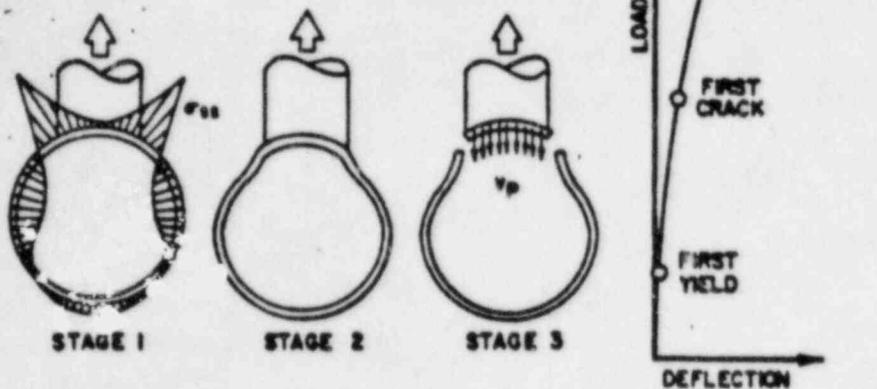
Fig. 7 — Reserve strength of a tubular connection
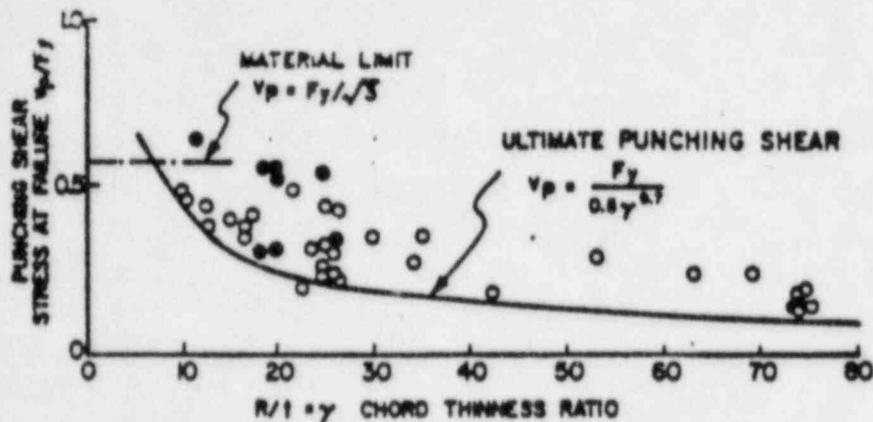

Fig. 10 — Static strength — β effects

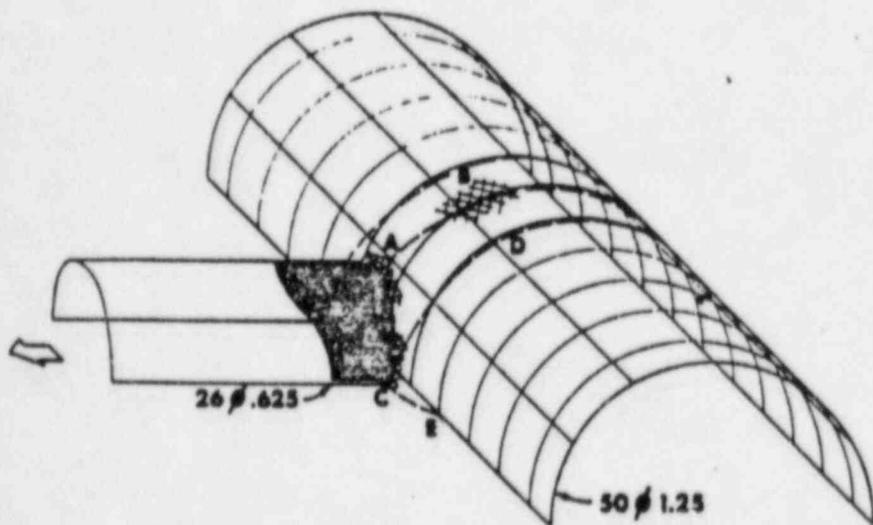Fig. 8 — Empirical design curve — static strength

Fig. 9 — Load redistribution. First yielding occurs at hot spot A. Cross hatched yield line is analogous to plastic hinge in a continuous frame. Full strength of ring AB is reached when yielding also occurs at B, after considerable angle change at hot spot. Ring AB continues to deform at constant load while rest of joint catches up, resulting in more uniform load distribution. Limit load of joint is reached when ring CD and stringer CE also yield. Deformed shape is indicated by dashed lines

where β and γ are defined in a manner analogous to the usage for circular tubes.

The second term on the right of equation (3) is quite similar to the empirical punching shear, equation (2); only the exponent of γ is different. The leading term corresponds to the β effect and has the following properties:

1. Minimum value of 1.0, which occurs at β = 0.5.
2. Increasing punching shear efficiency at larger and smaller β - ratios; this is comparable to the theoretical results for circular T-joints, Fig. 6.
3. Where β approaches its limits (0 and 1.0), punching shear is limited by the shear strength of the material (or by other considerations such as web crippling).

Test data (Ref. 10) for the specific case of 5 × 5 × 0.187 chord are also plotted in Fig. 11. Failure was defined as when joint deformation reached 3% of chord width. The strength increase for β -ratios over 0.5 appears to be confirmed, with the test data showing strengths ranging from 1.5 to 1.8 times the computed "upper bound" limit load. This reserve strength undoubtedly comes from some of the same sources discussed above for circular tube connections.

For β -ratios under 0.5, however, the test data show equation (3) to be increasingly less conservative as β decreases. The dotted line (Fig. 11) represents a punching shear criteria which is independent of the β -ratio, given by:

$$v_p = \frac{F_y}{0.5\,\gamma} \quad \text{for } \beta < 0.5 \quad (3a)$$

Note that this straight sloping line goes through the origin; total joint capacity goes to zero as the brace perimeter and β -ratio also approach zero. The combination of equations (3) and (3a) results in criteria with more or less consistent safety factors throughout the range of β.

punching shear capacity of tubular connections was gained from consideration of a limit analysis of square tubes. Using the yield line pattern of Fig. 11 and the upper bound theorem

of plastic design, the ultimate punching shear stress v_p is obtained as:

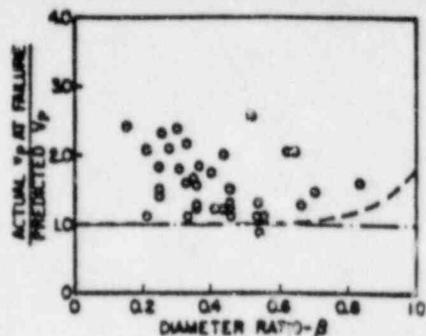$$v_p = \frac{0.25}{\beta(1-\beta)} \cdot \frac{F_y}{0.5 \times \gamma^{1.0}} \quad (3)$$

Fig. 11 — Ultimate strength analysis — square tubes

Fig. 12 — Japanese results — cross joints

Japanese Research

A simplified limit analysis of cross joints with circular tubes has been reported (Ref. 11), which employs the physical model of Fig. 12 to derive an expression for theoretical ultimate strength which can be reduced to the following:

$$v_p = \frac{0.5}{\beta(1-\beta)} \cdot \frac{F_y}{0.5\gamma} \cdot \frac{B_e}{2\pi R} \quad (4)$$

When the effective length B_e is taken as equal to the chord circumference, the last term becomes unity, and equation (4) becomes identical with equation (3), with a term for the basic variation of v_p with F_y and γ, modified by a term expressing the β-effect.

Test data were used to justify an empirical modification of the expression for ultimate punching shear, leading to the results plotted in Fig. 12, and

$$v_p = \frac{0.3}{\beta(1-0.833\beta)} \cdot \frac{F_y}{0.304\gamma} \quad (4a)$$

In this expression the term for β-effect has the following properties and implications:

1. A value of 1.0 for $\beta = 0.6$
2. Increasing joint efficiency for larger β-ratios, up to a limiting increase of 1.8-fold for $\beta = 1.0$.

Note that for the mid-range of diameter ratios (β from 0.25 to 0.75) the assumption of constant punching shear also provides a reasonable fit to the data of Fig. 12, in line with earlier results. For very small β-ratios, there is little experimental justification for the large increases in joint efficiency predicted by the β-modifier in equation (4a). Accordingly, it has been recommended that a modifier of unity be used for values of β less than 0.6. This is consistent with the results for square tubes, and appears to be conservative with respect to theoretical results (Fig. 6).

Proposed β-Effect

Applying the modifier, Q_β, for the effects of diameter ratio, to the punching shear criteria of equations proposed earlier (equations (2) and (2a)) one obtains:

$$\text{Ultimate } v_p = Q_\beta \cdot \frac{F_y}{0.5 \times \gamma^{0.7}} \quad (5)$$

$$\text{Allowable } v_y = Q_\beta \cdot \frac{F_y}{0.9 \times \gamma^{0.7}}$$

where

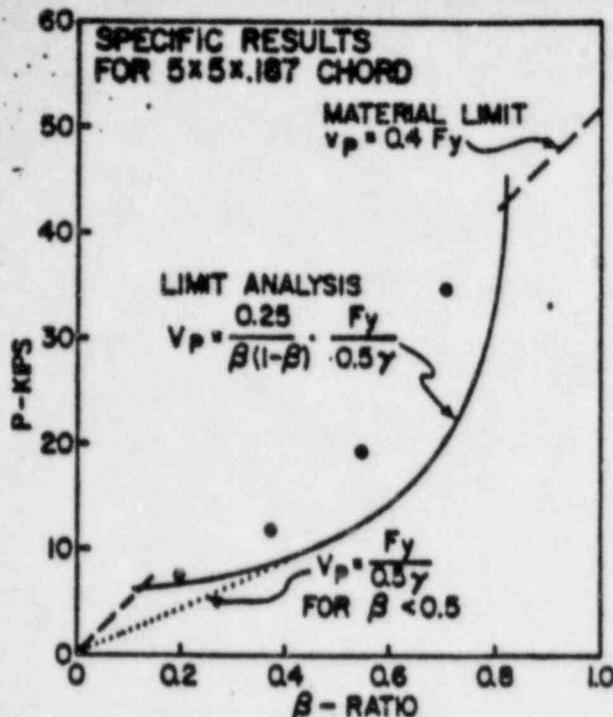$$Q_\beta = \frac{0.3}{\beta(1-0.833\beta)} \quad \text{for } \beta > 0.6$$

$$Q_f = \dfrac{P_{max} \text{ IN PRESENCE OF } P'}{P_{max} \text{ WITH CHORD UNLOADED}}$$

$Q_f = 1.0$

$Q_f = 1.22 - 0.5|U|$ FOR $|U| > 0.44$

P_max AT FAILURE

P' ← → P'

CHORD AREA Ac

P_max

COMPRESSION   CHORD UTILIZATION RATIO   TENSION
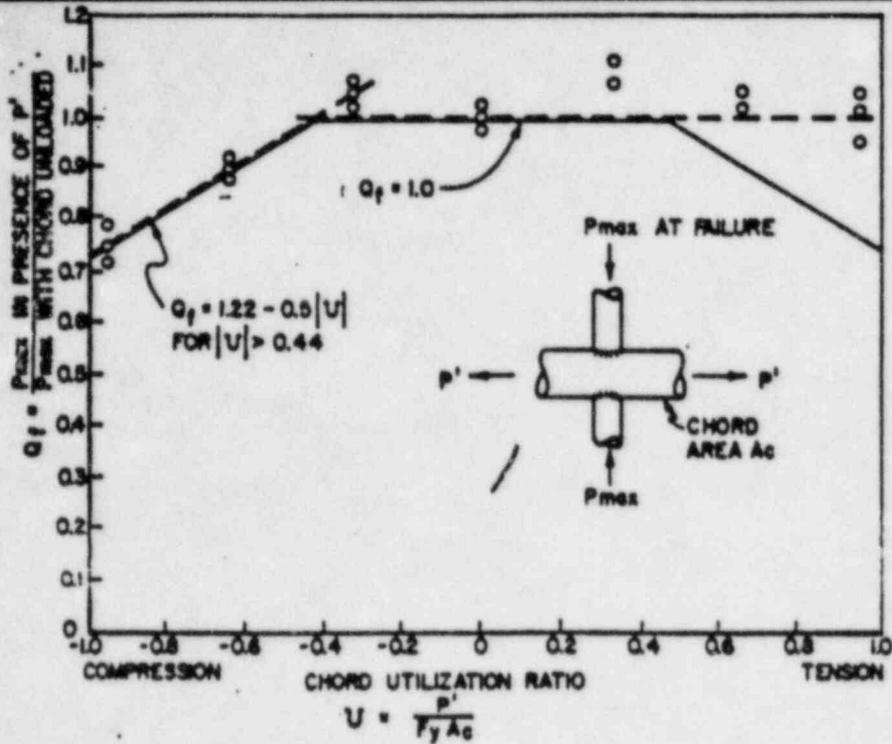
$$U = \dfrac{P'}{F_y A_c}$$
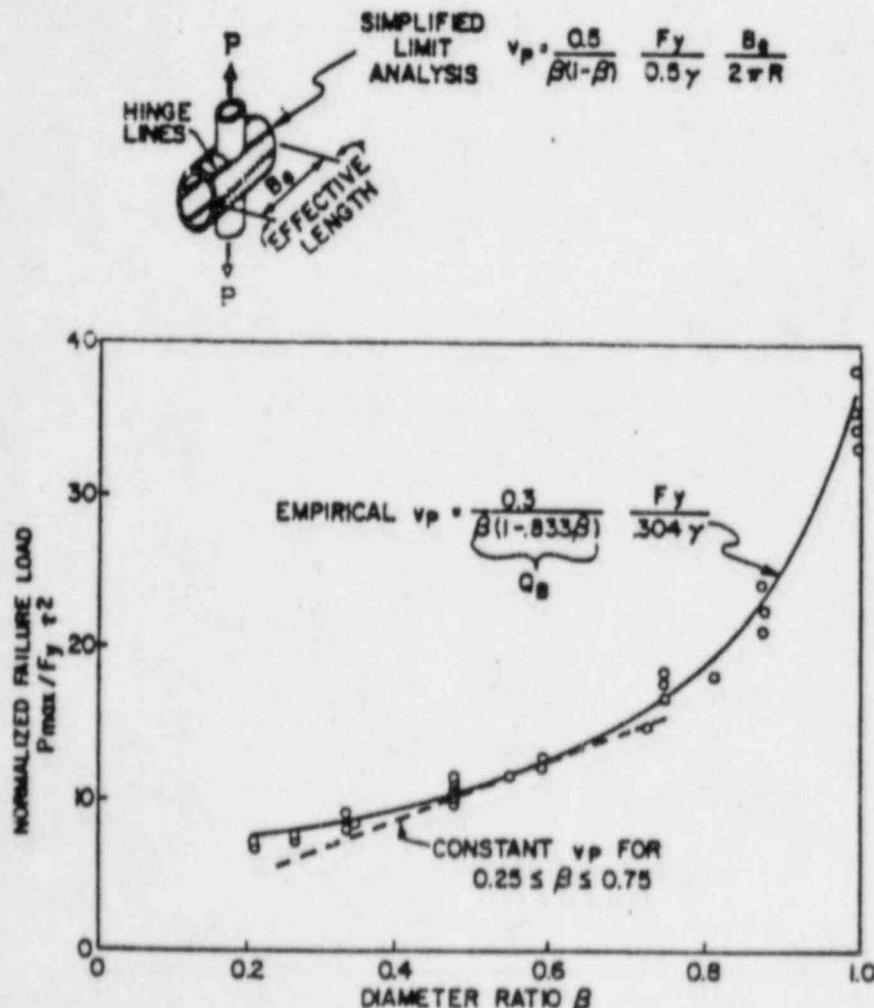
Fig. 13 — Interaction effects of stress in chord

and $Q_\beta = 1.0$ for $\beta \leq 0.6$

These criteria, including Q_β, are plotted as the heavy dashed line in Fig. 10.

Interaction Effects

Japanese data (Ref. 11), showing the extent to which axial load in the chord member reduces its capacity to carry punching shear, are plotted in Fig. 13. The proposed modifier Q_f for interaction effects would be used in design as follows:
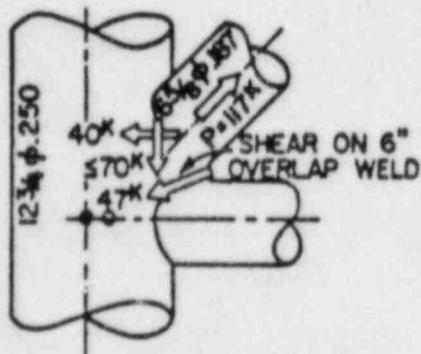
Allowable $v_p =$ (6)

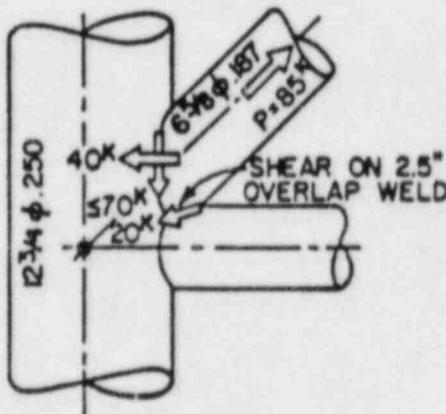$$Q_f \cdot Q_\beta \cdot \dfrac{F_y}{0.9 \cdot \gamma \tau}$$

where $Q_f = 1.22 - 0.5|U|$ for $|U| > 0.44$
$Q_f = 1.0$ for $|U| \leq 0.44$

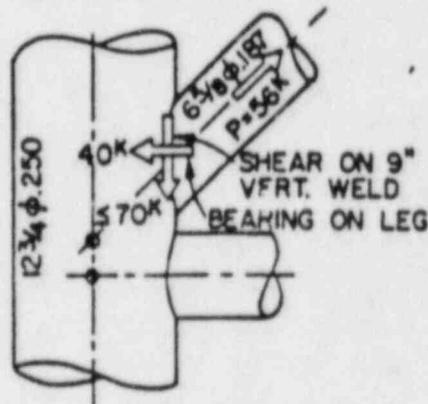and $|U| =$ chord utilization ratio at the connection.

NEGATIVE ECCENTRICITY   ZERO ECCENTRICITY   POSITIVE ECCENTRICITY

COMPARISON OF JOINT EFFICIENCIES		
TYPE OF JOINT	CALCULATED BASED ON NOM. YIELD 137^K IN 6⅝ϕ	TEST RESULTS BASED ON ULTIMATE 255^K IN 6⅝ϕ
POSITIVE ECCENTRICITY	41%	54%
ZERO ECCENTRICITY	62%	82%
NEGATIVE ECCENTRICITY	86%	108%

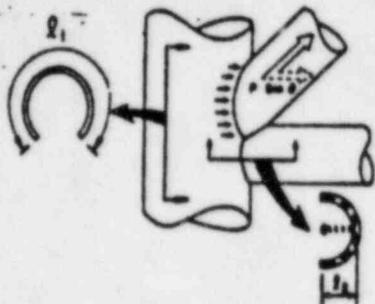Fig. 14 — Joints of various eccentricities

Fig. 15 — Components of resistance for overlapping joints

In design |U| would be taken as the AISC ratio for the chord at the tubular connection (with respect to criteria based on yield). Equation (6) includes safety factors and corresponds to a symmetrical failure envelope, as shown by the solid line (Fig. 13). Where heavy wall joint cans are used at tubular connections, the utilization ratio will often be less than 0.44 for the joint can, corresponding to no reductions due to interaction. For highly stressed K and X-joints* without joint cans, but with equal diameters, the increase in joint efficiency over equation (2a) will be limited to about 30%, when both Q_β and Q_t are considered.

Overlapping Joints

In overlapping joints, the braces intersect each other as well as the chord, and part of the load is trans-ferred directly from one brace to another through their common weld. One advantage of such joints is that, since the chord no longer must transfer the entire load, its thickness can be reduced and "joint cans" eliminated. The amount of overlap can be controlled by adjusting the eccentricity of brace centerlines, as indicated in Fig. 14. Negative eccentricity (Ref. 12) can be used to increase the amount of overlap and the static load transfer capacity of the connection.

A crude ultimate strength analysis is proposed (see Fig. 15), in which the punching shear capacity for that portion of the brace reaching the main member and the membrane shear capacity of the common weld between braces are assumed to act simultaneously. Thus, the total capacity of the connection for transferring loads perpendicular to the chord becomes

$$P \sin \theta = v_p t \, l_1 + 2 v_w t_w l_2 \qquad (7)$$

where

v_p = allowable punching shear stress equation (6) for the main member

t = main member wall thickness

l_1 = circumferential length for that portion of the brace which contacts the main member

and

v_w = allowable shear stress for the common weld between the braces*

t_w = throat thickness for the common weld between braces*

l_2 = the projected chord length (one side) of the overlapping weld, measured in the plane of the braces and perpendicular to the main member**

A comparison of computed capacities, in terms of brace axial load, P, using ultimate v_p and yield $v_w \times t_w$, versus test results is given in Fig. 14. Equation (6) appears to be conservative in predicting static joint capacities, provided there is sufficient ductility that the stiffer element (the overlap) does not fail before the rest of the joint catches up. At elastic load levels the overlap is so much stiffer that it tries to carry the entire load, thus, where overlapping joints are intentionally used, some designers like to proportion the overlap to carry at least 50% of the acting transverse load.

Where extreme amounts of overlap are used, it may become necessary to check the capacity of the connection for transferring loads parallel to the main member as well as transverse loads. Both may be accomplished with vector combination of the various strength elements, as suggested in Figs. 14 and 15.

Fatigue

Few members or connections in conventional buildings need to be designed for fatigue, since most load changes occur infrequently or produce only minor cyclic stresses. The full design wind or earthquake loads are sufficiently rare that fatigue need not be considered.

However, crane runways and supporting structures for machinery are often subject to fatigue loading conditions. Offshore structures are subject to a continuous spectrum of cyclic wave loadings, which require consideration of cumulative fatigue damage (Ref. 13).

Welded tubular connections, in particular, require special attention to fatigue, since statically acceptable designs may be subject to localized plastic strains, even at nominally allowable stress levels.

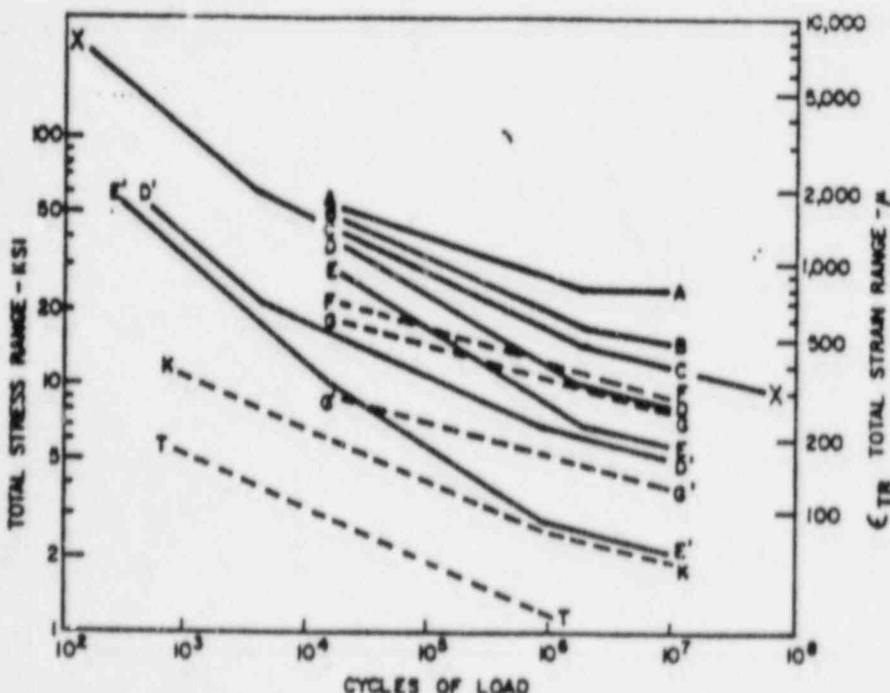Fatigue may be defined as damage that results in fracture after a suffi-

Fig. 16 — Family of fatigue design curves (see Table 1)

---

*Except that the line load capacity v_w * t_w should not exceed the shearing capacity of the thinner adjoining base metal.

**Projected chord length is proportional to the resultant of membrane shear, acting at peak value along the full length of the overlapping weld.

Table 2 — Fatigue Categories

Stress category	Situation	Kinds of stress[a]
A	Plain unwelded tube.	TCBR
A	Butt splices, no change in section, full penetration groove welds, ground flush, and inspected by x-ray or UT.	TCBR
B	Tube with longitudinal seam.	TCBR
B	Butt splices, full penetration groove welds, ground flush.	TCBR
B	Members with continuously welded longitudinal stiffeners.	TCBR
C	Butt splices, full penetration groove welds, as welded.	TCBR
D	Members with transverse (ring) stiffeners, or miscellaneous attachments such as clips, brackets, etc.	TCBR
D	Tee and cruciform joints with full penetration welds (except at tubular connections).	TCBR
D'[b]	Simple T, Y, or K connections with full penetration tubular groove welds.	TCBR in branch member (main member must be checked separately per Category K or T)
E	Balanced T and cruciform joints with partial penetration groove welds or fillet welds (except at tubular connections).	TCBR in member (weld must also be checked per Category G).
E	Members where doubler wrap, cover plates, longitudinal stiffeners, gusset plates, etc., terminate (except at tubular connections).	TCBR in member.
E'[b]	Simple T, Y, and K type tubular connections with partial penetration groove welds or fillet welds; also complex tubular connections in which load transfer is accomplished by overlap (negative eccentricity,) gusset plates, ring stiffeners, etc.	TCBR in branch member (main member in simple T, Y, or K connections must be checked separately per Category K or T; weld must also be checked per Category G').
F	End weld of cover plate or doubler wrap; welds on gusset plates, stiffeners, etc.	Shear in weld.
G	T and cruciform joints, loaded in tension or bending, having fillet or partial penetration groove welds.	Shear in weld (regardless of direction of loading)
G'	Simple T, Y, or K connections having fillet or partial penetration groove welds.	Nominal shear in weld (P/A + M/S)
X	Main member at simple T, Y, and K connection.	Hot spot, stress or strain on the outside surface of the main member, at the toe of weld joining branch member — measured in model of prototype connection, or calculated with best available theory.
X	Unreinforced cone-cylinder intersection.	Hot spot stress at angle change.
X	Connections whose adequacy is determined by testing an accurately scaled steel model.	Worst measured hot spot strain, after shake down.
K[c]	Simple K type tubular connections in which gamma ratio R/T of main member does not exceed 24.	Punching shear on shear area[d] of main member.
T[c]	Simple T and Y tubular connections in which gamma ratio R/T of main member does not exceed 24.	Punching shear on shear area[d] of main member.

(a) T = tension, C = compression, B = bending, R = reversal.
(b, c) Empirical curves based on "typical" connection geometries, if actual stress concentration factors or hot spot strains are known, use of curve X is to be preferred.
(d) Equation 1

---

cient number of fluctuations of stress. Where the fatigue environment involves stress cycles of varying magnitude and varying numbers of applications, failure is usually assumed to occur (or reach a given probability level) when the cumulative damage ratio, D, reaches unity, where

$$D = \Sigma n/N \qquad (8)$$

and n = number of cycles applied at a given stress range

N = number of cycles at that stress range corresponding to failure (or a given probability of failure)

Some designers limit the damage ratio to 0.33 when using median or best fit fatigue curves, corresponding to a safety factor of 3 on computed fatigue life. An alternative approach, which will be presented here, is to use fatigue curves which fall on the safe side of most of the data. It might be noted that a linear cumulative damage rule is consistent with the fracture mechanics approach to fatigue crack propagation (Ref. 14).

Stress fluctuations will be defined in terms of stress range, the peak-to-trough magnitude of these fluctuations. Mean stress is ignored. In welded structures we usually do not know the zero point, as there are residual stresses as high as yield which result from the heat of welding. Where there is localized plastic deformation during shakedown, a new set of resid-

ual stresses develop. What is usually measured on the actual structure (or a scale model) is the strain range, with the zero point undefined. The constant strain range approximation is in fair agreement with the results of fatigue tests on practical as-welded joints, particularly in the low cycle range.

Fatigue criteria are presented as a set of S-N design curves (Fig. 16) for the various situations categorized in Table 2.

Curves A, B, C, D, E, F, and G are consistent with AISC fatigue criteria (Ref. 15), which appear in turn to reflect the data published earlier by WRC (Ref. 16). Curves rather than tabulated (step function) allowables
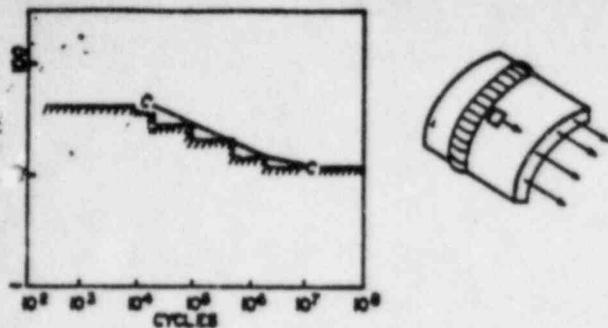
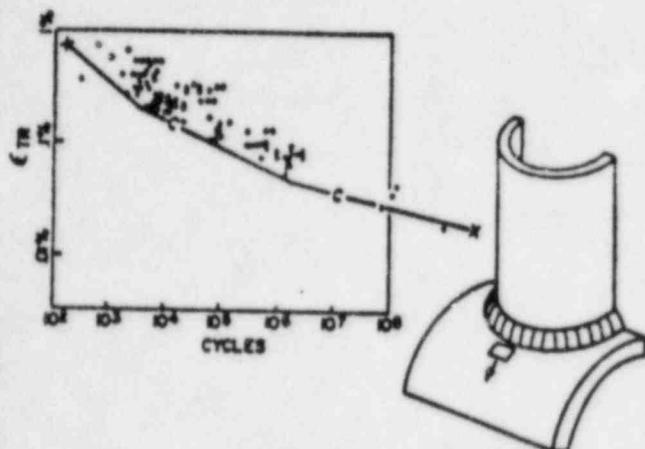Fig. 17 — Fatigue curve C — nominal stress adjacent to weld

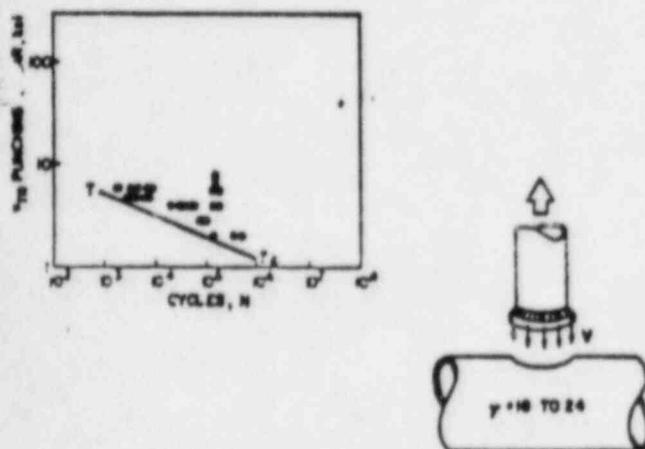Fig. 18 — Fatigue curves C and X — hot spot strain adjacent to weld

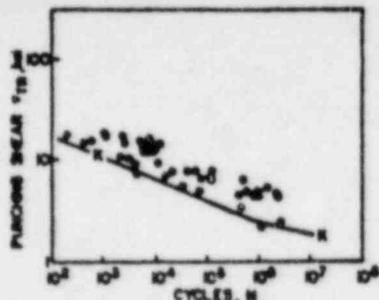Fig. 19 — Punching shear fatigue strength of T-connections

Fig. 20 — Punching shear fatigue strength of K-connections
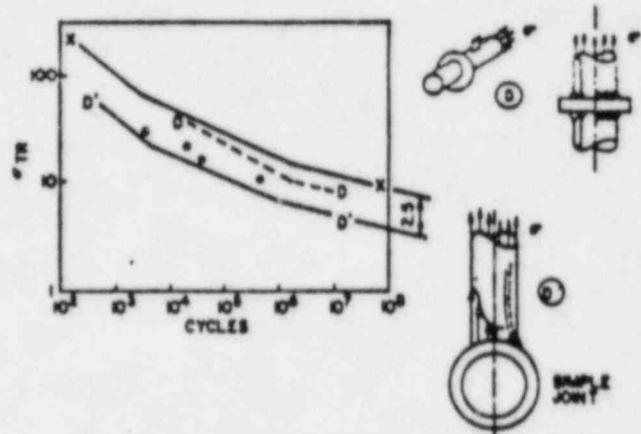

Fig. 21 — Fatigue curves D and D' — nominal member stress at full penetration T welds and simple joints
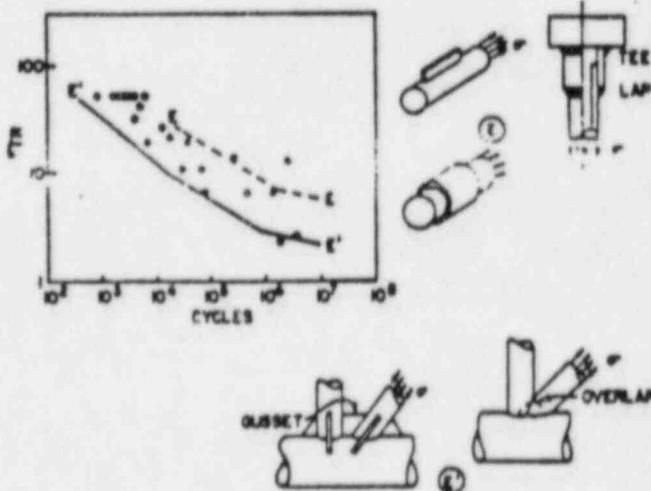

Fig. 22 — Fatigue curves E and E' — nominal member stress at fillet welds and complex joints

are used because they are more appropriate to tubular structures exposed to a continuous spectrum of cyclic loads. In these simple situations the nominal member stress $(f_a + f_b)$ fairly well represents the actual stress as would be measured adjacent to the weld. See Fig. 17.

Curve X is based on current design practices for offshore structures (Ref. 8). The relevant stress for fatigue failure of tubular connections is the hot spot stress measured adjacent to the weld, as shown in Fig. 18. This is usually considerably higher than the nominal member stress, and would normally be determined from a detailed theoretical (Refs. 5, 6), or experimental (Refs. 4, 7), analysis of the connection. Category X is consistent with category C since the local transverse stress adjacent to the weld is considered in both cases. In the range of inelastic stresses and low cycle fatigue (Ref. 17) it is more realistic to deal in terms of hot spot strain rather than stress.

The data plotted in Fig. 18 represent hot spot stress (or strain) from actual as-welded hardware — tubular connections, pressure vessels, laboratory models and prototype failures — from a variety of sources (Refs. 13, 14, 16, 18, 19, 20, 21). In the low cycle range, the design curve corresponds to roughly 95% survival (5% failure probability) based on test data which are spread out over a scatter band more than one log cycle wide. Within this range, all structural qual-

ity steels show similar fatigue behavior, independent of yield strength in the range of 36 to 100 ksi. Differences which show up' for smooth polished laboratory specimens in the high cycle range simply do not apply to practical as-welded (notched) hardware subjected to localized plastic strains in the presence of a corrosive environment (e.g., seawater).

Little data are available for the high cycle range, over 2×10^8 cycles. In the presence of initial flaws and/or corrosive environments, there is no endurance limit, and the fatigue strength continues to drop off.

Unfortunately, use of curve X requires knowledge of stress concentration factors and hot spot stresses within the tubular connections — information which would not be available to many designers. However, anyone should be able to calculate punching shear (equation 1) and make use of the empirical design curves T and K (Figs. 19 and 20) for cyclic punching shear in, respectively, T and K connections. These are based on data assembled by Toprac (Ref. 21) from tests in which the chord thinness ratio, γ, was limited to the range of 18 to 24. Thus the curves may err on the safe side for very heavy chord members (γ under 18), and they could be unconservative for chords with γ over 24. Since the theoretical elastic punching shear efficiency (Fig. 6) varies inversely with $\gamma^{0.7}$, it is suggested that, for chords having γ greater than 24, the allowable cyclic punching shear be reduced in proportion to $(24/\gamma)^{0.7}$.

Once failure of the chord in the punching shear mode has been prevented, by the use of heavy wall "joint cans" or by means of other joint reinforcement, the problem of possible fatigue failure in the braces remains. In simple joints, localized stresses in the brace may reach 2.5 times nominal $f_a + f_b$, due to non-uniform load transfer (a factor of about 2, Fig. 5), restraint to Poisson's-ratio breathing (a factor of 1.6 for perfect axisymmetric restraint), and continuity with the severely deformed chord. Accordingly, curve D' (Fig. 21) when applied to nominal brace stress takes these factors into account. Data points are for thick walled simple joints tested by Bouwkamp et al (Refs. 14, 19), for which failure occurred in the brace (branch member) rather than in the chord (main member).

Where some other form of joint reinforcement is used (such as brace overlap, gussets, or rings) localized stresses in the brace may become larger and more difficult to ascertain and thus have to be designed according to curve E' (Fig. 22), which implies stress concentration factors as high as 6. However, it should be stated

also that for some connections of this type curve E is too conservative but unfortunately at this stage no distinction can be made.

Curves D, E, F, and G are limited to situations in which nominal member stresses represent actual load transfer across the weld. Curve G' is shifted down to a factor of 2.0 to account for the uneven distribution of load transfer across the weld at the tube-to-tube intersection (Ref. 5).

The data supporting the empirical design curves, T, K, D', and E' generally show more scatter than the more basic data of Fig. 18, primarily because they neglect some of the relevant factors, and only represent "typical" connection geometries. Where actual stress concentration factors are known, the use of curve X is to be preferred.

Because of the uncertainty and scatter involved, calculated fatigue lives should be taken with a healthy amount of skepticism, and should be viewed more as a design guideline than as an absolute requirement of the code.

Concluding Remarks

The criteria presented have been developed primarily on the basis of research and experience with fixed offshore platforms. These structures are highly redundant, and localized tubular joint failures can occur without leading to collapse of the structure.

One purpose in presenting this paper is to let potential designers of other classes of tubular structures see just how the data fall relative to the proposed criteria, and what the scatter is, so that they may be in a position to evaluate the suitability of the criteria for their particular application.

Also, it is hoped that, as additional data become available, they will be compared against the criteria and data given herein. Such comparison, discussion, and re-examination should eventually lead to a better design.

The authors are indebted to their colleagues in the various API, AWS, WRC, and ASCE task groups concerned with welded tubular structures, whose prodding and comments helped shape the guidelines presented here.

References

1. *API Recommended Practice for Planning, Designing, and Constructing Fixed Offshore Platforms*, API RP 2A, Fourth Edition (1973).
2. *American Welding Society Structural Welding Code*, AWS D1.1-72 (1972).
3. British Standard 449-1959 Appendix C, "Determination of the Length of the Curve of Intersection of a Tube with Another Tube or with a Flat Plate", and British Standard 938-1962, *Spec. for Gen-*

eral Requirements for the Metal Arc Welding of Structural Steel Tubes to B.S. 1775.
4. Toprac, A. A., et al., "Welded Tubular Connections: An Investigation of Stresses in T-Joints," *Welding Journal*, Vol. 45, No. 1, January 1966, Res. Suppl., pp. 1-s to 12-s.
5. Dundrova, V., *Stresses at Intersection of Tubes — Cross and T-Joints*, The University of Texas, S.F.R.L. Technical Report P-550-5 (1966).
6. Greste, Ojars, *A Computer Program for the Analysis of Tubular K-Joints*, University of California Structural Engineering Lab. Report No. 69-19 (1969).
7. Beale, L. A., and Toprac, A. A., *Analysis of In-Plane T, Y and K Welded Tubular Connections*, Welding Research Council Bulletin 125, New York, N.Y., October 1967.
8. Marshall, P. W., et al., "Materials Problems in Offshore Platforms," Offshore Technology Conference Preprint No. OTC 1043 (1969).
9. Reber, J. B., "Ultimate Strength Design of Tubular Joints," Offshore Technology Conference Preprint No. OTC 1664 (1972).
10. Graff, W. J., "Welded Tubular Connections of Rectangular and Circular Hollow Sections," paper for presentation to the Texas Section, ASCE, El Paso, October 8-10, 1970.
11. Toprac, A. A., et al., *Studies on Tubular Joints in Japan — Part I — Review of Research Reports*, report prepared for Welding Research Council, Tubular Structures Committee, September, 1968.
12. Bouwkamp, J. G., *Research on Tubular Connections in Structural Work*, Welding Research Council Bulletin No. 71, 1961.
13. Bell, A. O., and Walker, R. C., "Stresses Experienced by an Offshore Mobile Drilling Unit," Offshore Technology Conference Preprint No. OTC 1440 (1971).
14. Becker, J. F., et al., "Fatigue Failure of Welded Tubular Joints," Offshore Technology Conference Preprint No. OTC 1228 (1970).
15. American Institute of Steel Construction, *Specifications for Design, Fabrication and Erection of Structural Steel for Buildings*, New York, N.Y., February 12, 1969.
16. Munse, W. H., and Grover, L., *Fatigue of Welded Steel Structures*, Welding Research Council, New York, N.Y. 1964.
17. Peterson, R. E., "Fatigue of Metals in Engineering and Design," ASTM Marburg Lecture, 1962.
18. Kooistra, L. F., Lange, E. A., and Pickett, A. G., "Full-Size Pressure Vessel Testing and its Application to Design," ASME Paper 63-Wa-293, 1963.
19. Bouwkamp, J. G., *Tubular Joints Under Static and Alternating Loads*, University of California, Structures and Materials Research Report No. 66-15, Berkeley, June 1966.
20. Toprac, A. A., and Natarajan, M., *An Investigation of Welded Tubular Joints: Progress Report*, International Institute of Welding Comm XV Doc XV-265-69, June 1969.
21. Toprac, A. A., *Design Considerations for Welded Tubular Connections*, Report prepared for Welding Research Council, Tubular Structures Committee, December 1970.

TEXAS UTILITIES GENERATING COMPANY

P. O. BOX 1002 · GLEN ROSE. TEXAS 76043

November 16, 1984

Ms. N. H. Williams
Project Manager
CYGNA Energy Services
101 California Street, Suite 1000
San Francisco, California 94111-5894

COMANCHE PEAK STEAM ELECTRIC STATION
Independent Assessment Program Phase 3
Cinched U-Bolt Testing & Analyses Program
Additional Information

REF: 1) J. B. George (TUGCO) letter to N. H. Williams (CYGNA), dated
November 1, 1984 - same subject

2) N. H. Williams (CYGNA) letter to J. B. George (TUGCO), "Status
of Cinched U-Bolt Testing and Analy s Program", 84042.018
dated October 1, 1984

Dear Ms. Williams:

Reference 1 provided in its attachment the information requested by Reference
2. Included in the attachment as part of the answer provided to Item 2 of
Reference 2 were results of a finite difference heat transfer analysis con-
ducted for an uninsulated and an insulated U-bolt configuration on a 10-inch
pipe.

A rechecking of the modelling of the contact areas between the U-bolt and
the pipe and the pipe and the crosspiece has indicated that the contact be-
tween the pipe and crosspiece was overestimated and that the contact between
the pipe and the U-bolt had been incorrectly assumed to extend for an arc of
180°. Accordingly, we are providing in the attachment to this letter the
results obtained for the uninsulated case of the pipe at 250° F and the in-
sulated case with the pipe at 350° F, where the boundary conditions of the
model are changed to reflect the more realistic contact areas. We will be
glad to discuss the details of the model, if CYGNA so desires.

Please call if you have any questions.

Very truly yours,

TEXAS UTILITIES GENERATING COMPANY

11/16/84

J. B. George
Vice President/Project General Manager

JBG/RCI/gh

cc: S. Burwell   R. Iotti
    J. Van Amerongen   D. Wade

CYGNA	
JOB NO :	84042
DATE REC'D/LOGGED:	11/19/84
LOG NO.:	498
FILE:	2.1.1 &c. 4A
CROSS REF. FILE	2.1 &c. 4A log

A DIVISION OF TEXAS UTILITIES ELECTRIC COMPANY

ATTACHMENT 1

Revision to Item 2 of Reference 1.

Please replace Item 2 response with the following:

A. The answer to this question is best worded by first restating that the choice of 250°F for the 10-inch pipe temperature is a compromise choice which bounds the majority of the systems in the plant, and where used with an uninsulated U-bolt configuration is also representative of the case where the pipe temperature may be 350°F but the U-bolt configuration is insulated.

Second, it is important to point out that there is a single cinched-up U-bolt which is used on the 10-inch portion of the RHR system. This is support RH-1-024-007-S22R which is on line 10-RH-1-24-601-R-2, which is connected to the outlet line of the RHR heat exchanger. The maximum normal temperature seen by the line is 280°F during initiation of RHR operation. Only under upset conditions, where component water cooling may be lost, can the maximum temperature of this line reach 350°F. There are no cinched-up U-bolts on the inlet side of the RHR heat exchangers.

Third, it is germane to point out that the tests conducted on the 10-inch pipe specimens had a corresponding average temperature of the U-bolt equal to approximately 150°F. For the particular configuration examined here, i.e., stainless steel pipe and carbon steel U-bolt, the approximate 150°F represents the equilibrium temperature of the U-bolt. The following describes the temperature history during the thermal cycling test and the creep test for both the U-bolt and the crosspiece.

Thermal Cycle 1:

The pipe reached the test temperature of 250°F at 30 minutes, but then continued to climb to over 280°F before settling back down ot 258°F. The U-bolt radius and leg stabilized around 195°F and 150°F, respectively, near the end of the cycle. See Figure 3.

Thermocouples 2, 9 and 10 on the crosspiece reached temperatures of 129°F, 136°F and 144°F, respectively, at che end of Cycle 1. These are less than the equilibrium temperatures reached during the creep test. Figure 4 shows that temperatures had not leveled off. Refer to Figure 9 for location of thermocouples.

Thermal Cycle 6:

The pipe reached an equilibrium temperature of 250°F within 20 minutes. The U-bolt radius and leg reached 183°F and 144°F, respectively, around 1 hour. See Figure 5.

Thermcouples 2, 9 and 10 on the crosspiece reached temperatures of 125°F, 132°F and 139°F, respectively, at the end of Cycle 6. These are less than the equilibrium temperatures reached during the creep test. Figure 6 shows that temperatures had not leveled off.

Creep Test:

The pipe reached an equilibrium temperature of 250°F in less than 1 hour.
The U-bolt radius stabilized at 185°F within 1 hour. The U-bolt leg sta-
bilized at 148°F within 2 hours. See Figure 7.

Thermocouples 2, 9 and 10 on the crosspiece reached equilibrium tempera-
tures of 138°F, 146°F and 154°F, respectively, around 3 hours. See Figure
8.

10" Specimen Summary:

With a pipe test temperature of 250°F, the U-bolt reached thermal equili-
brium during each cycle of the thermal cycling test, but the crosspiece
didn't. The entire assembly reached thermal equilibrium shortly into the
creep test. A summary is provided in Table 1.

Results of finite difference thermal analyses are very sensitive to the assumed
area of contact between the pipe and the U-bolt and the pipe and the crosspiece.
When the U-bolt is cinched, the line contact between the pipe and the U-bolt
extends for an arc which is less than 180°, and the precise extent of which
depends on the cinching force and the spacing of the bolt holes in the cross-
piece. Similarly the cinching process tends to produce a loss of contact at
some points between the crosspiece and the pipe due to either bending of the
crosspiece or local deformation of the pipe. This loss of contact, however
small, profoundly affects the heat transferred from the pipe to the crosspiece.

A heat transfer model has been executed for the uninsulated U-bolt configura-
tion with the following assumptions. Heat transfer from the pipe to the U-
bolt is along an arc near the apex of the U-bolt. At the diametral location
there is a small gap (less than 1/16") between the pipe and U-bolt. No gaps
are assumed between the U-bolt and the crosspiece (the assumption is believed
to be inconsequential since both elements are roughly at the same temperature
at that location). Heat transfer between the pipe and the crosspiece takes
place through a line contact extending 2 inches along the pipe, and via gap
conductance, along the circumference of the pipe and through a gap increasing
from zero to 1/128" linearly from the end of the contact area to the end of
the plate. Likewise, the heat transfer between the pipe and the U-bolt also
considers the gap conductance with areas immediately adjacent to the line of
contact and extending out to the U-bolt radius. This model produced results
which more closely match the results of the test.

Results of the analyses are shown in Figure 1 for the uninsulated case. In
Figure 2 similar results are shown for the insulated case. The only difference
between the latter analyses and that of the uninsulated configuration are the
pipe temperature, which in the latter instance is 350°F, and the presence of
insulation.

For the uninsulated case the average temperature of the U-bolt in the curved
portion is 175-180°F, while the straight portion is at about 150°F. For the
insulated case the corresponding temperatures are approximately 300°F and
260°F respectively.

The effect of the temperature rise on the clamping forces acting on the pipe and the U-bolt for the two cases of 250°F pipe, uninsulated U-bolt and 350°F pipe, insulated U-bolt, can be estimated by comparing the _relative_ growth of the pipe to U-bolt for the two cases, neglecting any deformation of the pipe. Since only relative growth is pertinent here, the one-directional growth of the U-bolt due to thermal expansion given as Y_1 where

$$Y_1 = \alpha_1 \Delta TL$$

where L is the projected length of the U-bolt which is given as 2R and T is the temperature differential between the average U-bolt temperature and ambient (or a reference temperature), is compared to the diametral growth of the pipe, Y_2, which is given as

$$Y_2 = \alpha_2 \Delta TD$$

The worst case relative expansion will occur for the stainless steel pipe and the carbon steel U-bolt. For the 10-inch pipe (10.75 OD), coefficients of thermal expansions $\alpha_1 = 6.3 \times 10^{-6}$ in/in/°F at 150-180°F or 6.6×10^{-6} at 260-300°F and $\alpha_2 = 9.4 \times 10^{-6}$ at 250°F or 9.53×10^{-6} at 350°F and a reference ambient temperature of 70°F, the relative expansion for the two cases considered, i.e., 250°F pipe with bare U-bolt, and 350°F pipe with insulated U-bolt are as follows:

1. 250°F $\Delta Y = 0.011755$ inches

2. 350°F $\Delta Y = 0.0137$ inches

3. Finite Element Analysis $\Delta Y = 0.0141*$

(* Finite Element Analysis used 210°F.)

As seen from the above, theoretical, steadystate heat transfer analyses would predict that the case of 350°F pipe expanding against an insulated U-bolt could result in a differential pipe expansion which would be approximately 17% larger than could be expected for a 250°F pipe with uninsulated U-bolt. However, the finite element analysis has been conducted in a manner that would encompass the case of 350°F insulated U-bolt. As seen from the third row of relative expansion, the finite element analysis, which used a pipe temperature of 210°F but maintained the U-bolt temperature at 70°F, would yield a relative expansion which is comparable to the case of 350° insulated.

Another point to be discussed, is that the test has provided information on the transient thermal expansion differential between the pipe and the U-bolt. As seen from the data which is attached as Figures 3 and 5, the maximum temperature differential between the pipe and the U-bolt occurred when the U-bolt has reached a representative temperature of about 100-105° while the pipe had been heated to 250-255°, a difference in temperature of approximately 150°F. This difference is well simulated in the finite element analysis where there is a constant difference in temperature of 140°F. It should also be remembered that for these temperature differentials, the amount of stress caused by the thermal expansion is not very significant.

TABLE 1

U-BOLT THERMAL AND CREEP TEST
DATA EVALUATION

	EQUILIBRIUM TEMPERATURE, °F						TIME REQUIRED TO REACH EQUILIBRIUM TEMPERATURE, HOURS					
	PIPE	U-BOLT RADIUS	U-BOLT LEGS	T/C 2	T/C 9	T/C 10	PIPE	U-BOLT RADIUS	U-BOLT LEGS	T/C 2	T/C 9	T/C 10
" INSULATED SPECIMEN												
THERMAL CYCLE 1	559	498	451	*	*	*	2.5	2.5	2.5	*	*	*
THERMAL CYCLE 6	560	530	440	*	*	*	2.0	2.25	2.75	*	*	*
CREEP	564	495	451	322	340	365	2.0	2.0	2.0	3.0	3.0	3.0
10" UNINSULATED SPECIMEN												
THERMAL CYCLE 1	250	195	150	*	*	*	.50	1.5	1.5	*	*	*
THERMAL CYCLE 6	250	183	144	*	*	*	.25	1.0	1.0	*	*	*
CREEP	250	185	148	138	146	154	1.0	2.0	2.0	3.0	3.0	3.0
32" INSULATED SPECIMEN												
THERMAL CYCLE 1	560	*	*	*	*	*	4.0	*	*	*	*	*
THERMAL CYCLE 6	560	*	*	*	*	*	5.0	*	*	*	*	*
CREEP	563	440	353	154	175	251	4.5	11.5	12.5	14.5	14.5	14.5

* THERMAL EQUILIBRIUM WAS NOT ACHIEVED.

EBASCO SERVICES INCORPORATED

BY M Zurisky DATE 10/22/84

CHKD. BY _____ DATE _____

SHEET _____ OF _____

OFS NO _____ DEPT. NO _____
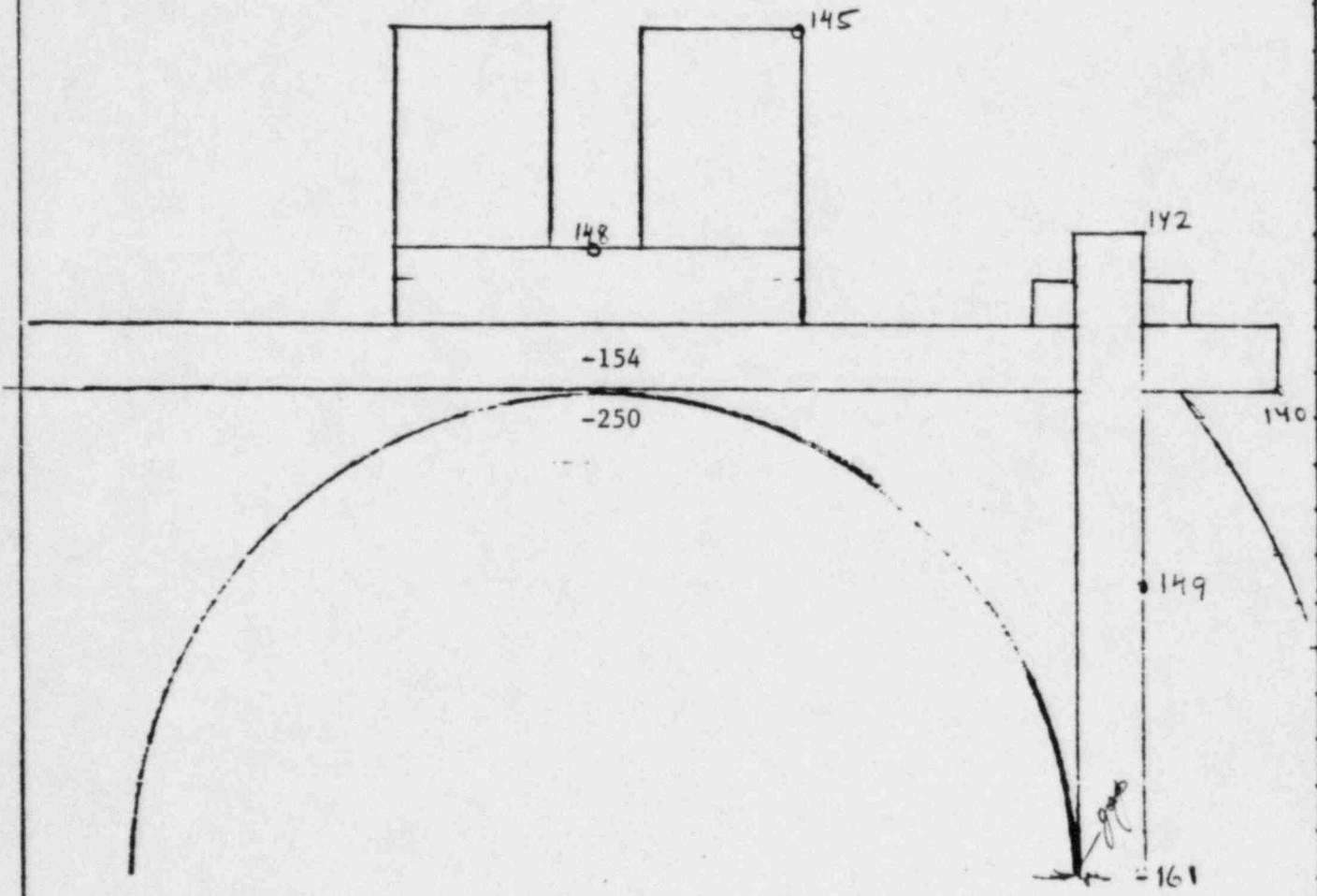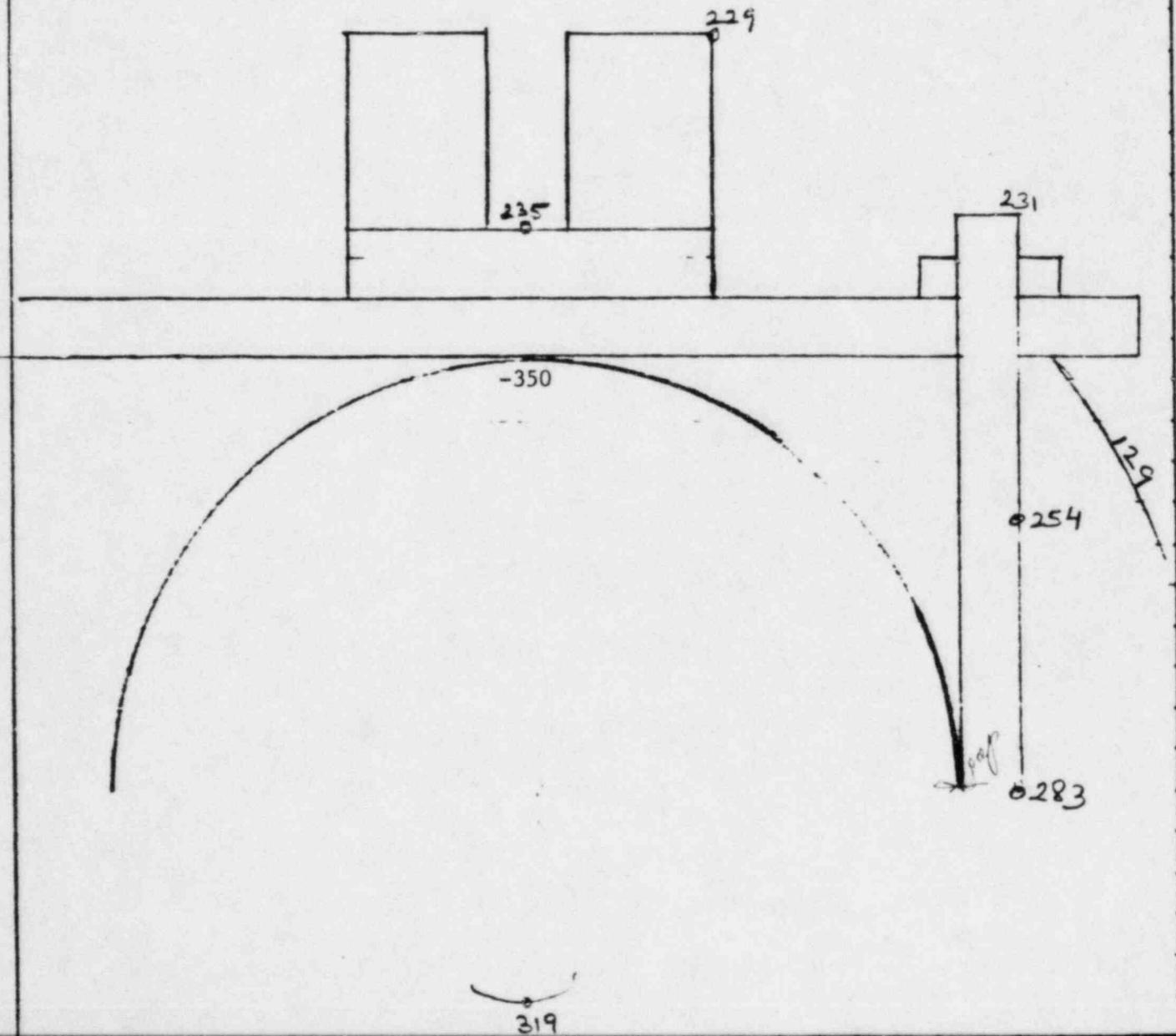
CLIENT _____ TUGC

PROJECT Comanche Peak

SUBJECT Temperature in 10" carbon steel pipe U-BOLT Assembly

Pipe at 250°F without insulation

FIGURE 1

189

BY M Zurisky DATE 10/22/84   SHEET _____ OF _____

CHKD. BY _____ DATE _____   OFS NO. _____   DEPT. NO. _____

CLIENT   TUGC

PROJECT   Comanche Peak

SUBJECT   Temperature in 10" carbon steel pipe U-BOLT Assembly

PIPE at 350°F with insulation

FIGURE 2

229

235

231

-350

129

⌀254

⌀283

319

10"SS - UNINSULATED

CYCLE 1

FIGURE 3

10" SS- UNINSULATED
CYCLE 1

CROSSPIECE
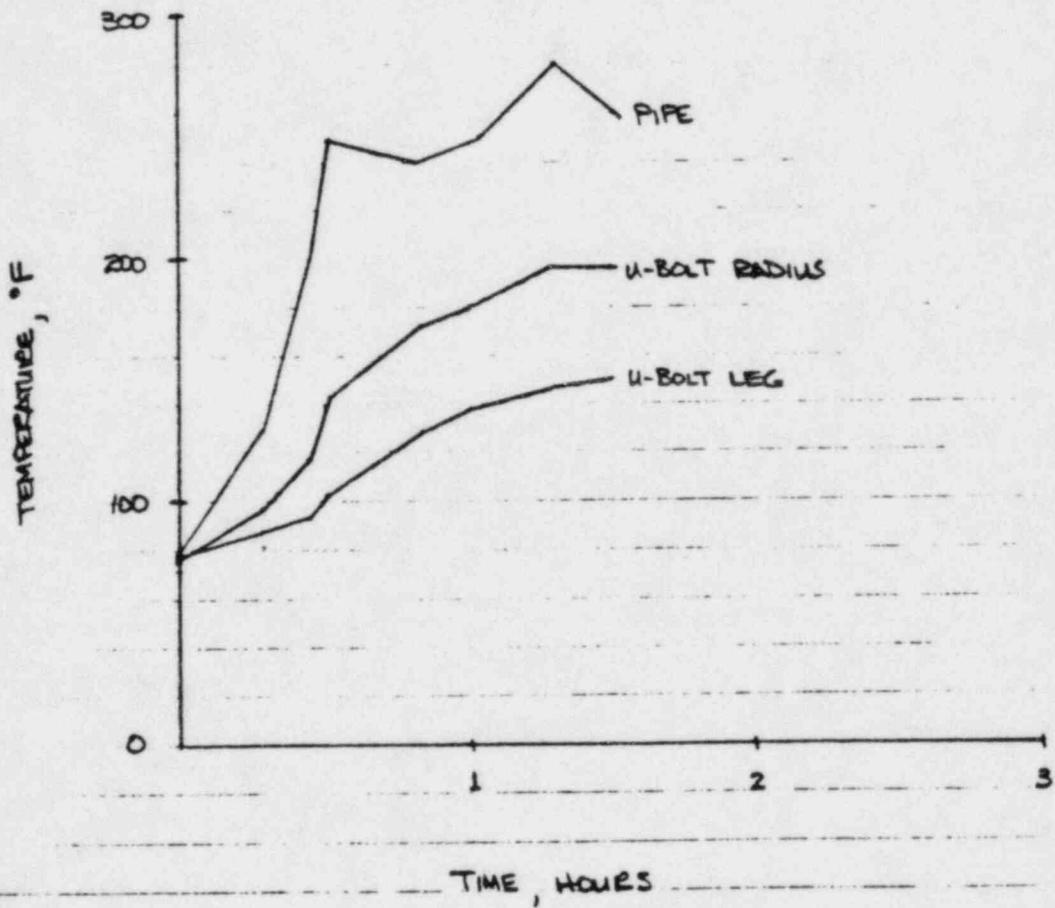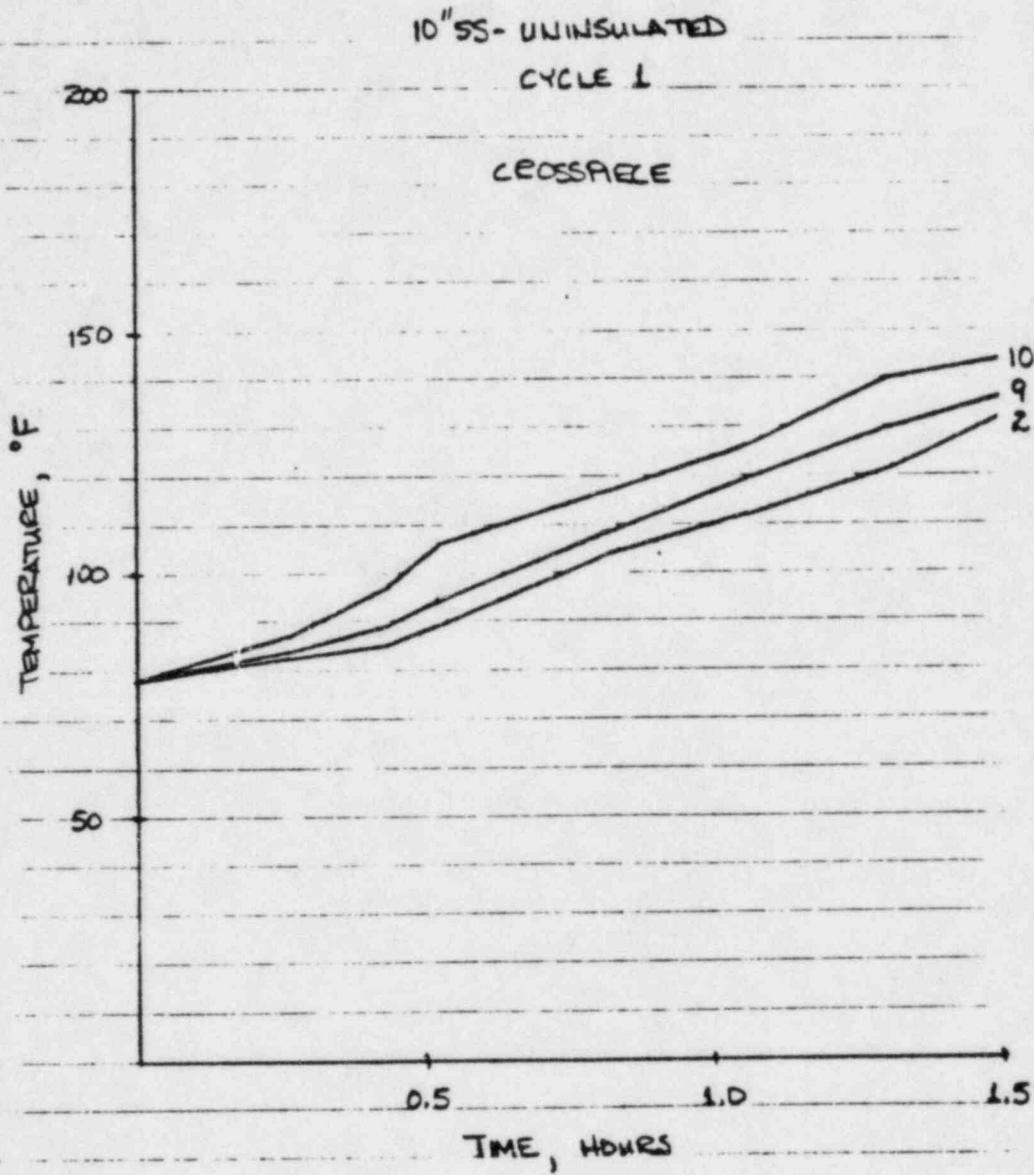
FIGURE 4

ID'SS - UNINSULATED
CYCLE 6
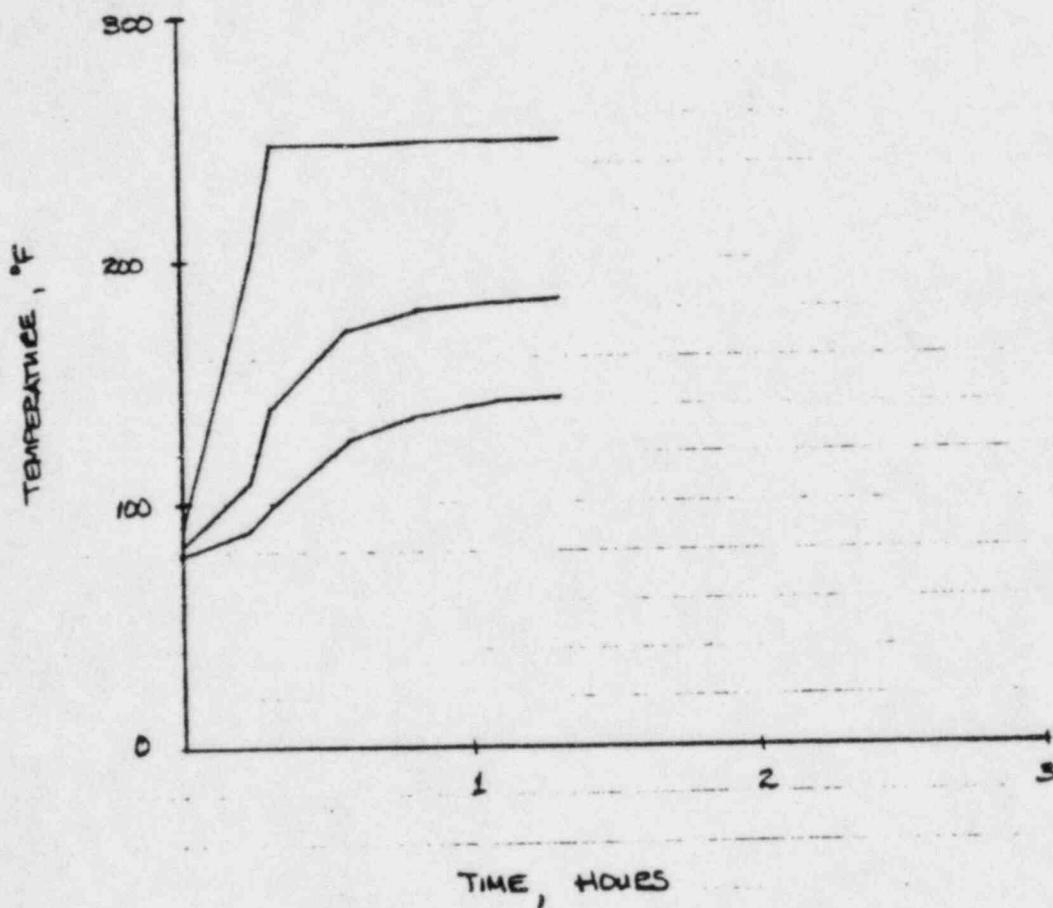
FIGURE 5

10"SS-UNINSULATED
CYCLE 6

CROSSPIECE

FIGURE 6

10" SS - UNINSULATED
CREEP TEST

PIPE 250
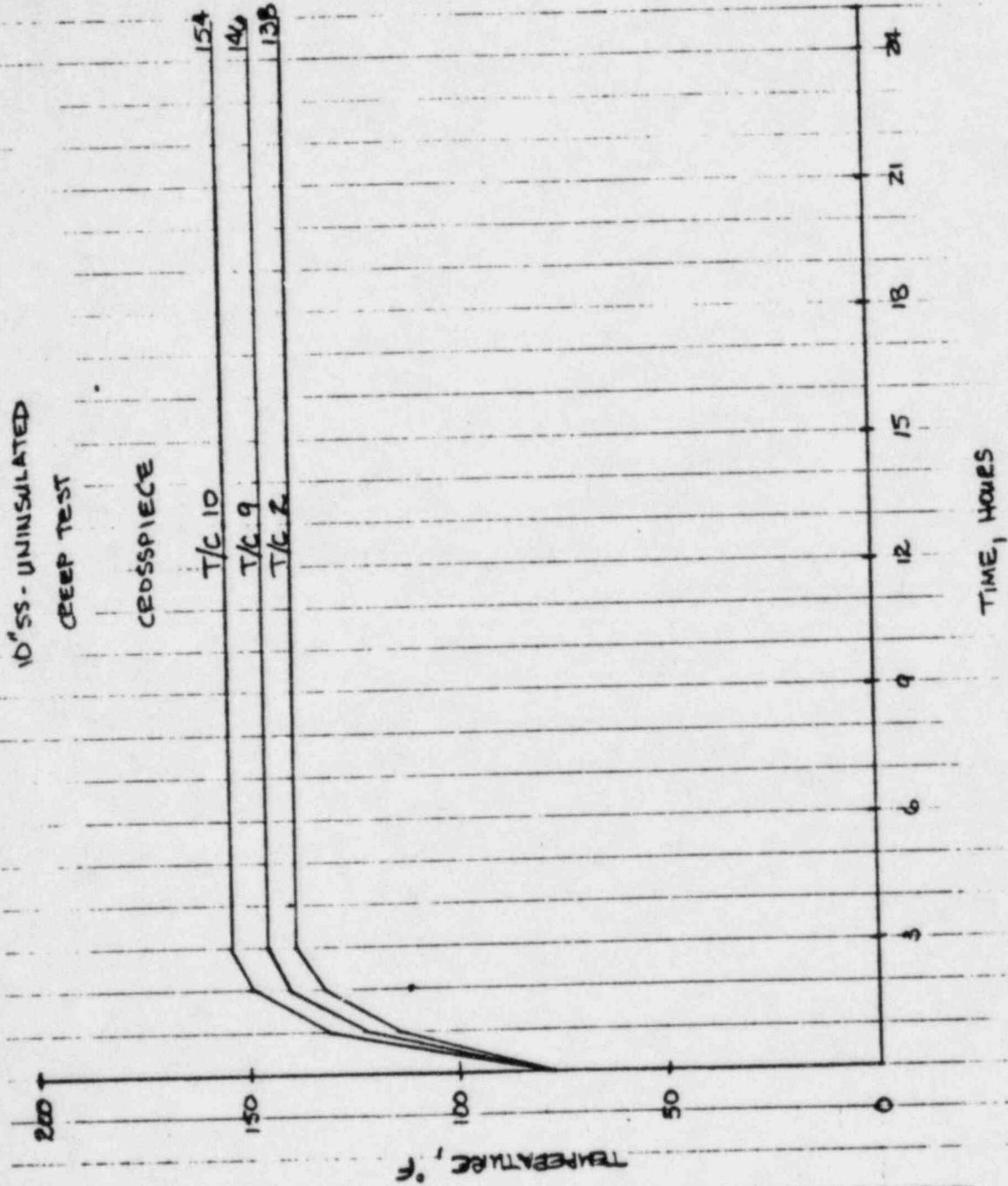
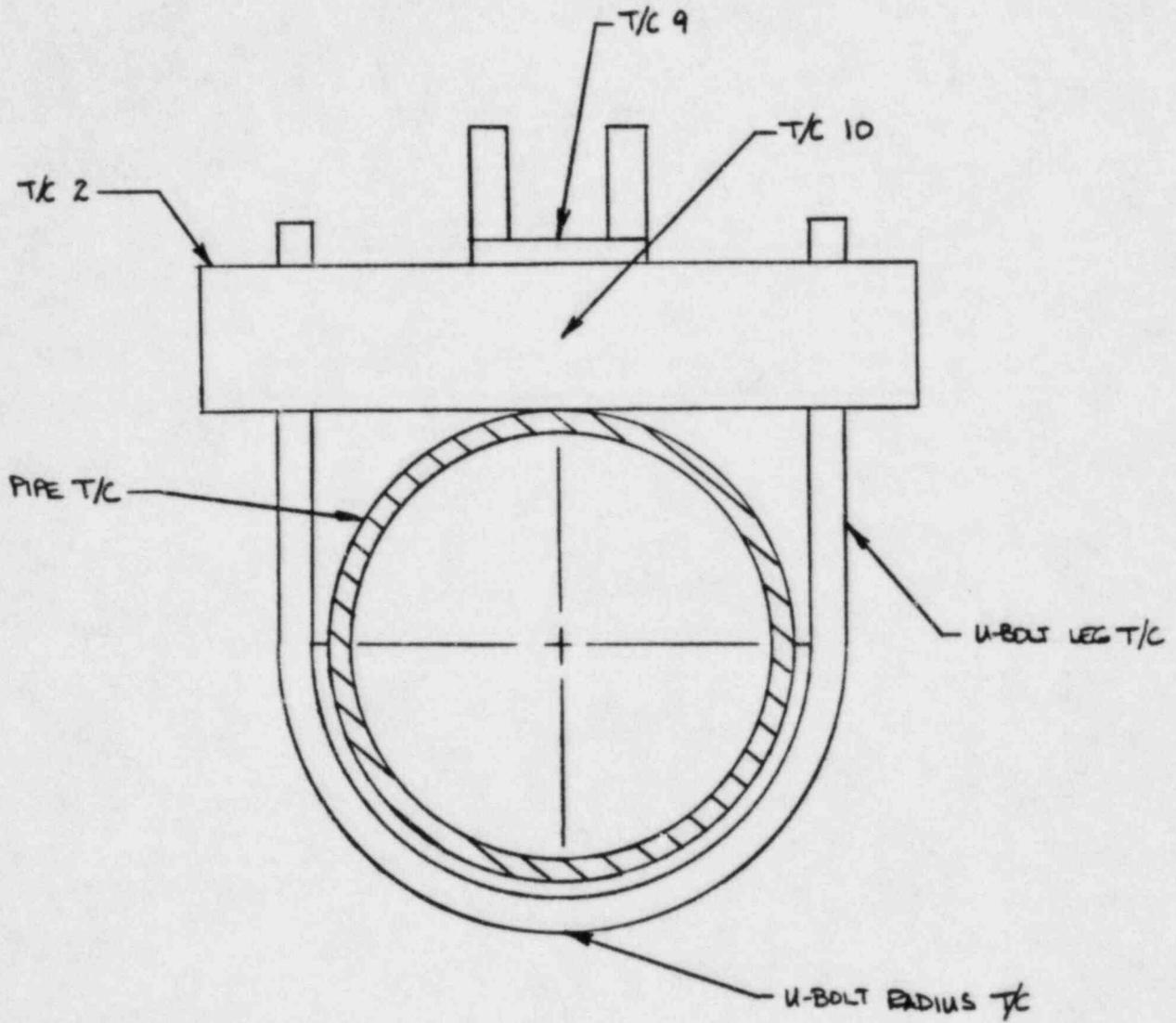U-BOLT RADIUS 185

U-BOLT LEG 140

TIME, HOURS
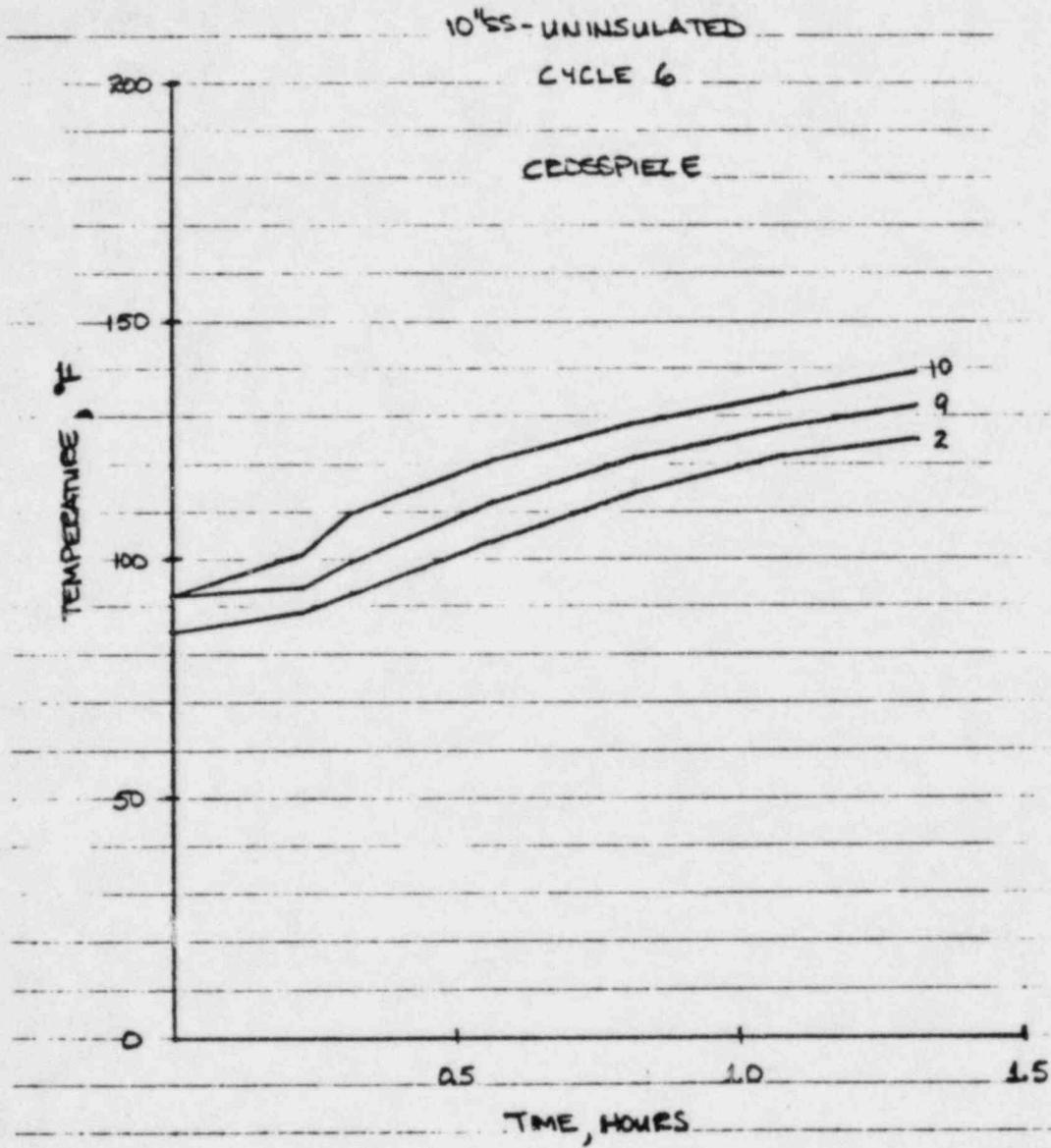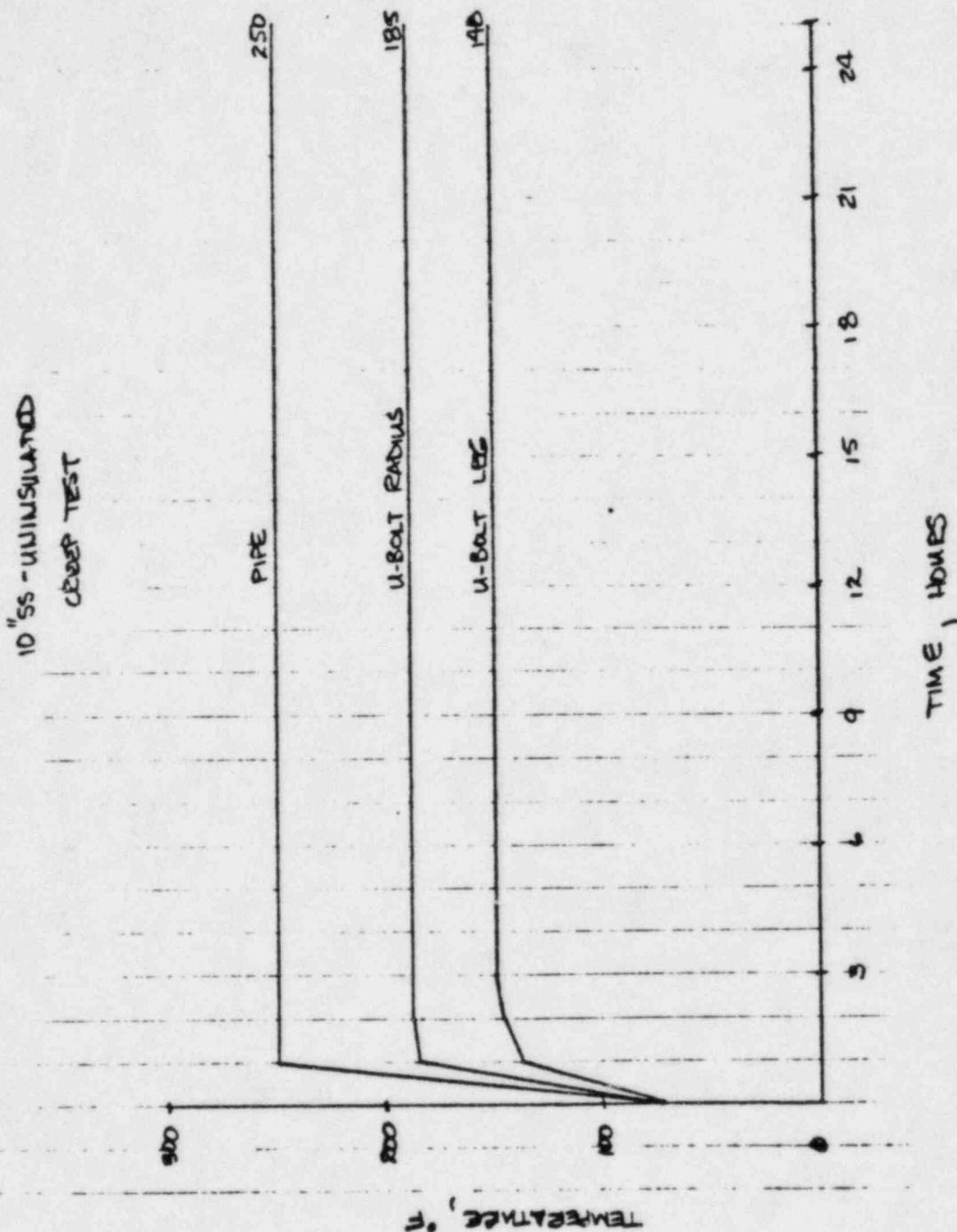
FIGURE 7

FIGURE 8

THERMAL AND CREEP TEST THERMOCOUPLE
LOCATIONS

FIGURE 9